AD-A089 402 AERONAUTICAL RESEARCH LABS MELBOURNE (AUSTRALIA) F/G 1/3
FATIGUE TESTING OF VAMPIRE WINGS,(U)
JUN 79 R A BRUTON, C A PATCHING
UNCLASSIFIED ARL/STRUC-378 NL

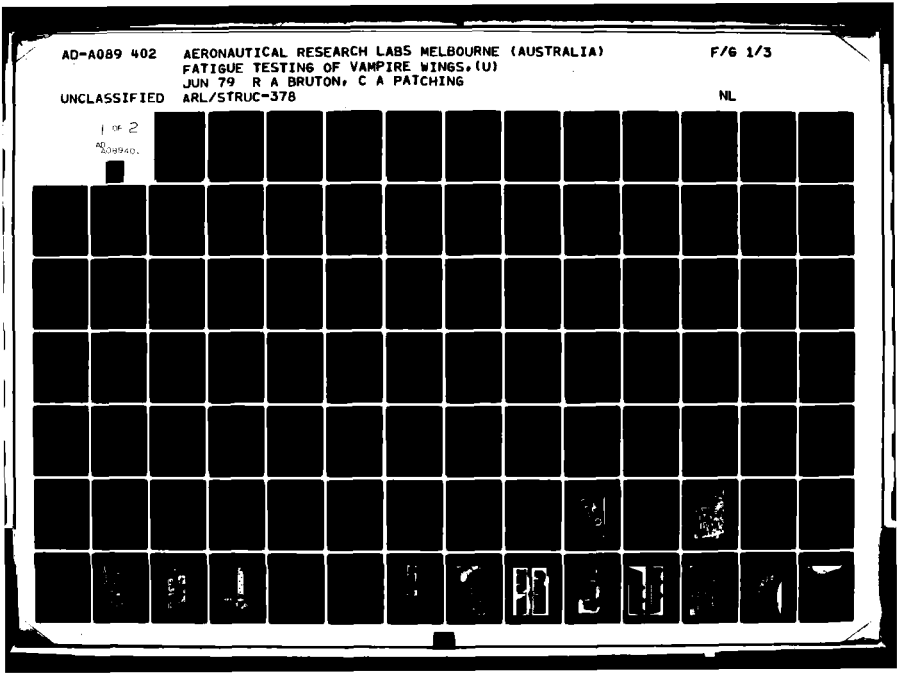

ARL-STRUC-REPORT-378

AR-001-742

DEPARTMENT OF DEFENCE

DEFENCE SCIENCE AND TECHNOLOGY ORGANISATION

AERONAUTICAL RESEARCH LABORATORIES

MELBOURNE, VICTORIA

STRUCTURES REPORT 378

FATIGUE TESTING OF VAMPIRE WINGS

by

R. A. BRUTON and C. A. PATCHING

Approved for Public Release

COPY No 10

JUNE 1979

AR-001-742

DEPARTMENT OF DEFENCE
DEFENCE SCIENCE AND TECHNOLOGY ORGANISATION
AERONAUTICAL RESEARCH LABORATORIES

STRUCTURES REPORT-378

FATIGUE TESTING OF VAMPIRE WINGS

by

R. A. BRUTON and C. A. PATCHING

SUMMARY

The fatigue behaviour of a total of 21 port and starboard Vampire wings has been investigated for a 12 load level programmed loading sequence, representative of an average Australian flight loading spectrum. An additional two wings were subjected to a randomised sequence of these loads.

This report describes the investigation and furnishes information on the following aspects:

(a) *the fatigue life of major components in the wing;*
(b) *the ineffectiveness of replacing Parker-Kalon self-tapping screws in the spar boom with pinned Chobert blind rivets;*
(c) *the increase in fatigue life achieved by replacing the lower spar boom;*
(d) *the residual strength of the cracked structure;*
(e) *the distribution of strain between screwed panels and the spar boom;*

and

(f) *the fatigue resistance of glued wooden fuselages.*

POSTAL ADDRESS: Chief Superintendent, Aeronautical Research Laboratories,
Box 4331, P.O., Melbourne, Victoria, 3001, Australia.

DOCUMENT CONTROL DATA

Security classification of this page: Unclassified

1. Document Numbers
   (a) AR Number: AR-001-742
   (b) Document Series and Number: Structures Report 378
   (c) Report Number: ARL-Struc.-Report-378

2. Security Classification
   (a) Complete document: Unclassified
   (b) Title in Isolation: Unclassified
   (c) Summary in Isolation: Unclassified

3. Title: FATIGUE TESTING OF VAMPIRE WINGS

4. Personal Author(s):
   Bruton, R. A.
   Patching, C. A.

5. Document Date:
   June, 1979

6. Type of Report and Period Covered:

7. Corporate Author(s):
   Aeronautical Research Laboratories

8. Reference Numbers
   (a) Task: AIR 99/01
   (b) Sponsoring Agency: DEFAIR

9. Cost Code: 26-1305

10. Imprint:
    Aeronautical Research Laboratories, Melbourne

11. Computer Program(s)
    (Title(s) and language(s)):

12. Release Limitations (of the document)
    Approved for public release

12-0. Overseas	N.O.		P.R.	1	A		B		C		D		E	

13. Announcement Limitations (of the information on this page):
    No limitation

14. Descriptors
    Fatigue tests
    Wings
    Loads (forces)
    Fatigue life
    Vampire aircraft

15. Cosati Codes: 1402, 1113, 01013

16.

ABSTRACT

The fatigue behaviour of 23 Vampire wings has been investigated for a 12 load level sequence applied in both a programmed and randomised order.

The effect on fatigue life of certain modifications and residual strength of the cracked structure were also ascertained.

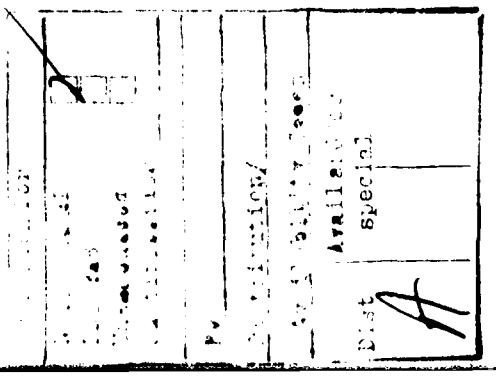

CONTENTS

1. INTRODUCTION

The fatigue life of RAAF Vampire trainer wings and of wing carry through structure in the fuselage in Australian operation was originally estimated by the use of fatigue data provided by the de Havilland Aircraft Co. Ltd., Airspeed Division, England.[1,2] These data had been obtained from fatigue tests in which failures were discovered in the following critical components:

Fuselage cross tube,
Cross tube fork end plugs,
Wing spar root end steel fittings,
Main spar boom at Rib 2.

The only other fatigue failure detected was in the main spar shear web at Rib 2, and this was not considered to be critical. The application of the data from these tests enabled the RAAF to determine safe lives and to schedule the replacement of the fuselage lower cross tube assembly and wing spar root end fittings.

However, limitations of the safe life of the wing itself, associated with fatigue in the lower spar boom at Rib 2 were not so readily amenable to alleviation by spar boom replacement, so the manufacturer had proposed a modification called the "Chobert rivet modification", or "Mod. No. 792", in which self-tapping screws at this station were to be removed, the holes enlarged to remove fatigue damaged material, and the enlarged (blind) holes filled by pinned Chobert rivets. Tests in the UK on wings built there had shown a substantial improvement to result from this modification.

Nevertheless the safe service life of the wing for Australian operations, as limited by the lower spar boom at Rib 2 was insufficient to meet the RAAF training schedule demands and, because of a minor variation in wings manufactured in Australia there were doubts that incorporation of the modification would effect an improvement in the safe life of Australian-built wings.

It was therefore decided to test Australian-built aircraft at the Aeronautical Research Laboratories.

This investigation, involving the fatigue testing of 23 half wings attached to a suitably mounted fuselage, had the following aims:

(1) To establish the fatigue life of Australian-built Vampire trainer wings under an Australian load spectrum.
(2) To establish the effectiveness of replacing the P-K screws at Rib 2 with pinned Chobert rivets in accordance with de Havilland Modification No. 792 which involved enlarging the holes from 3·28 to 4·85 mm (No. 30 to No. 11 drill size).
(3) To ascertain the lifetime at which the above modification should be incorporated.
(4) If the fatigue life shown by the investigation was insufficient, to find a suitable modification which would increase the safe flying life.
(5) To confirm the replacement lives then current for fuselage cross tube assemblies and the wing spar root end fittings.

The fatigue test was designed to conform as far as possible with the test conducted in England, except for the magnitude of the loads which were to be governed by Australian service conditions. Such conformity was expected to enable the findings from both investigations to be directly compared, and thus increase the body of data available.

A major concern of this report is the various failure regions which were found during the tests and their fatigue life, along with recommendations for increasing the life of the Vampire wing.

A number of other aspects arising from this comprehensive investigation were examined at RAAF request and details of these are described in Appendix I and Reference 3.

The estimation of safe service lives for the various components, and detailed regions where fatigue cracking occurred have been separately reported.[4,5]

Other pertinent findings of this investigation were reported to the RAAF by letter at the time of testing. Subsequently major research findings were reported externally in 1969, but the original draft comprehensive report remained unpublished. Because of the recurring need for reference within ARL to the many aspects of this extensive fatigue investigation, it was considered appropriate to publish the complete work in this form, thus adding to the total body of fatigue data for full-scale aircraft structures.

2. PRELIMINARY INVESTIGATIONS

Prior to and during preparation for the fatigue tests numerous investigations were made to provide information for both the formulation of the laboratory test and inspection of the wings during testing.

2.1 Inspection of Long Life Wings

Two pairs of wings which had been in RAAF service for 1200 and 1400 hours were subjected to an examination in the laboratory in order to establish:

(i) Whether there were any cracks appearing in the areas that had been identified by the fatigue tests in England.

(ii) Any other areas showing signs of fatigue cracks or fretting, which might lead to consideration of inspection procedures to be adopted during the testing programme.

(iii) An X-ray inspection procedure for examination of the lower spar boom at Rib 2.

The careful dismantling and detailed examination showed:

(*a*) looseness of the inboard five or six corner screws of No. 1 tank door along the main spar and root rib, and a similar number of corner screws of No. 2 tank door along the spar and forward along Rib 2;

(*b*) elongation of the screw holes detailed in (*a*);

(*c*) heavy fretting between the mating surfaces of the fuel tank doors and flanges at the area detailed in (*a*);

(*d*) fatigue cracks in the spar web at the end of the flange slot at Rib 2 (failure 4B, Fig. 1) and also in the outboard corner of the fuel transfer hole at Sta. 1524 (failure 9A, Fig. 1).

The establishing of a radiographic inspection procedure for the main spar at Rib 2 presented a major problem because the wing was 355·6 mm (14 in.) thick at that point and there were numerous heavy steel structural obstacles that could not be removed from the line of sight between the X-ray source and the photographic plate. Hence resolution was impaired, thus limiting the ability to detect cracks.

2.2 Residual Stress Measurements

From the fatigue tests conducted in England it was known that the fatigue failure in the lower spar boom at Rib 2 passed through the holes for the P-K screws attaching the skin to the boom. At this point the boom was bent through an angle of six degrees, and the forming process was known to produce residual tensile stresses on the surface, which would add to the stress concentration factor of the screw holes.

A multi-exposure X-ray back deflection technique[6] was used to evaluate the stresses for a distance of 100 mm on either side of the bend, and these are plotted in Figure 2. Due to the elongated grain structure in the boom, the values given are considered to have an accuracy of only $\pm$ 23 MPa.

Tensile surface stresses of about 40 MPa were found to be present over only a very restricted length of the boom, and the tensile stresses induced by flight loads greatly exceed this value. Hence the contribution of these residual stresses would have little influence on fatigue around the P-K screws.

2.3 Service Load Spectrum

Fatigue meters had been installed in a total of 11 aircraft operating from the three RAAF bases at Williamtown, Pearce and Sale. Analysis of the results obtained was carried out by de Havilland Aircraft Ltd. and was reported in References 7 and 8.

The analysis showed a considerable scatter of fatigue damaging loads from aircraft to aircraft and from base to base, which was mainly due to the different operational roles, and it was thus decided that the test loading spectrum would be based on the average of all fatigue meter readings obtained from RAAF Vampire aircraft.

During the analysis the effect of the ground-air-ground (G-A-G) cycle was estimated to be only $0{\cdot}4^{o}_{o}$, and it was decided not to incorporate this in the test loading spectrum.

2.4 Flight Strain Measurements

A series of test flights was conducted on an instrumented aircraft in order to ascertain the relationship between the strain in the lower spar boom at Rib 2 and the normal acceleration of the aircraft.[9] This information was required in order that a check could be made in the laboratory to ensure that the test was applying the desired bending moment per g at the wing root, and also at Rib 2. The fatigue test conditions were designed to represent the average of flight conditions that prevailed at the three RAAF bases, namely speed 330 knots EAS ($M = 0{\cdot}6$), height 5000 feet, all-up-weight 4536 kg (10,000 lb.) and centre of gravity location 30 mm (0·1 feet) aft of the wing transverse datum. Under these flight conditions the nominal stress in the lower spar boom was estimated to be 27·56 MPa (4000 psi) per g—the corresponding stress for the lighter English aircraft was 26·46 MPa (3840 psi) per g (see Section 8.8).

Details of the method of calibration for these flight tests which enabled measurement of absolute strain, and the values obtained are contained in Reference 9.

3. FORMULATION OF LABORATORY TESTS

Originally it was planned that the Australian tests would be identical with those conducted in England so that the data from both tests could be pooled. However, as preparations for the Australian tests proceeded two difficulties became apparent, the major one being the difference between UK and Australian service load spectrum and the other being the structural variations between wings manufactured in the two countries.

So that the results of the investigations could be directly related to Australian Vampires operated under RAAF service conditions, it was decided to use an average Australian load spectrum as outlined in Section 2.3. In all other aspects the two tests were similar giving the considerable advantage that common fatigue failures produced in the test specimens could be correlated. There were a number of other reasons for this decision including the following:

(i) There did not appear to be a straightforward relationship between the Australian flight spectrum and that from the UK Flying Command, which, for a given acceleration level showed more counts per hour.

(ii) The UK programme load test spectrum was more severe, except at its highest load level, than a stepped approximation to the average Australian flight load spectrum, and it was considered undesirable to conduct at ARL a test which would necessitate adjusting the test result to local service conditions by the use of a factor which could amount to 1·1 or more.

(iii) The spectrum could be considered representative of all RAAF operating conditions.

(iv) Because of the interchange of aircraft from base to base following modification or repair, a fatigue life estimation could not be made for particular aircraft.

NOTE: Fatigue meters were not fitted to every aircraft.

The various flight loading spectra are illustrated in Figure 3 and the example contained in Av. P970[10] has been included for comparison.

Since the average Australian flight spectrum was very similar in shape to the UK test spectrum it was decided also to use six load ranges for the ARL test representation.

The magnitude of each load range was determined by adopting the same number of load applications per load range as used in the UK test. The derivation of the load levels for each load range is described in Appendix II. These loads are listed and compared with UK equivalents in Table 1 and illustrated in Figure 4. Grouping of the load ranges was in ascending and descending order (Fig. 5) to form a block programme sequence of 3560 cycles equivalent to 80 hours of average service flying.

Subsequently for the comparison tests between random and block programmed load

sequences, the load peaks of the programmed loading representation were "randomised" and applied in two specimens. A typical "random" selection of load peaks is shown in Figure 6. The random load controller was designed to select and apply in random sequence the same distribution of peak and trough loads that occurred in the previous block programme sequence. Rotary switches having a limited number of contacts were used to select the load turning points, and the number of such contacts gave to the overall system a periodicity equivalent to 1·3 block programmes. Thereafter, this sequence was repeated unchanged until failure occurred.

The block programme sequence consisted of loads alternately above and below 1 *g* (straight and level flight) and there was a reversal in load direction after each load peak was reached. Inherent in randomising such a sequence was the possibility of selecting, in succession, a number of load peaks of the same sign and also progressively higher in magnitude. Without special precaution the load control system would apply these loads with no change in direction between successive peaks, causing a resultant fatigue damage to the structure as if only one load had been applied of the highest "*g*" value selected. This difficulty was overcome by designing the load controller to return the structure to the 1 *g* level between successive load peaks of the same sign. In this way there was a change in load direction after each load selection. The 1 *g* level was arbitrarily chosen.

An intrinsic discrepancy to arise from this solution of interspersing 1 *g* peaks or troughs between selected turning points of the same sign was the introduction of additional load fluctuations of smaller amplitude than existed in the block programmes. This can be seen in Table 2 where the number of excursions between selected turning points is listed for the random sequence. The load range magnitudes L4 (i.e. P_4–M_4), L5 and L6 in Table 1 for the block programme sequence do not occur as such in Table 2—they are modified in value and redistributed.

When comparing the number of load cycles in Table 1 and Table 2, it must be remembered that they are not equivalent. Table 2 includes the number of excursions between load turning points that occur for 9256 selections while Table 1 lists the number of cycles for each range totalling 3560 cycles and hence 7120 load turning points.

4. TEST SPECIMENS

4.1 General Description

A general view of the port lower surface of a Vampire trainer wing is shown in Figure 7.

The wing consisted essentially of a single spar for carrying the bending loads, with torsional stiffness being provided by a box formed by the spar and the leading edge. Aluminium alloy of the aluminium–copper type was used for the majority of the structure with the exception of steel for the wing to fuselage attachments. Table 3 lists the material specifications of the major structural components of the specimen.

In the design case, normal bending loads were reacted at the fuselage by vertical pins in the steel fittings bolted to the upper and lower spar booms. Chordwise bending was reacted by the spar fittings and a fitting located on the top of the wing root rib. This was attached with a horizontal pin to a fuselage bulkhead situated 660 mm (26 in.) forward of the spar. Vertical shear was carried by bending of the lugs on the spar lower fitting only. Torsion was considered to be reacted by both spar fittings. However, in practice the horizontal pin carried a small proportion of the normal bending and torsion. Undercarriage loads were reacted at Rib 2 and fed forward to the main spar.

All wings tested had been in service for periods of about five years and during this time had accumulated up to a maximum 1215 hours flying.

The wings were mounted on a fuselage which had a wooden skin and bulkheads, but the spar boom loads were transferred by steel cross tubes with forked plugged ends. Fatigue failures in these elements were regarded as relevant, and were reported.

4.2 Specimen Types Tested

To determine the service life of the fleet, 18 trainer "type" wings (semi span specimens) were used (specimens 1 to 17 and 24). These wings were the last to be manufactured for MK31 single seat fighter aircraft, but had been fitted with the strengthening modification at Rib 2 that made them structurally identical to MK35 and MK35A trainer aircraft. This modification

consisted of forged reinforcing brackets at the intersection of Rib 2 with the main spar, and were fitted to withstand the increased weight and demands of trainer aircraft.

Sixteen of these 18 specimens were tested under a programmed loading sequence and the remaining two under random loading conditions. Of the 16 programme load tested specimens, eight were tested with P-K screws attaching the skin at Rib 2, and eight were tested with the Chobert rivet modification No. 792 incorporated. Four of the latter wings had the modification incorporated before testing started, i.e. at an average equivalent service life of 8·5 programmes, and in the remaining four wings the modification was undertaken after 12·5 test programmes had been applied, i.e. at an average equivalent total life of 21 programmes. Two of these modified wings (specimens 13A and 16A) were selected for the boom replacement investigation where testing was continued until failure in the lower main spar boom was imminent. The replacement booms had the P-K screws removed and their holes filled with epoxy resin. Opportunity was also taken at this time to modify and test other areas that were shown by the test to be prone to fatigue cracking.

Five specimens from Mark 31 fighter aircraft of the original fighter design were used to complete the testing of unbroken port or starboard specimens. Because of the structural differences mentioned above they were regarded as making no contribution to the determination of fatigue performance of trainer wings as far as the spars are concerned. However, the fatigue performance of the spars was recorded, and has been tabulated separately from that of trainer wings. Data on failures in other locations were included with the data from trainer wings.

Two Mark 31 fighter fuselages were used alternately for all the wings tested. The steel cross tube assemblies were identical with those fitted to the trainer aircraft with the exception of engine attachment fittings. These fittings did not influence the mode of fatigue failure of the tubes or their forked end plugs.

Appendix I gives further information on the test life sustained by these two fuselages and the "Nene" engine mounts.

4.3 Preparation of Specimens

Prior to the testing of each wing a number of items including all the control surfaces, undercarriages, fuel tanks, pipelines, and other non-structural items were removed so as to facilitate inspections prior to and during the testing. Catapult hooks at Rib 2 had not been fitted to any of the wings tested.

Log books, where available, were examined for relevant information regarding damage and repairs made to the structure during service. The wings were then subjected to an extensive visual inspection for signs of overloading, fatigue cracks, fretting and normal corrosion, particularly in the region of the Rib 2 and spar junction. Some bolts were removed from the spar root end steel fittings to inspect inside the bolt holes.

An inspection was also made in the corners of the fuel transfer hole at Sta. 1524 where cracking had been observed in the long life service wings (Section 2.1 (*d*)). A mirror was installed in No. 2 tank bay opposite this hole so that visual inspections could be made during testing. The tank doors were then replaced and the screws fitted with a thread locking compound.

For specimens 1 to 6 inclusive all the fuel tank door screws were torqued to the manufacturer's recommended value of 11 Nm (96 in. lb.). From specimen 7 onwards till the end of the test, the screws were torqued to a set pattern that was determined from a survey of screw tightness found in service aircraft. This pattern is shown in Figure 8 and consisted of two torque values. Screws along the spar to Rib 5 and forward to the leading edge at Ribs 2 and 5 and aft to trailing edge at Rib 7 were torqued to 4·5 Nm (40 in. lb.). The remaining screws were torqued to 9 Nm (80 in. lb.).

The effect on the test of tightness of the fuel tank door screws is discussed in Section 6.1.2 and again in Appendix III.

Electric resistance strain gauges were attached to the lower spar boom at Rib 2, in order that the strain at this point could be monitored during each test.

4.4 Repair During Test

Fatigue cracks in two locations in the wing were repaired in a standard manner during testing. In the case of failure in the region of the rear spar at Rib 5 an avaliable service repair

scheme was used, and the other at the rear of the wheel well was repaired using conventional repair techniques. The remaining repairs did not necessarily return the structure to the fully factored strength, but sufficient care was taken to allow the fatigue test to proceed without the introduction of undesirable stress concentrations.

4.5 Boom Replacement

As the testing programme progressed a second major fatigue failure was found namely at Rib 1B, having the same life as the failure at Rib 2. Therefore, the modification of replacing the P-K screws at Rib 2 alone would not provide any extension of life whatsoever.

The de Havilland Aircraft Co. (Australia) had previously suggested replacement of the spar boom, omitting P-K screws at Rib 2, in order to extend the life for at least the period already flown. It was decided to investigate the feasibility of this suggestion by carrying out a boom change on two specimens which had previously been tested until collapse of the spar boom was immiment, and then subjecting these wings to further testing.

The opportunity was also taken to increase the fatigue life at Rib 1B by introducing a number of modifications in this region that were agreed to by the parties concerned. The modifications incorporated are shown in Figure 1. Those at B, C, and D were aimed at either inhibiting or delaying the cracking in the shear web flange and reinforcing angle. The change at C was the addition of a chrome-molybdenum steel strap, and at B the reinforcing angle had the vertical flange increased in width. At D the aluminium alloy reinforcing plate at Rib 2 was replaced by a longer steel plate extending from Rib 3 inboard to the root end fitting.

In the region of the root end fitting the changes A, B, and C were designed to reduce the load carried by the spar boom and shear web tongue at the section through the end bolt hole. This necessitated two 4·7 mm (2BA) bolts being omitted, and it was also found possible to remove a third bolt (4·7 mm (2BA)) which further improved the local stress conditions in the tongue. All three bolt holes in the replacement booms for wing specimens 13 and 16 were filled with an epoxy resin to prevent corrosion, as were also the P-K screw holes at Rib 2.

The replacement of the booms was carried out by the manufacturers without the necessity of jigging the wings or reworking them to cater for misalignment of holes.

5. DESCRIPTION OF TEST RIG

5.1 General

In keeping with the aims of the investigation the testing rig followed closely the design of the rig used for UK tests, e.g. the same method of applying load to the wing structure was employed.

A general view of the rig is shown in Figure 9 and a description is given in Appendix II together with the detail design of the rig.

The rig was capable of applying 12 load levels arranged either in pairs during a programmed loading sequence or separately in a randomised sequence.

As described in Appendix III the rig was fitted with various safety devices enabling it to run unattended. Table 4 contains information regarding the overall time involved for each specimen, and also lists the specimen number, maker's serial number, and wing type.

The cycling rate was approximately 25 c.p.m. thus taking 2 hours 20 minutes to apply one programme block, and giving a possible 10·3 blocks in a 24 hour test period. The greatest number of programme blocks applied in any 24 hour period was 8·31 which resulted in a maximum rig efficiency of 80·7%. An overall efficiency of 20·5% was achieved for the 16 wings listed in Table 4 and the total of 1713·3 blocks took 821 calendar days to apply.

5.2 Calibration

As mentioned in Appendix II it was possible to obtain an accurate estimation of the bending moment applied to the wing, by measurement of the strain in the lower cross tube joining the wing spars through the fuselage. However, it was known that the cross tubes would be replaced a number of times during each wing test, and so the base of the outer port side loading jack was constructed as a load transducer to provide a permanent load monitoring station for the duration of the tests.

Load transducers (electric weighing cells) were inserted at various locations in the loading system to verify the accuracy of the rig, and to investigate the effects of friction, which were found to be negligible.

A schematic diagram of the electrical and hydraulic control circuits is shown in Figure 10.

The procedure for both calibration and dynamic load monitoring was to display concurrently the output from the load transducer under the jack, and lines corresponding to calibrated load levels on a 433 mm persistent screen oscilloscope (CRO). The lines representing the load levels were established in a prior calibration run with the electric weighing cells.

During cycling of the wing the load controller was adjusted until the moving trace from the load transducer was bounded by the calibrated load lines of the particular range being applied. During random loading sequences the switching equipment was arranged to display the particular load level being applied, thus enabling attention to be focused on the appropriate load line.

Particular care was taken in the choice of components for the electronic equipment to minimise changes in signal strength. Also the method of multiplexing the input to the CRO enabled all signals to be displayed through a single channel, thus eliminating any differences in gain between signals.

In the early stages of the investigation calibration checks were made at frequent intervals. As the load controller and monitoring equipment proved reliable these intervals were extended to approximately 50 programmes.

6. TESTING PROCEDURE

6.1 First Specimen

A pair of wings (i.e. port and starboard) which had extensive flying service were chosen for the first two specimens so that there was every possible chance of propagating cracks that may have been initiated by service conditions. These specimens were also used for the following purposes:

(i) Correlation of the flight and laboratory strain measurements.
(ii) Checking the loading rig and establishing load calibration and monitoring procedures.
(iii) Development of inspection techniques.
(iv) Ascertaining areas in which fatigue cracking was likely to occur.
(v) Evaluation of radiographic inspection procedures.

During these particular investigations the wings were subjected to a variety of loading sequences not repeated on later specimens. However, all precautions were taken to ensure that the results obtained would be admissible.

6.1.1 Correlation of Flight and Laboratory Strain Measurements

The initial test rig calibration runs revealed a significant difference between the flight and laboratory measurements of the strain in the lower spar boom at Rib 2.

A series of tests was conducted which showed that the strain in the spar boom was directly controlled by the flexibility of the screwed attachments for the removable tank bay doors. The effect of screw tightness on strain in the spar boom is shown in Figure 11, where it can be seen that the strain variation could amount to 43% if all attachment screws were loose instead of being tight.

The load distribution through the structure, which has a large proportion of discontinuous panels with load transfer achieved by screwed connections was also investigated and this is discussed in Appendix III.

6.1.2 Screw Tightness Tests

In order to maintain a consistent load transfer condition into the lower spar boom at Rib 2, tests were conducted to establish how frequently the tank bay door screws should be retightened, or if there was a value of torque which could keep them tight.

In testing specimen No. 1, the screws were first tightened with a hand operated torque wrench to the manufacturer's recommended value of 11 Nm (96 in.lb.). However, the screws

did not remain tight and a pneumatic impact screwdriver was substituted with considerable success. The strain was measured before and after tightening at the beginning and end of the first, third, seventh, and fifteenth programmes, and then at intervals of eight until the fifty-fifth programme. After use of the pneumatic impact screwdriver, there was negligible difference in strain at Rib 2 and it was thus decided to proceed using the 11 Nm (96 in. lb.) value of torque.

However, starting from specimen No. 7 this procedure was changed when results of a survey[11] showed that aircraft were being operated with screws that had loosened to varying degrees. The values of torque used in the test were therefore reduced to simulate service conditions more closely. These values are shown in Figure 8. Checking of screw tightness during subsequent tests is described in Section 6.2.2.

6.1.3 Inspection Techniques

Visual inspection techniques involving the use of a penetrant dye and optical magnifiers were successfully used, particularly if the wing was loaded during the inspection. An "endascope" was used for the optical examination of holes and remote areas.

Ultrasonic equipment was unsuccessfully used to detect cracks emanating from holes in the spar boom, as it was not possible to resolve the "edge effect".

An electric resistance strain gauge was mounted on the spar boom at Rib 2 (see Fig. 12) close to the expected path of the fatigue crack. However, the measured strain from this gauge remained virtually unchanged until collapse was imminent. This could be attributed to a number of factors including the following:

(i) The crack propagated from the aft side of the screw holes in the boom, whereas the gauge could only be attached on the forward side.

(ii) An alternate load path was provided by bolted reinforcing brackets bridging the fatigue crack.

(iii) The boom area amounted to 20% of the wing tension surface, and thus the fatigue crack represented a loss of only approximately 4% in area.

Following failure, the first specimen was completely stripped for inspection. In some cases components were loaded during the examination using dye penetrant which revealed quite small cracks, e.g. 1·02 mm (0·04 in.) long. This inspection provided substantial evidence on where fatigue cracks and other contributing factors, particularly fretting corrosion could be expected to occur in subsequent wings tested.

6.1.4 Radiographic Inspections

Since it was expected that there may be a need to examine the lower spar boom in the region of Rib 2 of aircraft currently in service, a considerable amount of effort was spent in trying to develop a satisfactory radiographic inspection technique using X-rays. A technique was established on a separate wing which minimised the deleterious effect of copper electrical wiring, hydraulic lines, fuel tanks and steel bolts. However, on the first test wing inspections were made at intervals up to the penultimate programme without any indication of the presence of a crack.

On subsequent wings minor changes were made to improve the technique without success, except in one case, where a crack was detected 14·5 programmes before failure.

A record of the progress of these cracks is shown in Figure 12. The table in this figure gives the number of programmes before failure at which each X-ray exposure was taken. Inspection 1 made 14·5 programmes before failure, showed a crack propagating forward from hole 3. Inspection 2 showed that this crack had progressed into an area beyond the sensitivity of the X-ray beam. Examination after failure showed that this same crack had actually joined another crack progressing aft from hole 2. Inspection 3, only three programmes before final failure, detected a second crack progressing aft from hole 3. Subsequently, inspections 4 and 5 show further progress of this crack. The sixth inspection, only 20 cycles before collapse detected a crack propagating forward and aft from hole 4.

The crack that grew fore and aft from hole 1 could not be detected by radiographic means because of structural fittings obscuring the X-rays. Most of the forward crack length was due to overload failure and the amount propagated by fatigue is shown in the sectional view on the left of Figure 12.

The cracks found by the X-ray technique at this late stage were also easily detectable by eye,

and therefore should have been discovered in other specimens at similar stages of failure when X-ray inspections were made. The reason for detection in this case was fortuitous in that the crack propagated at the optimum angle giving maximum density change.

It was not possible during crack initiation to determine the angle of crack propagation. One solution to this problem was to take a number of shots at varying angles. This procedure demanded time and manpower which outweighed the possible results.

On two other occasions crack progress was followed using radiographic inspections. However, in each case the crack had already been detected during a visual inspection without any aids.

X-ray inspections, which were made only in the region of Rib 2, were discontinued after specimen No. 12.

6.2 Subsequent Specimens

Based on the findings of the test on the first specimens a procedure was followed during subsequent specimens in order to:

(i) Determine imminent failure of major components which would require replacement during the test, e.g. wing root fittings and fuselage cross tubes.

(ii) Discover cracks in members that could be repaired without altering the stress distribution along the spar boom from Rib 2 inboard to the root.

(iii) Maintain the initial strain level in the spar boom at Rib 2 by keeping the tank door screws at their appropriate tightness.

(iv) Detect initiation of cracking in the spar boom at Rib 2, and determine rate of growth using a radiographic inspection technique.

6.2.1 Strain Recording

An electric resistance strain gauge was mounted on the lower surface of the lower spar boom toward the leading edge at Rib 2, the only region which was relatively free of holes where the cross sectional area of the boom was approximately 1935 mm^2 (3 sq. in.) in extent (see Fig. 12). Mounting of the gauge was facilitated by removing a small portion of the No. 2 fuel tank bay door (see Fig. 13). The output of this gauge was monitored throughout the test life of each specimen, and a reading was taken at about every five programmes with the wing loaded to 4·5 *g*.

The gauge was used for two purposes, firstly to establish the nominal strain in the boom for each wing, and secondly, to check on the variation in tank door attachment effectiveness during the test.

Gauges were also mounted on the lower cross tube in the fuselage and used for load calibration purposes as mentioned in Section 5.2.

6.2.2 Screw Tightness

The tightness of the tank bay door screws was of paramount importance as mentioned in Section 6.1.2. Hence they were checked at regular intervals and tightened if necessary, with the wing at the 2 *g* ballast condition. This check was usually made in conjunction with a strain recording run.

The screws were installed with a thread locking adhesive to further resist loosening by turning, since the locking provided by the anchor nuts did not remain fully effective. Except for screws along the spar boom at Nos. 1 and 2 tanks, and along Ribs 2 and 5 forward of the spar, the screws remained tight.

6.2.3 Replacement of Fuselage Cross Tube Assemblies

The fuselage lower cross tube assemblies were replaced, either when found to contain a crack in the tube, or when convenient after 70 programmes of testing. This period was derived from a study of the UK fatigue test results. Replacement was necessary because a failure, particularly in the tube, could result in considerable damage to the fuselage, the spar root end fitting, and its surrounding structure.

Carrying out the test programme necessitated the replacement of cross tubes on 18 occasions. Replacement assemblies were obtained from redundant fighter-type aircraft. Delay to the test

programme was minimised by having the replacement cross tube assembly already mounted in a spare fuselage which could be exchanged for the fuselage with the time-expired cross tube assembly without removing the wings from the test rig.

6.2.4 Replacement of Root End Fittings

During the testing of the first wing these fittings were inspected regularly in the 8 mm ($\frac{5}{16}$ in.) diameter bolt holes between the fitting and the spar boom to prevent a failure producing damage to the surrounding structure that would have been difficult to repair.

As the test programme progressed it was found possible to inspect less frequently, and have the replacement of the fitting coincide with removal of the fuselage for cross tube changes. Despite these precautions four fittings did fail out of the 55 involved.

After removal from the wing, all of the fittings were examined using three visual methods to ascertain the extent of fatigue cracking present. The fittings were then loaded to failure and the actual extent of cracking measured.

Further comments on this investigation, in particular the inspection methods, are contained in Appendix I.

6.2.5 Crack Propagation at Rib 2

Since one of the main aims of the test was to investigate the effectiveness of replacing P-K screws with pinned Chobert rivets, it was necessary to establish the rate of crack propagation in the spar for both types of fasteners so that an assessment could be made of the optimum time and effectiveness of the replacement. It was not possible to quantitatively determine crack propagation during the test (refer Sections 6.1.3 and 6.1.4) because the methods used were ineffective.

However, after failure, a fractographic technique was used by Barnard and Hooke[12] to obtain crack propagation information relating to screw-holes in the spar boom at Rib 2, and to holes in the root-fittings.

Briefly, the technique involved photographic enlargement of the fracture face and measurements of the position of successive "bands" or "tide marks" which marked the position of the crack front at successive programmes. These bands could be traced back to the very early stages of the crack growth. Confirmation of reliability of the technique was obtained by comparison of the results with those obtained on the very few occasions when the crack was visually detected during the test, and also by the introduction into the test sequence of double-length and half-length programmes, whose effect was reproduced on the fracture surfaces. Further confirmation was obtained from an electron microscope mosaic technique by which the propagation of cracking by individual load cycles of the programme could be identified.

6.2.6 Chobert Rivet Modification

The principle of the de Havilland modification No. 792 was to replace P-K screws with pinned Chobert rivets. In so doing a blind hole was drilled to a pre-determined size that would guarantee removal of all fatigue damaged material surrounding the screw hole and also permit the fitting of a pinned Chobert rivet.

As stated in the introduction, there were two aims to be achieved in relation to the Chobert rivet modification. The first was to establish the fatigue life using this modification, and the second was to ascertain when it should be incorporated. Another inherent requirement was to establish the life of wings that had already been modified in service after 1000 hours flying.

The first aim was achieved by modifying four wings (Specimens 9, 10, 11, and 12) before testing started so that the effect of the modification alone could be evaluated.

The second aim was attained by making a crack propagation study[4] of the fracture faces of unmodified wings to determine how long the modification could be delayed and still be sure that all damaged material around the P-K screw hole was removed when the hole was enlarged to take the pinned Chobert rivet.

The third requirement was achieved by testing four specimens (Nos. 13, 14, 15, and 16) under prevailing service schedules, i.e. delaying the modifications until 12 test programmes (equivalent to 1000 flying hours) had been applied.

7. TEST RESULTS

All the failures that occurred during the testing of the 23 specimens are described in this section, and they have been classified as follows:

Major failures—Fatigue cracking which if not detected shortly after initiation would result in the structure not being able to withstand proof load, i.e. 6 *g*.

Minor failures—Failures which either propagated slowly or were easily detected, and in any case did not result in a significant lowering of strength.

Rivet failures—Areas where rivet failures occurred in most specimens.

The six areas of major failure, six areas of minor failure and seven areas of rivet failures are described in Tables 5(*a*), (*b*), and (*c*) respectively. Figures 1, 7, and 8 show the location of failures that occurred in the lower surface of the wing, while Figure 14 shows failure locations in the cross tube assembly, and Figure 15 the failure locations in the wing root fitting. In Tables 6, 7, and 8 full details are given concerning lives, failed areas, stress per *g*, etc., for the spar boom failures.

7.1 Major Failures

7.1.1 Cross Tube Assembly

Details of the amount of fatigue damage found in the cross tube assemblies used during the investigation are given in Table 9 and typical failures are shown in Figure 14.

It was not intended that collapse of any portion of the assembly should occur during the test (refer Section 6.2.3), the only exception being on one occasion when it was planned to provide data on crack growth during the last stage of fatigue. The results of this test are illustrated in Figure 16.

However, scheduling of the test resulted in assemblies being fatigued beyond the 70 programmes as proposed in Section 6.2.3 which resulted in two complete failures occurring in the tube, six in the upper lug, and one in the yoke plug end. The latter failure was initiated by a deep internal circumferential machining score passing through the centre of the two innermost attachment holes.

7.1.2 Wing Spar Lower Root End Fitting

A total of 55 root end fittings (REF), i.e. the steel fitting joining the main spar lower boom to the fuselage lower cross tube, were used during the investigation (see Table 3 for material specification). Of these, five failed completely, and a further 48 were found to be cracked after removal. In all cases the fatigue cracking originated from the two 8 mm ($\frac{5}{16}$ in.) diameter holes which were the inboard connection between the boom and the fitting as shown in Figure 15 (failure type 2). Following removal from the rig, those end fittings not broken in the test were statically loaded to failure and the fatigued areas were measured. The distribution of life (total = service and test) up to removal from the test rig is presented as a histogram in Figure 17. For each specimen represented in the histogram, the percentage of the nett cross sectional area which was cracked by fatigue is given in brackets. For each class interval of life in programmes, the mean percentage of area fatigue cracked is tabulated along the top of the diagram.

The fracture faces were also examined similarly to the spar booms at Rib 2 (Section 6.2.5) using fractographic techniques to obtain crack propagation data which has been reported in Reference 12.

7.1.3 Main Spar Assembly at Rib 1B

The prime failure point in this region was in the lower spar boom at the outboard REF attachment bolt hole failure 3A, Table 5.

During the test programme four wings collapsed at this location, where the load transfer is maximum in the spar boom, and all others were subsequently found to contain cracks. The mean life to collapse in this area was 103·6 programmes or 8288 hours (Table 7). A typical spar fracture face is shown in Figure 18 and a view of the lower surface at Rib 1B after failure is

shown in Figure 19. The measured fatigue areas at Rib 1B, whether collapse occurred there or at Rib 2, are given for all wings together with their total lives, in Tables 6 and 7.

Associated with the prime failure 3A in this region at Rib 1B were five other failure points in the adjacent web structure, namely 3B, 3C, 3D, 3E, and 3F, described in Table 5. Details of the amount of fatigue present at each point on termination of the test, and the extent to which they had failed are contained in Table 10. An illustration of the wing structure in this region (including boom replacement modifications), is provided in Figure 1.

7.1.4 Main Spar Assembly at Rib 2

Of the 23 specimens tested 18 failed completely in the lower spar boom at Rib 2. The mean life to collapse in this area in unmodified wings was 125·4 programmes, or 10,032 hours, and in modified wings was 106·2 programmes, or 8498 hours (Table 7). All the fatigue fractures passed through the P-K screw or Chobert rivet holes towards the rear of the boom immediately outboard of Rib 2.

The fractures did not always follow the same path across the boom, and Figure 20 shows two typical fracture faces, one through P-K screw holes alone and the other where the crack has diverted outboard into the neighbouring 9·5 mm ($\frac{3}{8}$ in.) diameter bolt hole. The characteristic "bands" or "tide marks" associated with the crack front in programmed loading sequences are also clearly seen in this figure.

An external view of the wing in this region is shown in Figure 13.

The fatigue lives and amount of fatigue damage sustained are contained in Table 6 for wings in the unmodified condition, and for modified wings in Table 7. Similar data obtained during testing of the Fighter type wings is contained in Table 8.

There were two more failures in this region as given in Table 5, one at the end of the slot in the shear web flange that extended up the spar web (4B), and the second in the aluminium alloy reinforcing strap (4C) that bridged the slot as shown in Figure 21. The latter failure also occurred in the extended steel strap fitted with the replacement boom (4D) as shown in Figure 1. These cracks could not be detected during the test. Table 11 lists the extent of fatigue cracking for these areas as measured on dismantling at the end of the test, and shows that fatigue cracks (type 4B) of various lengths were present in the shear web of every specimen except specimen No. 15. Slight cracking (type 4C) occurred in only two aluminium alloy straps, with 20% cracking in a third, whereas in the boom replacement specimen No. 13 the lengthened steel strap had completely failed by fatigue.

7.1.5 Butt Straps

The structural components transferring loads from the removable tank doors (Nos. 2 and 3) to the adjacent skin structure have been termed "butt straps". Fatigue cracking occurred at four such locations as listed in Table 5 (failure type 5) and shown in Figure 8.

However, these cracks proved to be not critical as in no case did they cause collapse, even at the highest load of the programme, viz. 6·55 g.

Cracks were found to occur or to have occurred in every specimen, except one, at the connection of Rib 5, and the No. 3 fuel tank door (failure 5D). The cracking started opposite each tank door attachment screw hole along a line which coincided both with a shallow bend line, and the edge of a skin panel. In some instances the cracks had grown together before the butt strap was removed, as shown in Figure 22.

In nine specimens (Table 12) cracks were observed late in the test life, and were repaired using a standard repair scheme. (Three of these repairs utilised straps removed from other wings.) No repairs were made to the other specimens. Tables 12 and 13 contain details of the amounts of fatigue cracking present when the straps were removed from the wings either at repair or final failure.

The remaining three type 5 failures (A, B, and C) occurred in four wings, of which two had been used for the spar boom replacement tests. From Table 14 it can be seen that in the four specimens cracking occurred in the butt strap (5B) forward of the spar at Rib 5, while at the same station in two specimens, cracking also occurred in the doubler plate (5C). A temporary repair executed on specimen 13 successfully retarded the fatigue cracking during the last 55 programmes. No repairs were effected on specimens 11, 14, and 16.

7.1.6 Rear Spar at Rib 5

Failure of the rear spar at Rib 5 (type 6) (see Fig. 8 and Table 5) occurred in the first three specimens tested, and did not appear again except in specimens 12 and 24.

This failure also occurred in service and was attributed to a high local stress produced by the presence of the dive brake hinge bracket loads. A standard service repair was available and it was considered unnecessary to let this type of failure develop if found during the tests. For the first seven specimens, test loads were applied to the structure through this hinge bracket. Subsequently the testing rig was modified, and the load acting downwards was distributed by means of a pad on the upper surface. Upwards loading was still applied directly to the fitting. Strain gauge readings on the lower flange of the rear spar did indicate a reduction in stress level achieved by this method of loading, and the modification was reasonably successful in delaying further failures.

The five results are shown in Table 15.

7.2. Minor Failures

7.2.1 Lower Skin between Rib 1 and Rib 2

There were two failure regions between these two ribs, one region (type 7A) was associated with the counter-sunk bolt holes parallel to and forward of the root end attachment fitting of the lower spar boom. The other region (type 7B and 7C) occurred in the aft outboard corner of an access hole located in the leading edge skin of starboard wings only. Both these regions are shown in Figure 8.

Failure type 7A is shown in Figure 23 and was present in 10 specimens. In seven cases the cracking had been initiated from all of the fourteen 6 mm ($\frac{1}{4}$ in.) diameter counter-sunk bolt holes and in three cases had propagated until there was one continuous zig-zag crack. This crack did not show any pattern in initiation nor was it peculiar to any test condition or type of wing. Fatigue lives for initiation of this failure were not recorded, and repairs were not made to any of the wings affected.

Fatigue cracking in failure types 7B and 7C emanated from the aft outboard corner of the access hole. It was not extensive and only occurred in two specimens. Repairs were deemed unnecessary.

7.2.2 Spar Assembly at Outboard Rocket Mount

Fatigue cracking occurred in the flange of the spar web at the location of the two mounting bolts for the rocket mount, and then mainly at the inboard bolt hole. These fatigue cracks are marked 8A and 8B in Figure 1 together with the fatigue crack 8C that initiated in the steel reinforcing strap fitted with the replacement booms. The location of these cracks was not inspectable during the test. There was no fatigue cracking found in any spar boom at this location.

The extent of the cracking in the spar web flange was quite small, except in two cases as given in Table 16, both from the same aircraft which had been subjected to a "wheels-up" landing.

7.2.3 Main Spar Web at Sta. 1524

The web of the main spar contained a "D"-shaped hole outboard of Rib 2 at Sta. 1524 to accommodate a fuel transfer pipe. From the outboard corner of this hole, fatigue cracks (failure type 9) propagated across the web flange in 21 of the 24 specimens tested. Cracking at this same point had been detected in wings inspected in service (see Section 2.1 (*d*)).

Figure 1 illustrates the position of failures 9A and 9B. The life to detection and the extent of the cracking produced during testing of each specimen is contained in Table 17. Failure type 9B refers to cracking of the steel reinforcing strap fitted to boom replacment wings only. It is to be noted that these cracks could be kept under observation during the test by viewing in the inspection mirror referred to in Section 4.3. In most cases this was the first crack to appear in a specimen, and thus it was very useful in initiating the inspection schedule during the test. None of the cracks was repaired.

7.2.4 Failures in Long Life Specimens

The two specimens in which booms were replaced contained three failures, types 10, 11, and 12 in Table 5, which were not observed to occur in any other specimen.

One failure, type 10, was in the flange of the main spar shear web at the hole for a fuel transfer pipe, just outboard of Rib 5, and it occurred in both wings.

The other two failures, types 11 and 12, occurred only in specimen 16 which endured a total life of 316 programmes. The type 11 failure consisted of a crack in the lower skin aft of the wheel well at Sta. 2248 which was allowed to propagate 133 mm (5¼ in.) before being repaired at 261 programmes. Figure 24 shows the extent of the repair and also illustrates the path of the crack before repair was made.

Failure type 12 occurred in the upper surface skin along the row of counter-sunk bolt holes at the rear of the root end fittings. These cracks were first detected at 263 programmes and advanced to the stage shown in Figure 25 by the end of the test.

7.3 Rivet Failures

There were very few rivet failures during testing, and they were confined to the seven areas as given in Table 5. Failures in the first three areas occurred in most wings, whilst those in the remaining four areas were only present in the long life boom replacement specimens. Examples of rivet failures can be seen in Figures 8, 13, 24, and 25. Failed rivets were not repaired.

7.4 Strain Measurement

The strains measured in the cross tubes showed virtually no variation between any of the tubes employed during the investigation, and thus proved that this member was an ideal choice for calibration purposes. The average value of strain per g was 300 micro strain which corresponds to a stress of 62·01 MPa/g (9000 psi) in this steel member.

By contrast, the value of strain measured in the lower spar boom at Rib 2 varied by a significant amount. For each specimen the strain varied slightly during the fatigue life, and this was related to variations in the tightness of the screwed connections as illustrated in Figure 26. However, between each specimen there was a considerable difference in the average stress value as shown in Tables 6, 7, and 8 for unmodified, modified, and Fighter type wings respectively.

Strains were measured at a number of other locations in the structure for the purpose of further investigations associated with calibration of the test rig, and as such, they have not been included in this report.

7.5 Replacement Boom Specimens

The two specimens 13B and 16B which had the lower spar booms replaced, both failed at Rib 2; however, fatigue cracks were also present at Rib 1B and other locations. The lives of the two replacement booms, are contained in Table 6 along with the other unmodified booms. Both these replacement booms had been removed from wings that had flown and hence had existing P-K screw holes at Rib 2. These screws were not fitted and the holes were filled with epoxy resin.

These two specimens were amongst those which suffered only a small amount of fatigue damage in the shear web assembly in the region of Rib 1B, and the actual fatigued area is given in Table 10. The amount of shear web flange cracking in the region of Rib 2 can be obtained from Table 11 by reference to specimens 13 and 16 at the bottom of the table. Butt strap failures at Rib 5 aft of the spar (failure type 5D) are given in Tables 12 and 13 and those forward of the spar (type 5A, 5B, and 5C) are contained in Table 14. Shear web flange cracks also occurred at Sta. 1219 and 1524 and the extent of these failures, types 8B, 8C, 9A, and 9B, is given in Tables 16 and 17.

8. DISCUSSION OF RESULTS

Final collapse of all wings tested resulted from failure in the lower spar boom either at Rib 2 or Rib 1B. At Rib 2 the failure originated from P-K screw holes in unmodified wings and from the same holes with Chobert rivets in modified wings. Failure at Rib 1B was at the further-

most outboard bolt hole of the six used to attach the steel root end fitting to the boom. At this point in the boom the end load was a maximum.

Cracking initiation in the spar at both Rib 2 and Rib 1B was detectable during the test by using unsophisticated visual means.

The only locations in the wing itself where cracking was observed and repairs made during the tests were in the butt straps at Rib 5 (in nine wings) and in the rear spar at Rib 5 (in three wings). All other failures were minor in their effect on the fatigue performance of the wing and their slow cracking was permitted to grow unchecked.

8.1 Spar Boom Failures

Evidence obtained from the UK tests on three wings revealed only one failure area in the wing, namely through P-K screw holes in the main spar at Rib 2.

However, the ARL tests showed that catastrophic failure could also occur at Rib 1B and at a similar life. Four specimens (all modified wings) failed in this new location, the first being No. 9 followed by Nos 10, 12, and finally 15. Fatigue, in varying degrees, was present in all other wings at this same point.

As mentioned in Section 6.1.2, a reduction was made in the torque value applied to the screws that attach the fuel tank skin panels to the spar boom in order to more accurately simulate service maintenance.[11] This reduction was from 11 Nm (96 in. lb.) to 4·5 Nm (40 in. lb.) and was first applied to specimen 7.

Table 18 shows the statistical comparisons that were made between the four test variables —two relating to the structure, i.e. modified and unmodified, and two relating to screw tightness, i.e. loose or tight. Unfortunately no modified wings were tested with tight screws and only two unmodified wings were tested with loose screws.

Primary comparisons were made between structural variations (modified or unmodified) that had similar conditions of screw tightness (i.e. screws loose), and between fastener variations (tight or loose) in wings that were structurally similar (i.e. unmodified). The results (Table 18) show that there were no significant differences in the means or standard deviation for either of these primary comparisons. The test data were then pooled to give larger populations so that secondary comparisons could be made, firstly between modified and unmodified structures and then between structures with loose or tight screws.

The secondary comparisons (Table 18) between modified and unmodified wings showed that there was a significance in means but no difference in the standard deviations. This is further discussed later. However, the secondary comparison between the condition of screw tightness showed that while there was still no significant difference in the standard deviations there was a highly significant difference in the means. This influence of screw tightness is also indicated by the increase in average strain recorded at Rib 2 for wings tested with screws torqued to the lesser value of 4.5 Nm. Figure 27 shows the relationship between average stress measured in the boom at Rib 2 and fatigue life to collapse for specimens 1 to 16A. The mean average strain for specimens 1 to 6 was 440 micro strain per g while that for specimens 7 to 16 was 514 micro strain per g, which is 16.8% higher. From Table 18 (Secondary Comparison—Pooling) the difference in log mean life between these two same groups of screw tightness is 130 programmes (10,400 hours) for specimens 1 to 6 and 107·4 programmes (8592 hours) for specimens 7 to 16A.

Screw tightness also had some influence on the area of collapse. This was particularly so at Rib 1B where no collapse had occurred in wings with tight screws even though cracking was established in all of these specimens. At this wing station the root rib intersects with the spar boom. Screws in this corner feed load into the spar adjacent to the root-end-fitting. When they loosen, more load is fed into the boom outboard of this alternative critical failure area and hence the damage rate there is accelerated.

In comparing modified with unmodified wings the results are not conclusive. Only one primary comparison could be made namely, with loose screws, of which there were two unmodified specimens and eight modified. When the data with different screw tightness were pooled giving eight specimens in each category the log mean life of the modified wings was significantly different and lower. The result is, however, confounded by the lack of data for modified wings with tight screws, which could have increased their log mean life in the same way that tight screws gave a higher mean life for unmodified wings 1 to 6. On balance the results are interpreted to

show that the modification at Rib 2 in which P-K screws were replaced by pinned Chobert rivets had no beneficial effect on the fatigue life of the spar. There appeared a reduction in the scatter of results, but this was not statistically significant.

The other main factor relating to the modification at Rib 2 was when it was to be done. The test results showed no influence on the total life to failure for either of the two conditions at which the modification was introduced, i.e. at the beginning of testing or after 12·5 programmes of testing (equivalent to 1000 hours of service flying). One reason for this could be that the separation of 12·5 programmes—which is 12% of pooled log mean life of modified wings—is within the accepted scatter band for fatigue testing of full-scale identical structures.

The mean life at Rib 2 was lower for modified wings, but not significantly so—an increase had been expected as a result of removing the self-tapped thread and replacing it with a reamed hole filled with an interference fit rivet. The lower life, or no increase in life, could perhaps be attributed to the deleterious effect of fretting which was found to be present in Chobert rivet holes. This apparently resulted from the smaller interference fit of the rivets as compared with that of the self-tapping screws which has also been reported in Reference 3.

The findings of the work to assess when the pinned Chobert rivet modification was to have been incorporated have been reported in Reference 4. This work, based on limited crack propagation data, showed that the modification should be carried out no later than 980 service flying hours. When done at this time, then there was a 1 in 1000 probability of having removed all fatigue damaged material from around the area of the P-K screw holes.

There is then one significant factor, namely screw tightness, that influences the fatigue life of the main spar in the two catastrophic areas at Rib 2 and Rib 1B. However, while tight screws gave an increase in life in laboratory testing it was not a practical assumption that this condition would be universal in squadron service. Specimens 7 to 16 were representative of average service conditions and therefore the log mean life of these wings provides an appropriate base for service life estimation.

8.2. Spar Boom Replacement

In Section 4.5 the reasons for a main spar boom replacement, along with the additional modifications to the structure surrounding the critical areas at Rib 2 and Rib 1B, have been discussed, together with the test procedure that followed in which two wings were fatigue tested until failure was imminent.

The modifications proved satisfactory for specimen 13, and very satisfactory for specimen 16 for which the life of the replacement boom was some 62% greater than the log mean life for unmodified wings. In addition the surrounding structure in specimen 16 was subjected to a total of 316 programmes (equivalent to 25,280 flying hours) thus giving ample opportunity for all failures to appear. It should be noted that the wing structure of specimen 13A suffered an unplanned spar boom failure at Rib 2, whereas the fatigue testing of specimen 16A was halted when failure was imminent. In the region of Rib 2, cracking had occurred in every specimen tested at the end of the web flange slot (failure 4B, Fig. 1), while only three of the reinforcing straps (failure 4C, Fig. 21) had shown any cracks, and the largest of these (specimen 2) only represented 20% of the strap area. In specimen 13 the fatigue damage at the end of the web flange slot was the second highest observed, and in addition the steel replacement reinforcing strap had failed completely. In the other specimen, No. 16, which withstood the longest life on any specimen tested, there was an average amount of cracking in the web and none in the steel strap.

The opportunity was also taken during the boom replacement investigation to strengthen the areas around the cut-out for the fuel transfer pipe at Sta. 1524, by extending the steel replacement reinforcing strap outboard to Rib 3. A true assessment of this modification could not be made because the flange had been partly failed in specimen 13A and completely in specimen 16A. However, in the continuing testing of specimen 13B the fitment of the steel strap proved most successful in that there was no further cracking in the web flange of that specimen.

The boom replacement scheme was successful in ways other than those which overcame, to a large extent, the fatigue weaknesses of the original design. It proved to be a relatively simple engineering task for this type of structure requiring no re-jigging. It also gave knowledge of the

behaviour of a fabricated wing structure at an extended fatigue life, and provided practical proof of the unique benefits that accrue from representative full-scale fatigue testing, in that modifications, be they major or minor, can be substantiated both in their engineering possibility and their operational achievement.

8.3 Effect of Loading Sequences

As previously discussed in Section 3, two wings were tested, for comparison, under a random load sequence. Section 2 of Appendix I gives further discussion on two reasons that also influenced the decision to test under a randomised load sequence.

The two specimens (17 and 24) used in this investigation were unmodified wings with screws tightened to represent in-service conditions, i.e. "loose".

The only true comparison that can be made is that between the results with these specimens and the results from specimens 7 and 8 under programme load with screws "loose". This comparison shows no significant difference in means or standard deviations of the fatigue lives to failure. However, a further comparison, supported by the statistical facts of Table 18, was permissible with specimens (7 to 16) of similar screw tightness, although structurally different. This comparison also showed no significant difference in means or standard deviation. In addition to the similarity in the fatigue life, these random load sequence specimens showed no changes in the amount or location of fatigue damage nor in the chronological order of its detection. For these reasons there appeared no need to test more than two wings.

This similarity between the lives to failure and locations of fatigue damage between the two sequences supports the conclusions of Payne[13] on Mustang wings and is generally similar to the findings of Schijve[14] for 7075 Al. Alloy tension skin wing panels, that a suitably proportioned programmed sequence will adequately represent a random sequence of the same loads.

Perhaps one explanation for this similarity is the fact that there was a considerable number (over 100) of programme blocks and over 75 repetitions of the random sequence before failure occurred. Other investigations have shown that if the number of programme blocks to failure is only 10 to 20, then there is no agreement with random loading sequences.

It must be remembered that the only factor that was changed in this aspect of the investigation was the sequence, resulting in a slight increase in the period of repeatability for the random sequence (which was 1·33 times that of the block programme sequence). This randomisation of block loads was not designed to represent an actual service flight-by-flight sequence in which periodic load cycles occur, e.g. flaps, landing, taxying and the predictable grouping of loads in particular flights. However the results could be expected to be the same if a flight-by-flight arrangement of the *g* spectrum had been applied.

8.4 Fatigue Crack Initiation and Propagation

The fatigue tests conducted in the UK revealed that fatigue cracking of the wing structure occurred in two locations only, and both at Rib 2, one being the main spar boom and the other the shear web.

In the Australian tests crack initiation at Rib 2 could be reliably observed during testing, but not so in the shear web. However, another crack (9A) was found in the cut-out for the fuel transfer pipe through the shear web at Sta. 1524, and in most specimens this was the first crack to appear in the wing structure. The initiation of this crack could be detected visually with the aid of a mirror. It started from the outboard corner and progressed via holes aft across the web flange (Figs. 1 and 21).

As can be seen from Table 17 cracking at this point was considerable in all wings. In some wings (6, 10, 19) it was detected as early as 30% of the test life.

Opportunity was taken in the boom replacement wings to alleviate this fatigue weakness in the web flange by replacing the existing aluminium alloy strap with a steel strap and extending it beyond Sta. 1524 (see Fig. 1). This modification proved only partly successful in as much that the steel strap virtually stopped further cracking in the flange by taking most, if not all of the load and as a consequence was totally failed in both specimens 13B and 16B.

As can be seen from the results contained in Table 17, the log mean life to detection of 46·6 programmes was about half the un-modified wing life of 131·2 programmes (Table 6, Note 2) and 105·3 programmes (Table 7, Note 2) for the modified wings.

Fatigue cracking of the main spar boom at Rib 2, in the case of the unmodified wings, invariably initiated at the P-K screw towards the rear of the boom. The cracks did not necessarily form at the stress concentration produced by the intersection of the hole and the spar surface. Examination of booms after failure produced evidence (see Fig. 28) that they originated at the peak of the thread.

The band markings on the boom fracture faces were counted in many instances, and they could be related to the number of programmes applied. Using the proven assumption that each band represented a programme, it was ascertained that cracking commenced early in the test life. However, it was extremely difficult to count the bands close to the origin of the crack and reference to Figures 20 and 28 shows that in the last three or four programmes the area of damage grew rapidly. Despite these difficulties with the technique, crack propagation in the spar boom and notched specimens of similar material has been examined, and reported in References 12 and 15. The rate of crack propagation in the spar boom was about $0{\cdot}02\%$ of the nett area for at least 50% of the fatigue life, which is quite a low rate.

Initiation of the fatigue crack at Rib 1 in both the spar boom and steel root end fitting could be attributed, in most instances, to fretting between the bolt and hole surface.

The fatigue cracks occurring in the butt straps were difficult to detect during testing since they coincided with the edge of a skin sheet, and hence the information contained in Tables 12, 13, and 14 was obtained following removal of the butt straps at the end of the test.

8.5 Butt Strap Failures

The failures (type 5A, 5B, 5C, and 5D) in the various butt straps presented a problem, as mentioned in Section 8.4, in that their detection was difficult. In type 5D the crack had many origins (see Fig. 22) which continued to grow individually and concurrently, producing rapid propagation as interconnection took place.

Of these four failure types or locations, type 5D (Tables 12 and 13) was by far the most common, being present in all but one specimen (specimen 18). This was a known service failure and a standard repair scheme existed. As mentioned in Section 7.1.5 this repair was successfully carried out on nine specimens.

In addition no wing collapsed (maximum load $6{\cdot}55\,g$) at this location even though the extent of cracking in the butt strap in five specimens had reached over 70%. However, the test load distribution was not representative of a rolling manoeuvre case, and hence the obvious reduction in torsional stiffness of the wing was not demonstrated. It is therefore most important to note that the test results do not confirm an adequate margin of safety, with type 5D cracking present, for other than the test load condition.

All other butt strap failures (5A, 5B and 5C) occurred in four wings (Table 14), two of which were boom replacement wings and hence long life specimens. Of these, type 5B (junction of fuel tank panel with Rib 5) was most advanced and occurred in all four wings. It must be noted also that if this type of failure occurred in conjunction with type 5D it would further reduce the torsional stiffness of the wing structure.

8.6 Cross Tube Assembly

As mentioned in Sections 6.2.3 and 7.1.1, no direct fatigue data was sought, because of possible damage being caused to the critical inboard end of the lower main spar boom, and also to the two valuable fuselages. However, some data was obtained from assemblies which did fail during the tests.

A crack propagation curve for specimen T4 is shown in Figure 16 from which the fatigue life to collapse was estimated for all the partly failed steel tubes (failure type 1A) used in the test. The log average of both the actual and estimated lives to collapse was $89{\cdot}3$ programmes, Table 9.

During the test it was not possible to detect cracking of the upper lug (failure type 1C) of the lower fork end fitting which accounts for the inadvertent failure of six of these fittings. Table 9 shows that only one other fitting (specimen T11) had partly failed during test. All the other lugs were either not cracked or were completely failed. The log average of the six complete and one estimated lug failures was $76{\cdot}5$ programmes.

8.7 Spar Root End Fittings

For similar reasons given in Section 8.6, the life to failure of the root end fittings was not a prime aim of the investigation. Indeed failure of one fitting of the five that did inadvertently fail during test caused considerable local damage to the wing structure. Generally fittings were therefore replaced before they collapsed.

Detection of cracks in the two 8 mm ($\frac{5}{16}$ in.) diameter holes (Fig. 15) was difficult because it was not always possible to remove the bolts for inspection of the holes. When this was possible and cracks detected, then the fitting was removed. Otherwise fittings were removed at any time convenient to the test schedule, e.g. an early fitting replacement could result from the convenience of combining it with a cross tube assembly replacement, or to give an uninterrupted test run to fail a specimen before a weekend, etc. As a consequence fittings were changed at times ranging from 20 to 110 programmes (see Fig. 17).

All fittings used during the test had been removed from service aircraft (a relatively simple task) as part of an established replacement schedule. Following their removal from the fatigue test specimens, they were inspected and then broken by static overload after judicious saw cutting, and the amount of fatigue cracking sustained during the test was measured. These results are shown as a histogram in Figure 17 which also shows that, on average, fatigue crack size at removal increased with time to removal. No attempt was made to estimate the life to final failure, but some indication can be drawn from the histogram using the data for the five fittings that completely failed, namely, that collapse was imminent after 85 programmes (6000 hours) or when over 50% of nett tension area had fatigued.

8.8 Comparison of UK and Australian Test Data

Initially it was envisaged that the Australian test would follow in detail that conducted in England, and results from both investigations would be pooled. For a number of reasons as outlined in Section 3, it was found necessary to depart from this plan and apply loads representative of Australian service conditions. Subsequently sufficient Australian specimens were tested which enabled the results to be analysed without inclusion of the overseas data. Nevertheless, the UK test results were used in the early stages of the investigations to supplement Australian data as it was being accumulated.

Since the UK tests were based on a lower aircraft AUW, it was estimated that the nominal stress in the lower spar boom at Rib 2 was 26·46 MPa (3840 psi) per g, as compared with 27·56 MPa (4000 psi) per g for the heavier Australian aircraft (see Section 2.4).

As a basis for comparison the fatigue damage was calculated for each AUW case using a linear damage hypothesis and the alternating stress–mean stress diagram for 24S-T structures contained in Reference 13, and the test lives adjusted accordingly. The service lives were converted on the basis of the aircraft being subjected to the same loading spectrum at the higher all-up-weight.

Before a direct comparison of results can be made, it must be remembered that there was a change in the Australian investigation after completion of the sixth unmodified wing (Section 6.1.2) in which the tightening torque applied to the fuel tank door panel screws was lowered to simulate service conditions more closely. As discussed in Section 8.1, this change proved to be fundamental in that it significantly shortened the life to failure of the wing.

No such change was made during the UK tests. The test report[1] mentioned screw looseness problems within application of 12 load programmes to the first wing tested. Subsequently the screws were checked and tightened after every programme. No mention was made of the tightening torque applied to the screws, but it is reasonable to assume that the manufacturer's specified figure of 11 Nm (96 in. lb) was used. A comparison could therefore be made between the two unmodified UK specimens and the first six unmodified Australian specimens on the basis that they were similar in structural detail and screw tightness.

The UK test report also stated that the rate of screw looseness increased as the test proceeded. During testing of the first Australian unmodified wing (Section 6.1.2) a similar problem occurred while using a hand-operated torque wrench. This was overcome by use of a pneumatic impact screwdrive, resulting in the maintaining of the correct load distribution through the wing structure. The most likely conclusion to be drawn from this is that the screws in the first six Australian wings remained tight for longer periods during test than did their counterpart in the

UK tests, and hence would lead to a longer life in Australian wings. In Table 19 are the test results which show a log mean life of 130 programmes for Australian unmodified wings and 71·7 programmes for wings tested in the UK. Table 19 also compares the results for modified wings. It is difficult to draw any direct conclusion from these results. The screw tightness of the eight Australian wings was maintained "loose". However, the log mean life of these eight is very close to that of the two UK wings in which it must be assumed the screws were "maintained" at the manufacturer's specified tightness. An explanation for this could be that for the tests on modified wings the screws in both countries were of similar tightness, i.e. "loose". If this be true, then the screws in the UK unmodified wings were "loose" also, and hence would explain why those wings had a much shorter fatigue life than Australian produced wings with tight screws.

This analysis leads to the fact that there is no real evidence to support a difference between the fatigue lives obtained in the UK or Australian tests, for either modified or unmodified wings.

8.9 Effect of Local Strain on Life

The UK tests revealed that fatigue cracking would occur in the main spar lower boom at Rib 2. Strain data at this station were recorded at regular intervals on every ARL specimen.

Another important reason for regular strain recording (Section 6.2.1) was to monitor the effect of screw tightness. The recording showed little variation throughout the test of each specimen. However, between specimens there was considerable variation in the average strain per g resulting in stresses* ranging from 24·83 to 40·90 MPa (3600 to 5940 psi) per g (Tables 6 and 7) for all wings tested. The nominal stress at Rib 2 estimated from the flight tests was 27·56 MPa (4000 psi) per g (Section 2.4).

The relationship between the average stress per g and fatigue life for the 16 specimens with tight and loose screws is shown in Figure 27. This figure shows that:

(1) Specimens (1 to 6) with tight screws formed a group with an average stress per g of 32·13 MPa (440 micro strain per g) and a mean life of 130·0 programmes (Table 18).

(2) Specimens (7 to 16) with loose screws formed another group with an average stress per g of 37·54 MPa (514 micro strain per g) and a mean life of 107·4 programmes (Table 18).

(3) Individual values of average stress did vary widely within each group; the scatter in life was rather less than the scatter in stress.

Inspection of Figure 27 shows clearly that there is no direct correlation between the local strain, as measured by a strain gauge, and the fatigue life of the redundant structure of the Vampire wing.

However, a statistical analysis of the averaged lives of (1) and (2) above showed a highly significant difference. The tight screw group with a 14% lower average stress per g gave a 21% higher fatigue life.

The gauge was positioned on the spar boom (Fig. 12) in an area free of fastener holes in order to give the best measure of the nominal strain in the boom. However, the boom represented only 20% of the effective tension area and hence the measured strain was sensitive to the variations in fabrication tolerances, and load transfer characteristics of the remaining 80%. These variations are additional to those contributed by the normal service tightness conditions of the tank door screws.

8.10 Comparison of Predicted and Actual Lives

The life of the wing in the region of the intersection of the lower spar boom with Rib 2 was predicted on the basis of the nominal stress, determined by the flight loadings, of 27·56 MPa (4000 psi) for a 1 g increment of load, and an aircraft AUW of 4634 kg (10,000 lb). The basic fatigue data used in the life prediction was taken from the alternating stress–mean stress diagram for 24S-T aluminium alloy structures given in Reference 13. These data were used in the absence of such data for L65, from which the spar boom was made, because it was considered satisfactory, based on equivalence of notched material data.

Two methods were used for determining the linear accumulation of fatigue damage, namely:

---

* Young's modulus for aluminium alloy was taken as $E = 73$ GPa.

ARL Method H_1 (which is a "peak count" method), where the load fluctuations determining fatigue damage are obtained by combining maximum "peaks" and minimum "troughs" irrespective of position in the sequence.

ARL Method H_4, where the load fluctuations are determined as in H_1, but the calculation of damage is based on the fatigue life of a structural preload by the highest load in the sequence.[13]

The lives predicted by each hypothesis, together with the actual endurances in programmes to failure, for modified and unmodified wings tested under programme and random load sequences are given in Table 20. The predicted endurances are identical for the two sequences investigated because they were based on a common load spectrum. A plot of the distribution between load ranges of predicted fatigue damage per programme is shown in Figure 29 for Method H_1, showing that maximum damage occurred at load range P5–M5.

It can be seen from Table 20 when compared with modified and unmodified results that both methods of prediction estimate greater lives to collapse than found by experiment, and hence are unconservative, though H_1 was more conservative than H_4.

These predicted lives, based as they were on a nominal stress of 27·56 MPa per g measured in flight, are plotted in Figure 27 with other lives predicted using appropriate stress values for tight and loose specimen groups, i.e. 32·13 MPa for tight screws and 37·54 MPa per g for the loose screw group. Only lives calculated by the ARL Method H_1 are plotted for the two specimen groups.

The three predicted lives (Method H_1) lie on a curve which shows that closer agreement with actual lives was achieved when the lower flight stress per g was the criteria for prediction than when the higher average test values were used.

8.11 Fatigue Behaviour of Fuselages

The Vampire fuselage was a laminated wooden structure bonded with an urea formaldehyde (Beetle Cement) glue.

Considerable interest had been aroused in what would be the fatigue performance of this type of fuselage because the findings of a UK investigation into glues and glueing had indicated that there was a fall-off in strength (after a period of 10 years or more) of wooden structures bonded with urea formaldehyde glues.

Both fuselages used in the ARL test were 15 years old and were subjected to the equivalent of 41,279 and 67,238 hours total life. On inspection no indications of any defect were found indicating that the design requirements were still being met. These findings were further supported by strength tests conducted by Hawker de Havilland Co. on glued joint specimens cut from similar fuselages up to 14 years old[16] in which it was found that the timber–glue joint strength exceeded the ultimate strength required in the aircraft structure by 50%.

9. CONCLUSIONS

(1) The fatigue life of the Vampire wing was dominated by collapse of the lower spar boom at Rib 2 and Rib 1B (see conclusion (4) for influence of screw tightness on failure location).

Fatigue cracking was detected in other areas and standard repairs were carried out on butt straps and the rear spar in the region of Rib 5. Other cracks were permitted to propagate since their growth rate was slow and the residual strength of the wing was not adversely affected.

All cracks were capable of detection using simple visual means except those in the butt strap areas forward of the main spar, and the upper lug of the lower cross tube assembly.

(2) Replacing the P-K screws at Rib 2 by pinned Chobert rivets in accordance with de Havilland modification No. 792 had no significant effect on fatigue life.

(3) Effective functioning of de Havilland modification No. 792 required that it should not be delayed beyond 980 flying hours.[1] This conclusion was based on:

(*a*) available crack propagation data;

(*b*) a 1 in 1000 probability of having removed all fatigue damaged material by drilling of the P-K screw holes.

(4) Tightness of fuel tank skin panel attaching screws had a significant effect on the strain per g at Rib 2, and made a highly significant difference to the fatigue life of the wing. Wings tested with screws tightened according to squadron service gave a log mean life to failure of 107·5 programmes or 8600 flying hours. Wings tested with screws tightened to manufacturer's specification gave a mean life of 130 programmes or 10,400 flying hours.

Screw tightness also influenced the area of collapse. Wings with tight screws failed at Rib 2 while those wings with loose screws, i.e. tightened to "service" conditions, failed at Rib 2 and Rib 1B.

(5) Replacement of the lower spar boom and incorporating two steel doublers provided an effective means of doubling the life of the wing.

(6) The six-load-range block programme sequence used in the test was well designed and adequately represented the average Australian service g spectrum in that:

(*a*) fatigue failures of various types occurred in 12 areas, plus numerous rivet failures;

(*b*) no adverse load sequence effects were discovered when compared with results from tests in which identical wings experienced a randomised sequence of loads of the same magnitudes and frequency of occurrence as contained in the block programme sequence;

(*c*) fatigue cracks and other defects detected during inspection of long life service wings also occurred in test specimens at similar lives.

(7) In most cases the first crack to become visible in the structure occurred at the cut-out for the fuel transfer pipe in the shear web at Sta. 1524 mm.

The mean life to detection of this crack was 46·6 programmes or 3728 hours of flying, but it was earliest detected on test at 2240 hours flying. This same crack was found in one of the long service (1400 hours) wings inspected before the investigation started.

(8) The butt strap failure at Rib 5 (failure 5D), which occurred in nearly half of the wings tested, should be regarded as serious because it reduced the torsional stiffness of the wing, and this could lead to catastrophic failure for some manoeuvres. The standard service repair scheme should be applied when a crack in the butt strap is found.

(9) The two ARL life prediction methods, H_1 and H_4, when applied to modified and unmodified wings tested under programme and random load sequences, gave reasonable prediction of fatigue life when the manufacturer's nominal design stress (confirmed by flight test) for the critical section was used. These same methods predicted lives that were very conservative when the measured, averaged, test strain in the spar boom for "identical" specimens was used.

(10) Maintenance of the manufacturer's specified torque of 11 Nm (96 in. lb) for the fuel tank skin panel attachment screws was of the utmost importance to achieve the best possible fatigue life for the wing.

The most effective method of achieving correct screw tightness was to use an impact type pneumatic screwdriver.

(11) A number of non-destructive inspection techniques were employed during the investigation with varying degrees of success. Despite considerable time and effort it was not possible to detect cracking in the spar boom by radiographic means using X-rays, even when the crack had been located visually.

During all inspections of the lower surface the wing was loaded to 1 g, and in this condition cracks as short as 1·0 mm (0·04 in.) could be found inside bolt holes with the aid of dye penetrants.

(12) Only two fuselages were used for the testing of 23 half wings and at the end of the investigation neither showed any signs of wood or glue deterioration. They had each been subjected to the equivalent of 41,219 and 67,238 flying hours.

10. ACKNOWLEDGMENTS

The authors wish to acknowledge the efforts of the team comprised of members of the staff of the Structures Experiment Group and RAAF personnel which conducted the tests over a period lasting 5½ years.

REFERENCES

1. Vampire T11 Aircraft Fatigue Tests. De Havilland Aircraft Co. Ltd., Airspeed Division. Test Report TR 115.060, June 1959.
2. Analyses of Vampire T11 Programme Fatigue Test. De Havilland Aircraft Co. Ltd., Airspeed Division. Stress Office Report SD570, June 1959.
3. Mann, J. Y., and Harris, F. G. An Investigation of the Fatigue Performance of Three Types of Aircraft Skin/Spar Boom Fastening Systems. Part 1: Constant-amplitude Fatigue Tests. Department of Defence, Aeronautical Research Laboratories, Structures and Materials Report 350, September 1974.
4. Barnard, J. M. H., and Agar, Elizabeth M. Safe Fatigue Life Predictions of Vampire Wing Components. Department of Supply, Aeronautical Research Laboratories, S.M. Note 289, March 1964.
5. Odbert, K. E. Vampire Trainer Fatigue of Mainplane Structure. De Havilland Aircraft Pty. Ltd. Report No. TOR 245, Bankstown, March 1963.
6. Hawkes, G. A. Residual Stresses Resulting from the Forming of High Strength Aluminium Alloys. Royal Aero. Society, Vol. 63, No. 578, February 1959.
7. Odbert, K. E. Interim Report on the Analysis of RAAF Vampire Trainer Fatigue Meter Results and Some Preliminary Estimates of Typical Service Lives. De Havilland Aircraft Pty. Ltd. Report No. TOR 157, Bankstown, November 1961.
8. Odbert, K. E. Queries Raised During a Visit to ARL on 15th March 1962. De Havilland Aircraft Pty. Ltd. Report No. TOR 174, Bankstown, March 1962.
9. Barnard, J. M. H., and Gee, S. W. Flight Tests of Vampire Mk. 35 Trainer Aircraft. Department of Supply, Aeronautical Research Laboratories, S. & M. Note 275, August 1962.
10. A.L. 72, Av.P. 970, Volume 1, Leaflet 200/7. August 1959.
11. Letter from RAAF containing reports from operating bases, dated 16th October, 1963.
12. Barnard, J. M. H., and Hooke, F. H. Fracture Study as an Aid to Fatigue Evaluation. Department of Supply, Aeronautcial Research Laboratories, S. & M. Tech. Memo. 123, 1963.
13. Payne, A. O. Determination of the Fatigue Resistance of Aircraft Wings by Full Scale Testing. *Full Scale Fatigue Testing of Aircraft Structures*, Pergamon Press, London 1961, pp. 76–132.
14. Schivje, J. Fatigue Life and Crack Propagation Under Random and Programmed Load Sequences. *Current Aeronautical Fatigue Problems*, Pergamon Press, London 1965, pp. 403–28.
15. Patching, C. A., and Mann J. Y. Comparison of an Aluminium Alloy Structure with Notched Specimens Under Programmed and Random Fatigue Loading Sequences. *Fatigue Design Procedures*, Pergamon Press, Oxford and New York 1969, pp. 395–432.
16. Downes, W. Estimated Life of the Vampire Trainer Fuselage Wooden Structure in Service with the RAAF. Report No. TOR 345, Hawker De Havilland, Australia Pty. Ltd., May 1964.
17. Becze, E. The Status of Knowledge of Residual Static Strength of Cracked Structures. Aeronautical Report L.R. 315, National Research Council of Canada, October 1961.
18. Fell, R. A., and Watson, Linda. The Accuracy of Several Methods for Measuring the Length of Fatigue Cracks. Tech. Memo. A.R.L./S.M. 167, Melbourne, June 1967.

APPENDIX I

Other Aspects of the Investigation

1. Residual Strength of the Cracked Structure

1.1 Aim of residual strength tests

These tests were carried out to examine the magnitude and variability in the failing load of four wings that contained identical cracks in the region of Rib 2.

1.2 Specimens

Although the Vampire wing can be described as being of single spar construction, it is sufficiently redundant to carry substantial load with the spar boom failed at Rib 2. The tests were carried out to provide data on the variability of residual strength with the spar boom failed.

A general description of the wing structure is contained in Section 4.

Three of the four specimens were Trainer type wings, and the other a Mark 31 Fighter wing. The significant difference between these wings in regard to residual strength, was in the size and placement of four brackets, one in each corner formed at the intersection of the lower spar boom, shear web and Rib 2. These brackets were riveted and bolted to all three adjacent elements, but were larger in the case of the Trainer type wings in order to accommodate loadings received from a catapult hook which could be attached at this station. None of the wings tested were actually fitted with the hook.

In all these four specimens the lower spar boom was completely fractured between the two pairs of brackets on either side of Rib 2. For the Fighter wing and two of the Trainer wings this failure was caused solely by fatigue loading. The boom in the remaining Trainer wing (specimen 25) was partially severed with a saw cut and then fatigued for less than one programme causing it to fail in a manner similar to the rest. Load could still be carried across the spar boom failure by the interconnection of the boom to the brackets through the rib and by the adjacent skin and tank doors, etc. In the Fighter type wings this load transfer was less effective because the brackets were much smaller and thus did not have such an efficient method of connection.

1.3 Instrumentation

From failures during the fatigue tests it was known where the fractures could occur and hence two specimens were instrumented to record the load at collapse, to photograph the failure path using a high speed camera, and to register crack propagation with a series of "jumper" wires, shown in Figure 30, that triggered lights in the field of view of the camera.

1.4 Loading technique

The specimens were loaded in the testing rig at a rate of 2 g per second until collapse. At failure the rig operator released the hydraulic pressure in the system in order to limit the extent of structural collapse; however, there was a two second delay in this operation in the case of specimen 25.

1.5 Discussion of Results

The failing load for each specimen is given in Table 21 and varied little between the four specimens. However, the mode of failure did vary between specimens in that specimen 25 which recorded the highest load failed at right angles to the spar across the tension surface at Rib 2, while the other three specimens all failed by spanwise tearing along a row of countersunk screws attaching skin to the forward edge of the spar boom, outboard of Rib 1B as shown in Figure 30.

It is interesting to note that the failure at right angles to the spar occurred in that specimen which had *not* been subjected to fatigue loading, viz. specimen 25. The resultant lack of "working" of the rivets, bolts and tank bay door screws meant that they were still functioning

efficiently. This enabled the skin panel between Ribs 1B and 2 to act as an alternative load path around the spar boom fracture. Assisting this path to carry the additional load was the absence of any fatigue cracking (failure type 7A, Fig. 8) in the region of the countersunk screws, along which the skin in the other three specimens failed by tearing. Collapse of specimen 25 was initiated by shearing of the rivets parallel to Rib 2 which transferred the load into the leading edge nose skin panel. Four rows of rivets sheared, which gave direction to the final failure path. Load was then re-distributed through the tightly bolted brackets and shear web at Rib 2, because the joints had not received the fatigue working of the other specimens; and hence these brackets received a sudden application of high load. This assumption was confirmed by the necking and failure of the bracket-to-rib bolts, and little or no deformation of the brackets. Failure in the shear web of the spar was along a vertical line through the bracket bolt holes because there was no fatigue at the end of the flange slot (failure type 4B, Figs. 1 and 2). While the bracket bolts and shear web were deforming, the load was redistributed aft through the skin between the main spar and the shear walls of the undercarriage leg well. Final collapse was by shearing of the rivets along Rib 2 aft to the rear spar, followed by failure of this spar in bending. This last stage could have been the result of a sudden transfer of load, or due to the two-second continuance of rig loading being sufficient to absorb the gross deflection and produce failure of the rear spar.

The failure of the other three specimens in the tearing mode parallel to the spar was the result of these specimens having been previously fatigue tested. The fatigue loading produced flexibilities in joints by both cracking in structural elements and slackening of rivets, bolts, and screwed fasteners. Initial distribution of load around the broken boom was still via the tank door and leading edge nose skin panel, but because of the relative looseness of the screw fasteners, a greater proportion was fed internally through the brackets bridging the fractured boom at Rib 2. Collapse in this mode originated at fatigue cracks of the root end fitting (in the nose skin), emanating from the holes of the countersunk screws of the root end fitting along the forward edge of the lower spar boom. These cracks allowed early shear buckling in this region, and this was a further reason why the failing load was lower in this case. Deformation of the brackets at Rib 2 was also taking place while the skin was tearing spanwise at the root. This was confirmed during examination after the test which also revealed bent and unbroken bolts in the brackets. The crack path in the skin proceeded along a chordwise row of rivets located between the spar and the shear wall of the undercarriage leg well. Failure of the shear web was initiated by the fatigue crack (failure type 4B) at the end of the flange slot.

No useful record of crack propagation was achieved. The progress of the crack was far too rapid for the "jumper" wire technique to resolve. This was almost true for the high speed camera which captured the stages of failure, but could not resolve the actual crack propagation during each stage.

1.6 Predicted failing load

Strength calculations by the authors using Engineers Bending Theory for both the cracked and uncracked structure produced completely inadmissible estimates of failing load in the region of Rib 2. An inspection of the structure revealed a major load diffusion situation, since the bending moment is reacted solely by the main spar at the fuselage connection. A simple calculation showed that the main spar alone can carry a load equivalent to $5 \cdot 5\,g$ with an area which is approximately 20% of the total cross section.

However, excellent agreement was obtained with the Becze[17] plot for residual strength of structures by estimating the ultimate failing load (UFL) of the structure using the following method:

The computed failing load for the main spar alone ($5 \cdot 5\,g$) was added to the load obtained during the residual strength test of the specimen containing the cut spar boom ($6 \cdot 74\,g$) giving a UFL of $12 \cdot 12\,g$ for an uncracked wing. *Note* – the design failing load of the wing was $10\,g$. This method assumes that the main spar and the rest of the structure are working independently of each other, which is reasonable since in the specimens tested there were no fatigue cracks of appreciable length to cause load redistribution.

1.7 Conclusions

(i) The variation between failing loads was quite small as may be expected, since there was an identical reduction in tension areas in each instance.

(ii) The presence of two modes of failure shows how fatigue damage can affect the balance between the various load paths and ultimate fracture, even in a structure with limited redundancies.

(iii) Using rather simple assumptions the results are in close agreement with other experimental data, indicating that in this instance a 20% loss of tension area results in 46% drop in UFL.

(iv) The residual strength of the Vampire wing containing a failure of the spar boom at Rib 2 was approximately 6·7 *g*. However, a similar failure in the spar boom at Rib 1B would produce a very much greater drop in residual strength, because there is far less redundancy surrounding this area.

2. Random Load Tests

2.1 Introduction

During the investigation it was decided to subject at least two specimens to a randomised sequence. This was done for two reasons, both concerned with the accepted assumption that a service load spectrum may be adequately represented by a programmed sequence of loads.

The first reason arose from the fact that in a programmed load test there is only one way of assessing fatigue damage, i.e. load amplitude is clearly defined by each peak and succeeding trough.

The second reason arose from work done in measuring crack propagation per programme, by counting the distinctive rings produced on the fracture faces of both steel and aluminium alloy components of the lower spar boom. This work[12] indicated that when the number of cycles per programme was changed the crack growth did not respond accordingly. Contrary to expectation the crack growth rate increased when the programme was shortened and decreased on the application of long programmes. This implied that the programme length could effect the life to failure.

It was therefore decided to test under a random load condition where firstly, the period of repeatability was longer than that of the programmed load sequence, and secondly there was no correlation between successive load cycles. All other parameters of frequency and magnitude of loads were unchanged.

2.2 Method of loading

A load controller was devised which selected individual loads at random instead of load ranges in order. Inherent in this random selection of loads was the possibility of two of the same sign, i.e. above or below the mean load level occurring in succession. Under the circumstances of this test and load counting the load controller was therefore designed to return the wing to an arbitrary 1 *g* load level between any two selected loads of similar sign. Because the 1 *g* to M_1 load excursion of 0·56 *g* was too small for the load controller to resolve, an arbitrary value of 0·645 *g* was chosen, i.e. midway between the P_1 and M_1 range of 1·29 *g* (Fig. 5).

The periodicity of loads selected is shown in Table 2, which shows that a period (i.e. the length of the sequence which is repetitive) was equivalent to 1·3 programmes.

From Tables 1 and 2 it is possible to obtain the mean and alternating stresses along with frequency of occurrence using a 1 *g* stress of 27·56 MPa (4000 psi).

2.3 Results

Wings 17 and 24 having unmodified spar booms were used for the random loading sequence. The fatigue life and damage to the boom in each case is recorded in Table 7, at the foot of the Table.

2.4 Discussion

The log mean average of the two results for the random sequence was 116·3 programmes. This compares favourably with the equivalent value for unmodified wings, i.e. 125·4 programmes (see notes, Table 7).

Furthermore, one result was above and the other below this mean, with the lower result still greater than specimen 7 which had the shortest life, i.e. 99·6 programmes.

All other fatigue features in the two wings followed the same pattern as far as order and time

of appearance was concerned, as would be predicted from the programmed loading series of tests. The extent of damage sustained by each specimen was also similar.

Unfortunately, there was no record of detection of failures type 9A in the web flange at fuel transfer hole for specimen 17. However, the results contained in Table 17 show good agreement between specimen 24 and the others.

2.5 Conclusions

The fatigue lives and damage to spar boom, along with the evidence of other failures, showed that there were no significant differences in the life produced by subjecting the wings to either the programmed or random loading sequence as applied in these tests.

3. Detection of Cracks in Spar Root End Fittings

As mentioned in Section 6.2.4 it was not intended that the spar root end fittings would be tested to failure, because of the damage that would be done to the surrounding structure. Nevertheless, four out of the 55 used did fail during test, and the remainder were found to be cracked on removal.

A number of the cracked fittings were then examined[18] using the following non-destructive crack detection methods to ascertain the extent of cracking in the two 8 mm ($\frac{5}{16}$ in.) diameter bolt holes (see Fig. 15):

(*a*) Visual, employing a hand magnifying glass of $\times 2$ magnification.

(*b*) Microscopic: similar procedure followed as in (*a*), but using a microscope obtained from a Vickers harness machine with 2/3 objective and magnification $\times 140$ approximately.

(*c*) Dye penetrant: consisting of the penetrating dye whose presence in the cracks was revealed by a white "developer", applied after dye on surface has been removed.

(*d*) Fluorescent particle method: the magnetised fitting was immersed in a fluorescent carrier solution containing magnetic particles in suspension. When viewed under a suitable lighting source the collection of magnetic particles together with the fluorescent carrier at the cracks could be readily observed.

No end load was applied to the fitting for the purpose of aiding the inspection technique.

After inspection the fittings were notched and subjected to a bending load, to produce failure with a minimum of damage to the fatigued areas.

3.1 Discussion of Results

A comparison between the various methods involving six specimens containing 22 cracks showed that the percentages of cracks detected and estimated to within $\pm 0{\cdot}5$ mm (0·02 in.) of their true lengths were as follows:

Visual	20%
Microscopic	45%
Fluorescent particle	70%

The dye penetrant did not identify any crack, while approximately 25% of cracks remained undetected by any of the methods used.

A summary of indicated and actual crack length for 10 specimens is given in Table 22.

Both the visual and fluorescent particle methods indicated cracks which were subsequently shown to be non-existent after fracture of the fittings. It is considered in these cases that the false indications resulted from surface scratches.

During examination with the fluorescent particle technique the presence was revealed of several cracks in the bore of the 8 mm ($\frac{5}{16}$ in.) diameter holes, which had developed adjacent to one another. Another feature of cracking in the holes was that in some instances they did not extend to the surface. These cracks had been initiated by fretting between the bolts and the fittings.

3.2 Conclusions

(1) The investigation showed that an accurate indication of the number and length of fatigue cracks was not achieved by any of the methods employed. The fluorescent

magnetic particle method was the most satisfactory, detecting 70% of the cracks to within $\pm 0{\cdot}5$ mm (0·02 in.) of their true surface lengths.

(2) The lack of success with the dye penetrant method may have resulted from the ingress of lubricants or cleaning solvents into the cracks during prior service or laboratory fatigue testing.

(3) A major factor influencing the results of the investigation was the unloaded state of the specimen during the application of the inspection techniques.

However, during the fatigue test a 1 *g* load was applied to the wing when inspections were being made in order to open any cracks present, and this did enable cracks to be detected which otherwise would have passed unnoticed.

4. Behaviour of Fuselages

4.1 Fuselage construction

Only two fuselages were used for the duration of the test programme, and these were more or less alternated with each pair of wing specimens.

The fuselages from Vampire fighter aircraft were of glued wooden monococque construction and had been manufactured during the year 1950, i.e. 15 years prior to testing. Spruce was the timber used for the heavier laminated members with birch plywood reinforcing panels. The shell of the fuselage was fabricated from a birch ply/balsa/birch ply sandwich.

A urea formaldehyde glue (Beetle Cement) had been used as the main bonding agent, although a phenolic resin of the film type had been used in the manufacture of the imported birch plywood.

The complete wooden structure was covered externally by nitro-cellulose doped madapolam cloth and finally finished with silver paint.

4.2 Loading

The loads applied to the wings were reacted at the fuselage centreline and distributed into both the fuselage and engine.

Fuselage loads were applied through the cockpit floor and external loading blocks glued to the cockpit shell at the No. 2 bulkhead as shown in Figure 9.

4.3 Endurance

Both fuselages endured the following fatigue history:

Fuselage No.	A79-467	A79-915
Flying hours	1,078	1,159
Test hours	66,160	40,120
Total life hours	67,238	41,279

No repairs were necessary during the test programme and an examination involving destruction of the fuselage did not reveal any damage to either the wood or the glueing.

5. Engine Mount Fatigue Lives

Each fuselage was complete with the Rolls-Royce Nene Mark 2 engine installed. The engine mount was a welded chrome moly steel tubular structure shown in Figure 31 and was subjected to fatigue loading during the test.

The maximum load applied during the fatigue cycle was 53·400 N (12,000 lb) and this was distributed through two points located either side of the CG of the engine.

Only one engine mount incurred any fatigue damage during the whole investigation. The mount assembled to fuselage number A79-469 was found to contain two cracks at a total life of 35,440 hours in the following locations:

(*a*) starboard upper horizontal member, bulkhead end, adjacent to the welding; and

(*b*) port diagonal member, upper end, i.e. at bulkhead, adjacent to the welding.

Three other engine mounts of unknown service life used during the investigation were subjected to a cumulative total of 64,800 hours of testing.

APPENDIX II

Testing Rig

1. Introduction

The main assumption used in designing the rig was that it would closely follow the principles adopted in the UK test. As mentioned earlier this would enable the findings from both investigations to be directly compared.

2. Rig Structural Design

2.1 Maximum loading capacity

Since ultimate static strength tests were not envisaged, the structural framework and loading members were designed for fatigue loading conditions only. A design load factor of $8 \cdot 55\,g$ was used, being the sum of $6 \cdot 55\,g$ (maximum test load) and $2 \cdot 0\,g$ (negative ballast weight) applied to an aircraft all up weight of 4540 kg (10,000 lb).

2.2 Load application

A structurally complete airframe was used so that the flexibilities at the wing root in reacting the applied loads would be identical to an actual airframe.

The aircraft was anchored to the floor at one point, and to an overhead structure at two points, all three on the fuselage centre line. These reactions being proportionally distributed into the fuselage and engine according to their mass distribution. The aircraft was free to roll but restrained in pitch, and was prevented from yawing or moving fore and aft by hinged links attached to the nose wheel axle. A view of the aircraft installed in the test rig is shown in Figure 9.

Hydraulic jacks were used to apply the positive loads, while the wing was loaded with ballast to $2 \cdot 0\,g$ which provided negative load levels.

Felt lined contour boards were attached to 12 rib stations on each wing, and apart from connections to the rear spar at Rib 5, and the transport joints in the fuselage booms, these were the only locations of positive load input to the structure. Three loading jacks per side were connected through a lever system, shown schematically in Figure 10, and were supplied with oil from a common pressure line.

3. Load Distribution

3.1 Design

The loads to be applied were calculated from data supplied by the Stress Office at De Havilland Aircraft Co. Ltd., England, which covered normal shear, torque and drag for the two cases of 1 g level flight and a positive load factor of $4 \cdot 66\,g$. The shift in centre of pressure between these two cases was rather large, but as the test rig had to be designed with a constant loading geometry, only one centre of pressure was simulated.

By assuming a linear relationship between the two cases, a 1 g increment of load was calculated for each of the three parameters, i.e. shear, torque, and drag. Thus, by starting with the 1 g level flight case, any other g condition could be obtained by the addition of an appropriate multiple of the 1 g increment of load.

Since the UK tests had shown the wing to be critical in fatigue in the region of Rib 2, the differences between desired and applied loading conditions were minimised at this station. However, the changes in torque were not represented inboard of Rib 2. The required bending moment, shear, and torque curves for the 1 g increment are shown with those that were actually applied, in Figures 32 and 33.

3.2 Flight loading

From the flight tests[9] it was possible to obtain a strain per g relationship for both the spar

boom at Rib 2 and the fuselage cross tube. This was then converted to bending moment per g by conducting a subsequent ground calibration.

The flight strain relationship was used directly to check the design loads, while the bending moment relationship was used in the final calibration of the testing rig.

3.3 Resolution of flight and design loading

The correctness of the applied loads was established by the insertion of electric weighing cells under the loading jacks and in the linkages. This check also verified that the jacks had negligible friction. Subsequent calibrations were conducted using load measurements at one of the jacks.

The test rig strain per 1 g increment of load was ascertained for both the lower spar boom at Rib 2 and the cross tubes, and compared with the flight tests. This showed an unacceptably large difference in the values for the spar at Rib 2, and from an investigation into the cause of this error (refer to Section 6.1.1) it was apparent that control of the test could not be related to boom strain at Rib 2 as first thought necessary. On the other hand the strain per g in the lower cross tube was within 5% (see Fig. 34), and hence it was concluded that the rig was satisfactorily representing flight conditions.

Therefore, the wing root bending moment was taken as the parameter to be controlled and used for calibration. This was achieved by monitoring the strain in the cross tube, and by measuring the applied load and position of the loading jacks from the aircraft centreline.

4. Test Loading

4.1 g Load spectrum

The average Australian flight load spectrum was approximated by six load ranges, L_1 to L_6 (see Fig. 4). The load ranges, although different in magnitude to those used in the UK test, were derived using the same counts per hour. The peak g values for each range were the average for the counting period, e.g. the value of $6{\cdot}55g$ for P_6 is the average of $7{\cdot}17g$ and $5{\cdot}93g$. The maximum and minimum g values obtained in this manner for each load range are shown in Figure 4 together with the number of cycles in each counting period. Differences in magnitude of load range between Australian and UK tests are listed in Table 1.

4.2 Rig bending moment

Because of the 5% difference in strain rate between flight strain and that produced by the design load in the lower cross tube, a modified plot of strain versus bending moment was drawn which coincided at the 1 g flight condition. This reduced the error in applied bending moment to $1{\cdot}7\%$ at the $6{\cdot}55\,g$ load.

From this modified plot (see Fig. 34) and the g values obtained from Figure 4, the bending moment versus g relationship was established (see Fig. 35), from which the bending moments appropriate to the 12 load levels of the six load ranges were obtained. These values were converted to jack force and used to calibrate the test rig.

5. Load Control

A schematic of the hydraulic loading and control circuits is shown in Figure 10, and Figure 36 shows the electrical circuit in detail. Control of the loading was by means of a multi-level pressure switch (MLPS) (F4, Fig. 36), actuating a solenoid valve (F6) in the hydraulic system. This pressure switch consisted of a small spring-loaded jack (packless ram), with micro switches representing each load level, so arranged that their vertical setting gave a direct measure and control of the applied load.

In a programme load test the "P" and "M" micro switches were selcted in pairs, as shown in Figure 10 (F1) and Figure 36, by the load selector. Each pair remained active until the required number of cycles at that load range was applied, at which stage the micro switches corresponding to the next load range were motivated.

For random loading another load selector was installed which activated single micro switches consecutively in an order which approximated a random sequence. However, as mentioned in Appendix I, the load selector equipment was designed so that when two loads of the same sign were selected consecutively an intervening 1 g load was applied.

Under both test conditions individual load applications about the 1 *g* level were counted for both positive and negative loads.

Various safety devices including overload protection, excessive roll, tip deflection, loss of oil, fire, etc., were installed as shown at A8 (Fig. 36) and the rig was consequently allowed to run unattended.

6. *Rig Calibration*

6.1 *Load transducers*

A permanent load transducer was built into the port outboard loading jack to monitor loads during each test. This arrangement was chosen instead of the cross tube strain gauge station, mainly because there would be at least one cross tube replacement during each specimen tested, which would involve re-gauging and calibration. Also there was a small degree of redundancy in the tube assemblies, which could have lead to the possibility of variation in total bending moment measured, especially after fatigue cracking had occurred.

During calibration runs only, an electrical weighing cell was installed at the base of the port outboard loading jack and hence in series with the transducer, as a continuing check on the accuracy of the transducer.

6.2 *Method of calibration*

6.2.1 *Programmed loading*

The output signal from the permanent load transducer was displayed on a 433 mm (17 in.) oscilloscope (CRO) along with adjustable load limit lines. The procedure was to load the rig up to the peak of a loading cycle and unload down to a trough. On reaching the required jack force as indicated by the weighing cell, the appropriate load level line was set to coincide with the transducer output. At any one time there were six load level lines displayed, representing the peaks and troughs of three load ranges. Switching of the display was automatic and appropriate to the load ranges being applied to the specimen.

On completion of the setting of all 12 load lines, the weighing cell was removed and the rig cycled. The controlling pressures in the system were then adjusted until the transducer output traversed the bounds set by the appropriate load limit lines. This critical visual operation was facilitated by the oscilloscope having a persistent screen.

To avoid most of the drift problems associated with electronic equipment, the signals of the transducer and load limit lines were multiplexed at the input of the oscilloscope. In addition stable and drift free components were used, which resulted in the calibrating and monitoring equipment giving accurate and reliable service during the testing programme.

6.2.2 *Random loading*

The procedure for establishing the load limit lines on the oscilloscope was identical with that for programmed loading.

However, when the rig was running there was a difficulty in switching the various attenuation settings for the load transducer, which were pecular to each load range. In the case of programmed loading only the peak load values varied between ranges, and the corresponding attenuation was automatically switched. It was still possible to do this during random loading for the peak loads only.

Adjustment of the minimum loads or troughs was done by selecting an attenuation setting and waiting until the corresponding load was applied. Since the interval of time between identical loads was not long this was quite a feasible operation. Because of the slower rate of loading on higher loads, the error between the static and dynamic settings was quite small, and thus the adjustment required was negligible.

6.3 *Accuracy*

The accuracy of the electrical weighing cells was $\pm 0{\cdot}1\%$ of measured load, and this coupled with a similar accuracy for the load transducer and oscilloscope made it possible to set the load limit lines to within 1% of the maximum load applied. The dynamic load control was less accurate but was considered to be within 2% of applied load.

Early in the tests, calibration checks were made every 10 programmes but as the load controller and monitoring equipment proved their stability, these intervals were extended to about 50 programmes. On the average this occurred every 12 days of testing time.

APPENDIX III

Load Transfer by Screwed Panels

1. Introduction

A large proportion of the wing lower surface consisted of fuel tank bay access panels (tank doors), attached along their edges by countersunk screws (see Figs. 7 and 8). During calibration runs it became apparent that the distribution of load between the panels and surrounding structure was dependent upon the tightness of the screws, i.e. the stiffness of the attachment joints.

A series of tests was conducted to ascertain the initial affect of screw tightness on the strain in the spar boom at Rib 2, and the variation during a test due to changing screw tightness.

2. *Effectiveness of Screwed Fasteners*

The transfer of load from the panels into the surrounding structure was mainly by friction produced by clamping. The countersunk screws passed through clearance holes in the spar boom and ribs, which were fitted with floating anchor nuts. Countersunk washers were fitted to some wings, because the holes in the panels had become enlarged from working and repeated tightening of the screws.

The initial tests were conducted by loading the wing with a single jack on each side at Rib 6; however, the maximum bending moment applied was limited to an equivalent load of 2 *g*.

The effect of strain in the spar boom at Rib 2 for various conditions of screw tightness in specimen 1 can be seen in Figure 11. From this it can be seen that the strain/*g* varied from 480 to 680 micro strain between the condition with all screws tight and all screws half turn loose.

But in tests, strain/*g* varied from lowest 340 to highest 560 micro strain. The difference in strain/g could be explained by the fact that one specimen was used to obtain Figure 11 results while the other values were the range of 22 specimens, six of which were maintained tight, and the remainder at a set value.

The distribution of strain between the spar boom at Rib 2 and the panel for No. 2 tank for panel screws tight and half turn loose is illustrated in Figure 37. Case C shows that with all panel screws one half turn loose, the strain in the spar boom increased by 46%, compared to Case A when all screws were tight, while strain in the panel decreased 64%, cases D and B (Fig. 37).

The degree of slippage that took place between the panel and the boom is indicated by the difference between the loading and unloading lines. With the screws tight there was some reduction in load carried by the panel during unloading, and this was reflected by an increase in boom strain. These results indicated that even with the screws tight there was still relative movement within the attachment joint.

The effect of slippage produced a departure from a straight line by individual strain gauge readings, and a non-return to zero for both gauges. Both of these features being more pronounced in cases C and D when the screws were loose (see Fig. 37).

3. Change in Joint Stiffness

Shortly after testing began on specimen 1 the strain per unit bending moment in the spar boom decreased by 37·6%, to a value close to that measured in flight. Strain measurements were repeated in the spar boom at Rib 2 and the panel for No. 2 fuel tank. However, a much larger bending moment was applied on this occasion as the readings were taken during calibration runs on the rig with all jacks in circuit.

The strains measured are shown in Figure 38 and agree closely up to the corresponding bending moment applied in Figure 37. However, at the higher loads there was an increase in the proportion of load carried by the boom, case A (Fig. 38), with a corresponding decrease in panel load, case B (Fig. 38).

The non-linearity produced by slippage between the panels and adjacent structure is readily observable in these illustrations. Also the changeover in effect on strain between loading and unloading is quite evident.

A repeat of the strain measurements at a later stage showed a remarkable difference, see cases C and D (Fig. 38). The load–strain relationship for both spar boom and panel were almost linear, which indicated that the attachment joints were functioning more efficiently. This is further supported by the narrowness of the hysteresis loop.

The reasons why the screw fasteners should have become more efficient during this test were never established, and there was no further change until failure. No other specimens displayed such a large change during testing although in some spar booms the value of strain was just as high as that originally present on specimen 1.

4. Subsequent specimens

Similar measurements of strain were recorded for the next specimen to ascertain:

(*a*) if there was a sudden or gradual change in joint efficiency with successive screw tightening; and

(*b*) if high values of strain in the spar boom at Rib 2 were indicative of low joint stiffness.

The results showed that throughout the test there was little variation in the proportion of load carried by the boom and tank door.

A typical plot of strain is shown in Figure 38, cases E and F, which when compared with cases A and B are very similar.

The variation in boom strain throughout a test is shown for two specimens in Figure 26.

TABLE 1
Test Load Ranges—Programmed Sequence

Load Range	Number Applied per Programme	Australian Load Range			U.K. Load Range g	Difference Between Aust. and U.K. Load Range g
		Maximum g 'P' Load	Minimum g 'M' Load	Range g		
(1)	(2)	(3)	(4)	(5)	(6)	(7)
L6	10	+6·55	−1·63	8·18	7·71	+0·47
L5	50	+5·38	−0·83	6·21	6·56	−0·35
L4	150	+4·25	−0·30	4·55	5·26	−0·71
L3	300	+3·14	0·03	3·11	3·96	−0·85
L2	550	+2·32	0·24	2·08	2·86	−0·78
L1	2500	+1·73	0·44	1·29	1·61	−0·32
Total	*3560*					

Column: (1)—Load Range Symbol;
(2)—Refer Figure 4 and Appendix II;
(3) and (4)—From Figure 4;
(5) = (3)–(4);
(6)—From Reference 1;
(7) = (5)–(6).

TABLE 2
Number of Excursions Between Turning Points P_N and M_N or '1 g' under Random Loading, per 9256 Selections

	'1 g'	P_1	P_2	P_3	P_4	P_5	P_6	Totals Across
'1 g'	—	3153	814	356	234	39	26	4622*
M_1	3083	2385	432	257	104	65	0	6326
M_2	626	541	145	82	13	26	0	1433
M_3	353	322	13	78	13	0	0	779
M_4	260	104	13	13	0	0	0	390
M_5	52	39	13	0	26	0	0	130
M_6	13	13	0	0	0	0	0	26
Totals Down	4387*	6557	1430	786	390	130	26	13706

Note: 1. The period length of the load selection equipment was 9256 selections, which is equivalent to 1·3 programmes of 3560 cycles. (7120 selected load turning points).
2. P_1 and M_1 etc., are the peak and trough load levels for the load range L_1, etc. with the P loads being those above the 1 g level, and M loads those below. See Figs 5 and 6.
3. The '1 g' level for the random sequence was actually displaced to 1·08 g to satisfy a test rig control limitation.

* Total excursions between nominal '1 g' level and selected load peaks were inserted automatically by the control equipment.

TABLE 3
Materials Specification (Minimum Values)
Major Structural Components

Component	Material	0·1% Proof Strength Tons/in² (MPa)	Ultimate Strength Tons/in² (MPa)	Elongation %
Cross Tube	T 60 Cr-Mo Steel (Weldable)	78 (1200) [0·2% Value]	85 (1310)	10
Root End Fitting	S 98 2·5% Ni-Cr-Mo Steel (High carbon)	65 (1000)	85 (1310)	14
Wing Lower Spar Boom	L 65 Cu-Mg-Si-Mn Type Aluminium Alloy	26 (400)	30 (460)	8

TABLE 4
Test Rig Utilization Time

Specimen No.	Maker's Serial No.	Test Time		Stoppages			Running Time		Specimen Test Life—Programme	Programmes per Day
		Total Days	Working Days	Fuselage Changes—days	Repairs —Days	Opposite wing Changes—days	Testing —Hours	Nett Days		
(1)	(2)	(3)	(4)	(5)	(6)	(7)	(8)	(9)	(10)	(11)
1	VMP-179	71	53	8	—	4	246·5	41	107·5	2·62
2	VMS-179	59	47	8	—	—	224·6	39	98·0	2·51
3	VMP-174	67	47	11	1	3	360·4	32	159·5	4·98
4	VMS-183	70	50	10	1	8	328·4	31	140·5	4·53
5	VMP-173	34	24	4	3	2	258·7	15	114·0	7·60
6	VMS-173	29	21	4	3	—	226·1	14	99·0	7·07
7	VMP-175	44	32	4	5	—	215·6	23	90·0	3·91
8	VMS-175	55	39	3	6	2	269·2	28	117·5	4·20
9	VMP-176	36	26	7	—	2	260·3	17	100·5	5·91
10	VMS-176	41	29	7	—	4	262·8	18	99·4	5·50
11	VMP-187	29	21	4	—	—	245·2	17	100·9	5·94
12	VMS-187	25	14	—	—	4	190·6	10	83·1	8·31

13A	VMP-180	50	36	8	—	5	265·8	23	105·2	4·57
13B	VMP-180	68	48	6	—	3	345·8	39	117·4	3·01
14	VMS-180	35	25	6	—	5	233·2	14	93·5	6·68
15	VMP-178	108	76	10	1	19	377·0	46	105·3	2·29
16A	VMS-177	60	42	2	1	5	302·5	34	106·5	3·13
16B	VMS-177	58	42	5	1	2	546·8	34	203·5	5·99
17	VMP-177	209	148	7	5	—	Not known	136	125·0	0·92
18	VMS-166	38	26	—	—	—	176·2	26	45·5	1·75
19	VMP-166	22	16	—	1	—	308·0	15	112·3	7·49
20	VMS-147	49	35	3	—	—	210·2	32	68·9	2·15
21	VMP-143	34	24	5	—	—	251·8	19	91·1	4·79
22	VMS-132	18	14	3	—	—	135·6	11	78·5	7·14
24	VMS-181	199	143	—	5	—	Not known	138	95·0	0·69

Col: (1) Specimen identification; (2) Manufacturers serial number; (3) Includes weekends and Public Holidays; (4) (3)—weekends, etc. (5), (6), (7) Working days involved; (8) Test rig time clock; (9) (4)—((5) + (6) + (7)); (10) Test programmes; (11) (10) ÷ (9).

Note: 1. Time to apply 1 block programme = 2 hrs. 20 min.
2. Rig was not run on a regular 24 hour basis.
3. Average number of programmes per day — 4·55.
4. All wings were Trainer construction except 18 to 22 incl. which were from Fighters.

TABLE 5
Vampire Wing Fatigue Failures

(a) Major Failures

Identification No.	Description
1	*Lower Cross Tube Assembly* (Fig. 14)
1A	Tube at Fork End Attachment Inner Bolt Hole.
1B	Fork End at Tube Attachment Outer Bolt Hole
1C	Fork End Upper (Threaded) Lug
2	*Lower Root End Fitting* (R.E.F.) Through Inboard 8 mm ($\frac{5}{16}$ in.) Dia. Bolt Holes, STA.747 (Fig.15)
3	*Main Spar Assembly at Rib 1B* (Figs. 1 and 8)
3A	Lower Boom at R.E.F. Attachment outboard Bolt Hole (Figs 18 and 19)
3B	Spar Web Lower Flange Tongue at R.E.F. Attachment Outboard Bolt Hole
3C	Spar Web Lower Flange Reinforcing Angle at R.E.F. Attachment Outboard Bolt Hole
3D	Web Lower Flange Reinforcing Angle at 4·7 mm (2BA) Bolt Holes Outboard of R.E.F.
3E	Web at End of Tongue Slot
3F	Web Lower Flange Steel Reinforcing Strap (Boom Replacement Mod.) at R.E.F. Attachment Outboard Bolt Hole.
4	*Main Spar Assembly at Rib 2*
4A	Lower Boom at P-K Screws (Figs. 1 and 20)
4B	Web at End of Flange Slot (Figs. 1 and 21)
4C	Web Flange Aluminium Alloy Reinforcing Strap (Fig. 21)
4D	Web Flange Steel Reinforcing Strap (Boom Replacement Mod.) (Fig. 1)
5	*Butt Straps* (Fig. 8)
5A	Rib 2 No. 2 Fuel Tank Door
5B	Rib 5 No. 2 Fuel Tank Door
5C	Rib 5 Doubler No. 2 Fuel Tank Door
5D	Rib 5 No. 3 Fuel Tank Door (Fig. 22)
6	*Rear Spar at Rib 5* (Fig. 8) Dive Brake Hinge Bracket Attachment Point

Table 5 (Continued)

(b) Minor Failures

Identification No.	Description
7	*Lower Skin Between Rib 1A and Rib 2*
7A	Lower Skin at Row of Countersunk Bolt Holes Forward of Root End Fitting (Fig. 23)
7B	Skin at Rear Outboard Corner of Access Panel Sta.1346 (Starboard Wing Only)
7C	Butt Strap at Rear Outboard Corner of Access Panel Sta.1346 (Starboard Wing Only)
8	*Main Spar Assembly at Rocket Mounts*
8A	Web Lower Flange at Rocket Mount Inner Bolt Hole, Sta.1186
8B	Web Lower Flange at Rocket Mount Outboard Bolt Hole Sta.1250
8C	Web Lower Flange Steel Reinforcing Strap (Boom Replacement Mod.) at Rocket Mount Sta.1186
9	*Main Spar Assembly at Fuel Transfer Pipe Hole Outboard of Rib 2 at Sta.1524*
9A	Web Lower Flange at Outboard Corner of Fuel Transfer Pipe Hole (Fig. 21)
9B	Web Lower Flange Steel Reinforcing Strap (Boom Replacement Mod.)
10	*Main Spar Web Lower Flange at Fuel Transfer Pipe Hole Inboard of Rib 5 at Sta.2540*
11	*Lower Skin Rear of Wheel Well at Sta.2248*
12	*Upper Skin at Countersunk Bolt Holes Rear of Upper Root End Fitting*

(c) Rivet Failures

R1	Lower Skin at Rib 1A Forward from Main Spar
R2	Lower Skin at Rib 2 Forward from Main Spar
R3	Lower Skin at Rib 2 Rear of Main Spar
R4	Lower Skin at Butt Strap at Rib 5, in the Three Stringers Forward of Rear Spar
R5	Lower Skin on Main Spar Outboard from Rib 5
R6	Upper Skin on Main Spar at Rib 1B
R7	Upper Skin at Rib 2 Forward of Main Spar

TABLE 6
Unmodified Spar Boom (Trainer) Lives and Fatigue Damage

Spec. No.	Programmes		Position of Final Failure	Gross Boom Area mm^2	Nett Boom Area-Failure Pos'n mm^2	Fatigue Area mm^2	Residual Boom Area at Failure %	Average Stress/g MPa	Holes in Crack Path at Final Failure Position
	Test	Total							
(1)	(2)	(3)	(4)	(5)	(6)	(7)	(8)	(9)	(10)
1	107·5	121·0	RIB 2	1279	948	152	84·0	24·83	One P.K., One 4 mm Rivet One 4·8 mm and One 9·5 mm Bolt
			*	1468	1060	6	99·4		
2	98·0	111·5	RIB 2	1258	1121	186	83·4	37·25	Four P.K. Screws
			*	1497	1089	24	97·8		
3	159·5	166·0	RIB 2	1268	1164	232	80·0	32·86	Three P.K. Screws
			*	1477	1070	44	95·9		
4	140·5	146·2	RIB 2	1268	940	164	82·5	35·79	One P.K., One 4 mm Rivet One 4·8 mm and One 9·5 mm Bolt
			*	1495	1088	32	99·7		
5	114·0	129·2	RIB 2	1237	1140	187	83·6	33·60	Three P.K. Screws
			*	1475	1067	21	98·7		
6	99·0	114·2	RIB 2	1237	988	164	83·4	28·48	Three P.K. Screws One 9·5 mm Bolt
			*	1488	1081	74	93·1		
7	90·0	99·6	RIB 2	1246	969	193	80·0	37·98	Three P.K. Screws One 9·5 mm Bolt
			*	1468	1060	39	96·4		

(1)	(2)	(3)	(4)	(5)	(6)	(7)	(8)	(9)	(10)
8	117·5	127·1	RIB 2	1226	1138	148	86·9	39·44	Three P.K. Screws
			*	1497	1089	3	99·7		
13B†	117·4	121·9	RIB 2	1258	1137	255	77·5	35·79	Four P.K. Screws
			*	1476	1068	26	97·6		
16B†	203·5	203·5§	RIB 2	1246	1137	161	85·8	32·13	Three P.K. Screws
			*	1493	1086	3	99·7		
17‡	125·0	131·1	RIB 2	1260	1163	273	76·5	38·71	Three P.K. Screws
			*	1493	1086	26	97·6		
24‡	95·0	103·0	RIB 2	1246	1141	155	86·4	32·13	Three P.K. Screws
			*	1495	1088	55	95·0		

Col.: (1) Test specimen identification number.
(2) Test Programmes applied in rig.
(3) Total programmes—Test plus flying hours (Equivalent).
(4) Final and * alternative failure positions i.e. Rib 1B-(failure 3A)
(5) Gross boom area at failure position.
(6) Col. (5) less measured cross sectional area of holes on fracture surface.
(7) Measured fatigue area on fracture face.
(8) Col. (6) less Col. (7) as % of Col. (6).
(9) Average stress per g in spar boom at Rib 2, recorded during test.
(10) Holes in actual final failure crack path.

* Areas of subsidiary fatigue failure i.e. Rib 1B (failure 3A) established at strip-down specimen.
† Replacement spar booms—P.K. screw holes filled with epoxy resin.
‡ Random loading sequence applied to these specimens.
§ Flying hours not available for replacement boom used in specimen 16 B.

Notes 1. Mean fatigue area of Rib 2 failures Col. (7) = 178 mm².
2. Log mean Col. (3) programmed loading = 131·2 (including specimens 13B and 16B).
Log mean Col. (3) programmed loading = 125·4 (excluding specimens 13B and 16B).
Log mean Col. (3) random loading = 116·2 programmes (specimens 17 and 24).

TABLE 7
Modified Spar Boom (Trainer) Lives and Fatigue Damage

Spec. No.	Start of Mod DH 792 Programmes	Programmes		Position of Final Failure	Gross Boom Area mm^2	Nett Boom Area mm^2	Fatigue Area mm^2	Residual Boom Area at Failure %	Average Stress/g MPa	Holes in Crack Path at Final Failure Position
		Test	Total							
(1)	(2)	(3)	(4)	(5)	(6)	(7)	(8)	(9)	(10)	(11)
9	Zero	100·5	107·8	*	1246	1077	6	99·4	35·79	Two 5·5 mm Bolts One 11 mm Bolt
				RIB 1B	1468	1060	168	84·1		
10	,,	99·4	106·7	*	1246	1023	53	94·5	37·25	Two 5·5 mm Bolts One 11 mm Bolt
				RIB 1B	1468	1060	139	86·9		
11	,,	100·9	107·0	RIB 2	1267	1120	103	90·8	40·90	Three 4·8 mm Chobert Rivets
				*	1477	1070	19	98·2		
12	,,	83·1	89·2	*	1252	1077	6	99·4	35·06	Two 5·5 mm Bolts One 11 mm Bolt
				RIB 1B	1477	1070	181	83·1		
13A	12·5	105·2	113·9	RIB 2	1239	1026	116	88·7	37·25	Four 4·8 mm Chobert Rivets
				*	1493	1086	1	99·9		

14	,,	93·5	104·0	RIB 2	1252	1128	158	86·0	38·71	Two 4·8 mm Chobert Riverts
				*	1506	1098	1	99·9		
15	,,	105·3	110·8	*	1268	1035	16	98·5	35·79	Two 5·5 mm Bolts One 11 mm Bolt
				RIB 1B	1477	1070	181	83·1		
16A†	,,	106·5	112·6		1277	1103	48	95·6	37·25	Speciment not Completely Failed
				*	1493	1086	2	99·8		

Col. (1) Test specimen identification number—13A and 16A are original fitment spar booms in specimens used in boom replacement investigation.
(2) Number of test programmes (flying hours not included) after start of test at which mod. DH 792 was incorporated.
(3) Test programmes applied in Rig.
(4) Total programmes—Test plus flying hours (Equivalent).
(5) Final and * subsidiary failure positions i.e. Rib 1B (Failure 3A).
(6) Gross boom area at failure position.
(7) Col. (6) less measured cross sectional area of holes on fracture surface.
(8) Measured fatigue area on fracture face.
(9) Col. (7) less Col. (8) as % of Col. (7).
(10) Average stress per g in spar boom at Rib 2, recorded during test.
(11) Holes in actual final failure crack path.
* Areas for subsidiary fatigue position i.e. Rib 1B (Failure 3A) or Rib 2 established at strip-down of specimen.
† Specimen 16A removed from Rig prior to spar boom failure so that wing structure could be used for boom replacement test.

Notes
1. Mean fatigue area of final failure Rib 1B Col. (8) = 167 mm²; Rib 2B = 126 mm².
2. Log mean Col. (4) (8 specimens) = 106·2 programmes.

TABLE 8

Unmodified Spar Boom (Fighter) Lives and Fatigue Damage

Spec. No.	Programmes		Position of Final Failure	Gross Boom Area mm²	Nett Boom Area-Failure Pos'n mm²	Fatigue Area mm²	Residual Boom Area at Failure %	Average Stress/g MPa	Holes in Crack Path at Final Failure Position
	Test	Total							
(1)	(2)	(3)	(4)	(5)	(6)	(7)	(8)	(9)	(10)
18†	45·5	59·0		1187	1064	32	—	37·98	Specimen not Completely Failed
						Nil	—		
19	112·3	125·8	RIB 2	1258	1010	239	76·3	38·71	Four P.K. Screws One 8 mm Bolt
			*	1471	1063	1	99·9		
20	68·9	74·8	RIB 2	1253	1006	155	84·6	40·90	Three P.K. Screws One 8 mm Bolt
			*	1458	1050	6	99·4		
21†	91·1	97·5		1239	1142	16	—	39·44	Specimen not Completely Failed
				1471	1063	6	—		
22	78·5	84·3	RIB 2	1241	1011	135	86·6	37·25	Three P.K. Screws One 8 mm Bolt
			*	1471	1063	4	99·6		

Col. (1) Test specimen identification number.
(2) Test programmes applied to Rig.
(3) Total programmes—Test plus flying hours (Equivalent).
(4) Final and * subsidiary failure positions i.e. Rib 1B (Failure 3A)
(5) Gross boom area at failure position.
(6) Col. (5) less measured gross sectional area of holes on fracture surface.
(7) Measured fatigue area on fracture face.
(8) Col. (6) less Col. (7) as % of Col. (6).
(9) Average stress per g in spar boom at Rib 2, recorded during test.
(10) Holes in actual final failure crack path.

*Areas for subsidiary fatigue position i.e. Rib 1B (Failure 3A)
† These specimens not completely failed – Upper figures refer to Rib 2.

Notes 1. Mean fatigue area of failures—Rib 2 Col. (7) = 176 mm².
2. Log mean Col. (3) = 92·58 programmes (Excluding spec's 18 and 21)

TABLE 9

Service and Test Programmes on Lower Cross Tube Assemblies

Including crack data at failure or at estimated failure life

Specimen No.	Programmes to Tube Removal			Tube Failure 1A		Fork End Upper Lug Failure 1C		Fork End Tube Portion Failure 1B	
	Test	Flying	Total	% Fatigue	Total Programmes to Complete Failure	% Fatigue	Total Programmes to Complete Failure	% Fatigue	Total Programmes to Complete Failure
(1)	(2)	(3)	(4)	(5)	(6)	(7)	(8)	(9)	(10)
T1	81·5	13·4	94·9	48·2	94·9 Actual	Nil	—	Nil	—
T4	75	not known	>75	47·3	>75 Actual	Nil	—	Nil	—
T6	86	7·6	93·6	27·30	94·5 Estimated	Nil	—	Nil	—
T10	74	8·7	82·7	25·0	83·6 Estimated	Nil	—	Nil	—
T15	66·3	6·4	72·7	22·76	73·7 Estimated	Nil	—	Nil	—
T8	69	7·3	76·3	19·2	77·6 Estimated	100	76·3 Actual	Nil	—
T11	52·5	5·8	58·3	11·6	63·5 Estimated	65	59 Estimated	Nil	—
T17	66·4	5·7	72·1	8·93	79·0 Estimated	Nil	—	Nil	—
T18	63	16·3	79·3	8·0	89·3 Estimated	Nil	—	Nil	—
T12	73·5	8·7	82·2	7·14	92·2 Estimated	Nil	—	Nil	—
T19	61·2	16·3	77·5	4·3	94·5 Estimated	100	77·5 Actual	Nil	—

T5	90·5	3·5	94·0	3·6	119·0 Estimated	100	94·0 Actual	Nil	—
T3	60·5	not known	>60·5	3·6	>85·5 Estimated	Nil	—	49·05	>60·5 Actual
T14	64·7	6·4	71·1	3·5	99·5 Estimated	100	71·1 Actual	Nil	—
T2	61·0	14·5	75·5	3·0	103·5 Estimated	100	75·5 Actual	Nil	—
T9	71·5	15·5	87·0	3·0	115·0 Estimated	100	87·0 Actual	Nil	—
T13	62·3	5·5	67·8	3·0	95·8 Estimated	Nil	—	Nil	—
T16	38·4	not known	>38·4	Nil	—	Nil	—	Nil	—
T7	25·5	9·5	35·0	Nil	—	Nil	—	Nil	—

Col. (1)—Specimen identification number.
(2)—Total test programmes.
(3)—Total flying hours as programmes.
(4)—(2) + (3).
(5)—Fatigue crack length as per cent of 180.3 mm (7.1 in.) i.e. tube circumference less holes.
(6)—'Estimated' totals from *Figure 16*: '*Actual*' as (4).
(7)—Measured fatigue area as per cent of typical complete failure, fracture face area.
(8)—'Estimated' totals from typical lug crack propagation rate. (unpublished)
(9)—Crack length as per cent of 153·01 mm (6·024 in.) i.e. fork end tube portion circumference less holes.
(10)—As (4).

Notes: Log average Col. (6) = 89·3 Programmes
Log average Col. (8) = 76·5 Programmes

TABLE 10
Shear Web Assembly Failures in Region of Rib 1B

Specimen No.	Total Programmes	Flange Tongue Failure 3B		Tongue Slot Failure 3E		Reinforcing Angle Failure 3C		3D	Remarks
		% Failed	% Fatigue	% Failed	% Fatigue	% Failed	% Fatigue	% Fatigue	
(1)	(2)	(3)	(4)	(5)	(6)	(7)	(8)	(9)	(10)
1	121·0	52	52	2	2	Nil	Nil	67	Rib 2 Failure
2	111·5	Nil	Nil	Nil	Nil	Nil	Nil	12	Rib 2 Failure
3	165·9	100	100	Nil	Nil	Nil	Nil	44	Rib 2 Failure
4	146·2	8	8	Nil	Nil	Nil	Nil	44	Rib 2 Failure
5	129·2	41	41	2	2	Nil	Nil	42	Rib 2 Failure
6	114·2	100	100	Nil	Nil	36	36	18	Rib 2 Failure
7	99·6	Nil	Nil	Nil	Nil	Nil	Nil	71	Rib 2 Failure
8	127·1	Nil	Nil	Nil	Nil	Nil	Nil	Nil	Rib 2 Failure
9	107·8	100	100	95	9	Nil	Nil	100	Rib 1B Failure
10	106·7	100	100	93	16	Nil	Nil	100	Rib 1B Failure
11	107·0	100	100	Nil	Nil	Nil	Nil	71	Rib 2 Failure
12	89·1	37	37	Nil	Nil	Nil	Nil	Nil	Rib 1B Failure

13B	121·9	Nil	Nil	Nil	Nil	Nil	Nil	Nil	24% Failure of Steel Strap, Rib 2 Failure
14	104·0	40	40	Nil	Nil	Nil	Nil	71	Rib 2 Failure
15	110·8	100	52	Nil	Nil	100	95	Nil	Rib 1B Failure
16B	203·5	Nil	Nil	Nil	Nil	50	50	Nil	100% Failure of Steel Strap, Rib 2 Failure
17	131·1	84	84	Nil	Nil	Nil	Nil	71	Rib 2 Failure, Random Load
18	59·0	Nil	Nil	Nil	Nil	Nil	Nil	Nil	Wing Not Completely Failed
19	125·8	Nil	Nil	Nil	Nil	Nil	Nil	Nil	Rib 2 Failure
20	74·8	38	38	Nil	Nil	Nil	Nil	41	Rib 2 Failure
21	97·5	24	24	Nil	Nil	Nil	Nil	71	Wing Not Completely Failed
22	84·3	Nil	Nil	Nil	Nil	Nil	Nil	Nil	Rib 2 Failure
24	103·0	36	36	2	2	Nil	Nil	71	Rib 2 Failure, Random Load

Col. (1) *Specimen identification number.*
(2) Total programmes—Test + Flying hours.
(3) Total crack length (fatigue + static failure) as % of nett tongue width—39·6 mm.
(4) Fatigue portion of crack length as % of 39·6 mm.
(5) Total crack length [see (3) above] as % of shear web depth at Failure position less flanges—419 mm.
(6) Fatigue portion of crack length as % of 419 mm.
(7) Total crack length [see (3) above] as % of nett Angle width at failure Position—71·6 mm.
(8) Fatigue portion of crack length as % of 71·6 mm.
(9) Fatigue crack length as % of angle total width at failure Position—76 mm.
(10) Position of wing final failure.

Notes: 1. Specimens 16B and 13B had steel reinforcing strap fitted at boom replacement. Percentage figures Col. (10) express fatigue crack length as % of nett width at failure position—23·5 mm.
2. Specimens 17 and 24 experienced a random load sequence.

TABLE 11
Shear Web Failures in the Region of Rib 2

Specimen No.	Total Programme	Web Failure 4B		Reinforced Strap Failure 4C		Remarks
		% Failed	% Fatigue	% Failed	% Fatigue	
(1)	(2)	(3)	(4)	(5)	(6)	(7)
1	121·0	75	6	100	Nil	
2	111·5	11	7	80	20	
3	166·0	17	9	100	5	
4	146·2	6	6	Nil	Nil	
5	129·2	6	6	Nil	Nil	
6	114·2	7	5	Nil	Nil	
7	99·6	7	7	Nil	Nil	
8	127·1	7	7	Nil	Nil	
9	107·8	5	5	Nil	Nil	Rib 1B Failure
10	106·7	10	10	Nil	Nil	Rib 1B Failure
11	107·0	100	12	100	Nil	Residual Strength Test
12	89·2	3	3	Nil	Nil	Rib 1B Failure

13A	113·9	19	17	Nil	Nil	Al. Alloy Strap Removed at Boom Replacement
13B	121·9	—	—	100	100	Steel Strap Fitted at Boom Replacement
14	104·0	17	6	100	5	
15	110·8	Nil	Nil	Nil	Nil	Rib 1B Failure
16A	112·6	6	6	Nil	Nil	Al. Alloy Strap Removed at Boom Replacement
16B	203·5	—	—	Nil	Nil	Steel Strap Fitted at Boom Replacement
17	131·1	86	32	100	Nil	Random Load and Residual Strength Test
18	59·0	6	6	Nil	Nil	Specimen Not Completely Failed
19	125·8	10	10	Nil	Nil	
20	74·8	45	7	100	Nil	
21	97·5	11	11	Nil	Nil	Specimen Not Completely Failed
22	84·3	88	9	100	Nil	Residual Strength Test
24	103·0	100	3	100	Nil	Random Load

Col. (1) Specimen identification number.
(2) Total programmes—Test + Flying hours.
(3) Total crack length—Fatigue + Static failure as % of web less flanges—311 mm.
(4) Fatigue portion of crack length as % of 311 mm.
(5) Total crack length (see 3 above) as % of strap width—57 mm.
(6) Fatigue portion of crack length as % of 57 mm.

TABLE 12
Butt Strap—Failure 5D—Replacements

Wing Specimen No.	Programmes			% Failed	Remarks
	Test	Flying	Total		
(1)	(2)	(3)	(4)	(5)	(6)
1	7	Nil	7	Nil	New Replacement
3	9	17·9	26·9	Nil	Removed from Untested Wing VMP 135
5	25	14·5	39·5	Nil	Removed from Untested Wing VMP 168
6	98 + 14	13·5	125·5	17	Removed from Specimen 2 at 98·0 Programmes
10	23·8	Nil	23·8	Nil	New Replacement
12	22·9	Nil	22·9	Nil	New Replacement
16 (A & B)	203·5 + 27·5	Nil	231·0	52	New Butt Strap Fitted at 27·5 Programmes before Fitting of Replacement Booms
19	38·4	Nil	38·4	Nil	New Replacement
24	12·5	Nil	12·5	Nil	New Replacement Test under Random Load

Col. (1) Specimen identification number.
(2) Test programmes.
(3) Flying hours expressed as programmes.
(4) Total programmes (2) + (3).
(5) Crack length as a % of butt strap length of 432 mm.

TABLE 13
Butt Strap—Failure 5D—Original Assembly

Wing Specimen No.	Programmes			% Failed
	Test	Flying	Total	
(1)	(2)	(3)	(4)	(5)
1	100·5	13·5	114·0	100
2	98·0	13·5	111·5*	5
3†	151·0	6·5	157·5	71
4	140·5	5·7	146·2*	6
5	89·0	15·2	104·2	94
6	85·0	15·2	100·2	69
7	90·0	9·6	99·6*	9
8	117·5	9·6	127·1*	Surface cracks
9	100·5	7·3	107·8*	,,
10	75·5	7·3	82·8	93
11	100·9	6·1	107·0*	Surface cracks
12	66·2	6·1	72·3	,,
13 (A + B)	222·6	8·7	231·3*	,,
14	93·5	10·5	104·0*	,,
15	105·3	5·5	110·8*	,,
16A	79·0	6·1	85·1	78
17‡	125·0	6·1	131·1*	5
18	45·5	13·5	59·0	Nil
19	74·0	13·5	87·5	60
20	68·9	5·9	74·8*	Surface cracks
21	91·1	6·4	97·5	,,
22	78·5	5·8	84·3*	,,
24‡	82·5	8·0	90·5	,,

Col. (1) Specimen Identification Number.
(2) Test Programmes.
(3) Flying Hours Expressed in Programmes.
(4) Total Programmes (2) + (3).
(5) Crack Length as a % of Butt Strap Length of 432 mm.

† Wing Removed at 120 Programmes with 10·3% of Butt Strap Failed. Wing Refitted and Further Tested Another 31 Programmes

‡ Random Load Test.
* Butt Straps Endured Till Final Failure of Wing.

TABLE 14
Butt Strap Failures 5A, 5B and 5C at Rib Nos. 2 and 5

Wing Specimen No.	Wing Programmes to Failure			Rib No. 2		Rib No. 5				Remarks
				Failure 5A		Failure 5B		Failure 5C (Doubler)		
	Test	Flying	Total	% Failed	Total Programmes at Measurement	% Failed	Total Programmes at Measurement	% Failed	Total Programmes at Measurement	
(1)	(2)	(3)	(4)	(5)	(6)	(7)	(8)	(9)	(10)	(11)
11	100·9	6·1	107·0*	Nil	*	3·6	107·0*	Nil	*	Nil
13A & B	222·6	8·7	231·3	Nil	*	70·0	176·3	66·7	176·3	Temporary repair carried out at Rib 5 at 176·3 Programmes
13A & B	222·6	8·7	231·3	24·4	231·3*	76·7	231·3*	73·3	231·3*	Damage at wing final failure
14	93·5	10·5	104·0	Nil	*	28·9	104·0*	2·7	104·0*	Crack in outer plate originating at a deep score (5B)
16A & B	310·0	6·1	316·1	Nil	*	11·1	316·1*	Nil	*	Nil

Col. (1) Wing specimen identification number.
(2) Test programmes.
(3) Flying hours expressed in test programmes.
(4) (2) + (3)
(5) Crack length as a % of butt strap total length i.e. 648 mm.
(7) Crack length as a % of butt strap total length i.e. 564 mm.
(9) Crack length as a % of doubler strap total length i.e. 564 mm.
* Total programmes as at end of test.

TABLE 15
Rear Spar at Rib 5—Failure Type 6

Wing Specimen No.	Programmes to Detection			% Failed
	Test	Flying	Total	
(1)	(2)	(3)	(4)	(5)
3	120·5	6·5	127	100
1	100·5	13·5	114	100
24*	82·5	8·0	90·5	100
12	66·3	6·1	72·4	100
2	98	13·5	111·5**	15

Col. (1) Specimen indentification number.
(2) Programmes in test rig.
(3) Flying hours expressed as programmes.
(4) Cols (2) + (3).
(5) Crack length as a % of rear spar i.e. Flange width of 32 mm plus web distance of 48 mm to lightening hole.

Note: All failures traversed the lower flange and up web to the lightening hole.
* Random loading sequence.
** Rear spar failure at final failure of wing.

TABLE 16
Spar Web Lower Flange Failures at Rocket Mount Positions
Failures 8A, 8B and 8C

Wing Specimen No.	Programmes to Wing Failure			% Failed		
	Test	Flying	Total	Failure 8A I/B Bolt	Failure 8B O/B Bolt	Failure 8C Steel Strap
(1)	(2)	(3)	(4)	(5)	(6)	(7)
1†	107·5	13·5	121·0	17	3·24	Not Applicable
2†	98·0	13·5	111·5	29	1–2	,,
3	159·5	6·5	166·0	3	Nil	,,
4	140·5	5·7	146·2	2	2	,,
5	114·0	15·2	129·2	Nil	3	,,
6	99·0	15·2	114·2	2	2	,,
8	117·5	9·6	127·1	2	3	,,
9	100·5	7·3	107·8	Nil	2	,,
11	100·9	6·1	107·0	2	2	,,
13A & B*	222·6	8·7	231·3	4	2	66
16A & B*	310·0	6·1	316·1	4	2	100

Col. (1) Wing specimen identification number.
(2) Programmes in test rig.
(3) Service flying hours expressed as programmes.
(4) Total programmes (2) + (3).
(5) & (6) Crack length as a % of spar web total length i.e. 508 mm.
(7) Crack length as a % of steel strap total width i.e. 44 mm.
† Specimens 1 and 2 subjected to one "Wheels-up" landing and one excess 'g' load during service.
* Steel reinforcing strap fitted during boom replacement.

Note. The remaining twelve wings had no damage at the rocket mount holes.

TABLE 17
Initiation Time and Extent of Failure at Hole in Spar Web at Sta. 1524
Failures 9A and 9B

Wing Specimen No.	Programmes			% Failed
	Flying	Total to Detection	Total to Final Wing Failure	
(1)	(2)	(3)	(4)	(5)
1	13·5	49	121·0	40
2	13·5	40	111·5	45
3	6·5	47	166·0	65
4	5·7	48	146·2	60
5	15·2	103	129·2	49
6	15·2	28	114·2	65
7	9·6	40	99·6	60
8	9·6	68	127·1	70
9	7·3	88	107·8	45
10	7·3	29	106·7	100
11	6·1	41	107·0	70
12	6·1	50	89·2	39
13A 13B†	8·7 —	38 27	113·9§ 117·4	70 100
14	10·5	36	104·0	70
15	5·5	110·8	110·8	15
16A 16B†	6·1 —	80 46	112·6‡ 203·5	100 100
17*	6·1	131·1	131·1	55
18	13·5	50	59·0	37
19	13·5	39	125·8	45
20	5·9	68	74·8	68
21	6·4	37	97·5	70
22	5·8	84·3	84·3	62
24*	8·0	59	103·0	58

Col.
(1) Wing specimen identification number.
(2) Service flying hours expressed as programmes.
(3) (2) + Test programmes to crack detection.
(4) Total programmes to removal of specimen from rig.
(5) Crack length at time of final wing failure expressed as a % of web lower flange i.e. 61 mm

† Failure of Steel reinforcing strap fitted at boom change, (Failure 9B).

* Random loading sequence.

§ Failure 9A was 70% failed at boom change i.e. 113·9 Programmes and fitment of steel strap stopped further cracking.

‡ Failure 9A was 100% failed at boom change i.e. 112·6 Programmes.

Note.
Log mean Col. (3) = 46·6 programmes.

TABLE 18
Statistical Check of Spar Boom Lives

PRIMARY COMPARISON

VARIABLES:

Structural—Modified or un-modified specimens.
Fasteners—Tight or loose screws.

Fasteners	Structure		Statistical Parameters
	Modified	Un-modified	
Tight	—	6 (1 to 6)	n
	—	2·114 (130·0 progs.)	$\bar{x}$
	—	0·067	S
Loose	8 (9 to 16A)	2 (7 to 8)	n
	2·026 (106·2 progs.)	2·051 (112·5 progs.)	$\bar{x}$
	0·033	0·0748	S

n = Number of specimens

$\bar{x}$ = Mean log life

S = Standard deviation of log lives where $S = \sqrt{\dfrac{\Sigma x^2 - \dfrac{(\Sigma x)^2}{n}}{n-1}}$

RESULTS:

Structural Variations — 8 Modified Specimens (9–16A) vs 2 Un-Modified Spec.
(With similar conditions for fasteners) Standard deviations — Not significantly different.
Means — Not significantly different.

Fasteners — 6 Specimens, Tight-Screws (1–6) vs 2 Specimens, Loose Screw.
(With similar conditions of structure) Standard deviations — Not significantly different.
Means — Not significantly different.

TABLE 18—continued

SECONDARY COMPARISON — Pooling

1. Pooling the results of tight and loose screws to give a larger population for comparison between modified and un-modified specimens.

Structure		Statistical Parameters
Modified	Un-Modified	
8 (9 to 16A)	8 (1 to 8)	n
2·026 (106·2 progs.)	2·098 (125·4 progs.)	$\bar{x}$
0·033	0·070	S

RESULTS:

Standard deviations — Not significantly different.
Means — Are significantly different.

2. Pooling of results of modified and un-modified specimens to give a larger population for comparison between tight and loose screws.

Fasteners		Statistical Parameters
Tight	Loose	
6 (1 to 6)	10 (7 to 16A)	n
2·114 (130·0 progs.)	2·031 (107·4 progs.)	$\bar{x}$
0·067	0·040	S

n = Number of specimens

$\bar{x}$ = Mean log life

S = Standard deviation of log lives where $S = \sqrt{\dfrac{\Sigma x^2 - \dfrac{(\Sigma x)^2}{n}}{n-1}}$

RESULTS:

Standard deviations — Not significantly different.
Means — Highly significantly different.

TABLE 19
Comparison of UK and Australian Rest Tesults

Specimen Type	Total Life to Failure — Programmes			
	UK Results			Australian Results
	Actual	Equivalent		
(1)	(2)	(3)		(4)
Un-modified	64·1	86·5	71·7 (2 specimens)	130·0 (6 specimens)
			$\bar{x}$ 1·856	$\bar{x}$ 2·114
	45·6	59·5	S 0·115	S 0·067
Modified	63·2	88·5 (unbroken)	101·1 (2 specimens)	106·2 (8 specimens)
			$\bar{x}$ 2·005	$\bar{x}$ 2·026
	81·7	115·5	S 0·081	S 0·033

Col. (1) — Un-modified specimens: Fitted with P.K. screws.
Modified specimens: P.K. screws replaced by pinned Chobert Rivets.

(2) — Actual service life plus test life converted to programmes i.e. 80 hours flying equivalent to 1 programme.

(3) — Service life converted on basis of aircraft weight plus test life converted on a damage basis.

(4) — Log mean life (Table 18).

TABLE 20
Comparison of Actual and Predicted Fatigue Lives at Rib 2

Loading Sequence	Life Source	Spar Boom Condition			
		Un-modified		Modified	
		Life-Progs.	Life Ratio	Life-Progs.	Life Ratio
(1)	(2)	(3)	(4)	(5)	(6)
Programmed	Actual	130	—	106	—
	H_1	134	0·97	134	0·79
	H_4	146	0·89	146	0·73
Random	Actual	116	—	—	—
	H_1	134	0·87	—	—
	H_4	146	0·79	—	—

Col. (3) Programmed actual from Table 19.
H_1 and H_4 computed for both loading sequencies.
Random actual from Table 6.

(5) Programmed actual from Table 19.

(4) and (6) Life ratio = Actual life/Predicted life.

TABLE 21
Residual Strength Test—Failing Loads

Specimen No.	Prior Fatigue Life		Failing Load g	Remarks
	Flying Hours	Test Programmes		
(1)	(2)	(3)	(4)	(5)
25*	500	Nil	7·11	Failure initiated by saw cut. Rig unload delayed
11	487·5	101	6·82	Initial failure at 1·73 g
17	490	125	6·56	
22	463	48·5	6·48	Fighter wing

Col. (1) Specimen identification number.
(2) Service flying hours.
(3) Test programmes to produce fatigue damage.
(4) As measured.
* This specimen was not fatigue tested.

Note: 1 Programme = 80 flying hours.
Average failure Load = 6·74 g.

TABLE 22
Crack Dimensions in Spar Root End Fittings

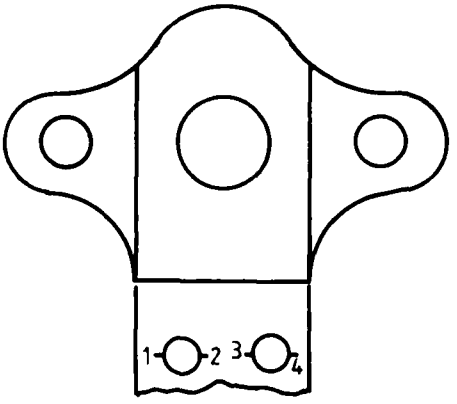

Crack No.

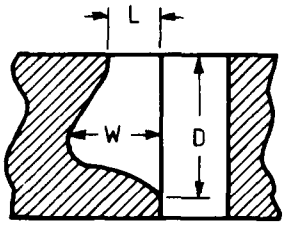

Crack dimensions

Specimen No.	Crack No.	Crack Dimensions — mm					
		Length 'L' Indicated by Method			Measured after Fracture		
		V*	M†	P‡	L	W_{max}	D
1	1	3·8	1·0		1·8	1·8	6·6
	2	1·8	Nil		1·8	1·8	4·1
	3	3·1	1·3		2·0	2·0	5·6
	4	2·3	2·3		3·0	3·3	7·1
2	1	2·8	1·8		2·3	2·0	5·1
	2	1·5	0·5		0·8	1·3	4·3
	3	1·5	1·0		Nil	0·5	2·5
	4	2·5	Nil	Method	Nil	0·8	4·3
3	1	8·4	5·1	not used	5·1	6·1	9·1
	2	3·3	Nil		1·3	3·3	7·1
	3	2·3	Nil		Nil	1·0	3·8
	4	1·8	Nil		1·5	1·5	5·1
4	1	3·3	4·3		4·3	4·6	7·6
	2	1·8	2·0		3·6	3·8	6·9
	3	1·8	2·5		3·0	3·3	5·6
	4	1·8	2·0		1·8	1·8	5·1
5	1	5·3	1·8	2·0	2·0	2·0	5·8
	2	2·0	Nil	Nil	0·8	0·8	2·0
	3	1·5	1·5	1·5	§	1·5	4·6
	4	1·5	Nil	Nil	1·0	1·0	3·0

TABLE 22—continued

Specimen No.	Crack No.	Crack Dimension — mm					
		Length 'L' Indicated by Method			Measured after Fracture		
		V*	M†	P‡	L	W_{max}	D
6	1	6·3	1·5	0·8	1·0	1·0	4·3
	2	2·8	1·5	1·3	Nil	0·5	4·6
	3	1·8	3·7	1·8	1·8	2·0	5·6
	4	1·0	2·5	1·8	2·0	2·0	4·1
7	1	3·3	0·5	2·0	2·0	2·0	5·6
	2	2·0	2·0	1·8	2·0	2·0	4·1
	3	1·8	1·0	1·3	0·8	0·8	4·6
	4	6·9	2·8	3·3	3·3	3·3	6·6
8	1	2·8	Nil	Nil	0·8	0·8	0·8
	2	2·5	Nil	Nil	2·5	0·3	5·1
	3	2·3	Nil	Nil	1·0	1·3	3·8
	4	3·0	Nil	Nil	1·5	1·5	1·8
9	1	6·1	1·5	1·8	2·0	2·3	4·6
	2	3·8	1·8	2·0	1·8	1·8	4·0
	3	6·9	3·0	3·6	3·6	4·1	7·1
	4	6·9	4·0	4·8	5·3	5·6	7·6
10	1	4·8	2·5	2·5	2·5	3·0	7·6
	2	1·5	Nil	1·5	1·8	2·0	6·1
	3	4·3	Nil	2·0	2·3	2·5	5·1
	4	7·6	Nil	2·0	2·5	2·5	6·1

* Visual examination with hand magnifying glass.
† Visual examination using microscope 140x.
‡ Fluorescent magnetic particle method of inspection.
§ Additional crack detected but failed in adjacent parent metal, because of subsurface cracking.

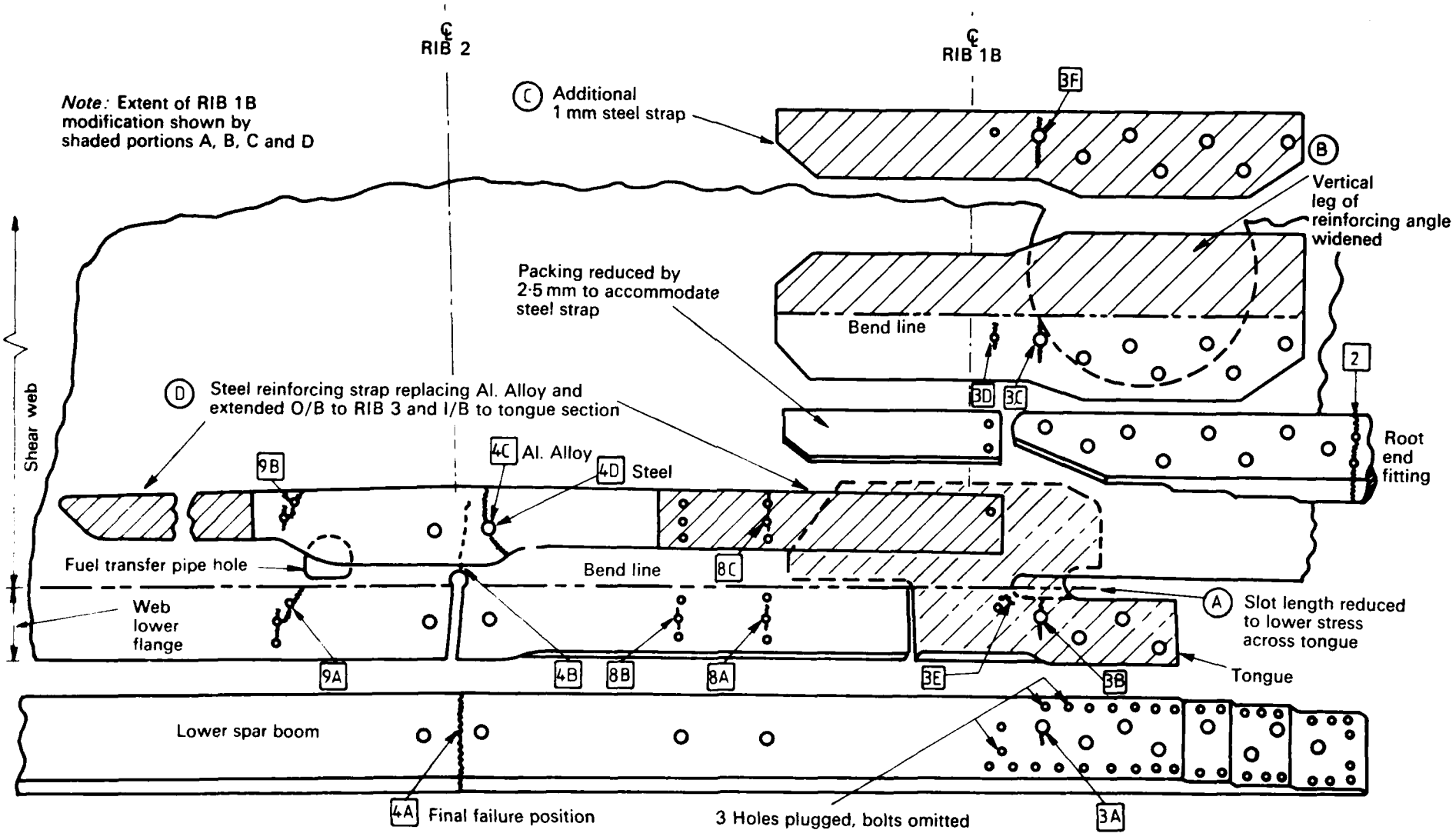

FIG. 1 : BOOM REPLACEMENT—MODIFICATIONS AND FAILURES
EXPLODED VIEW AT REAR FACE OF SPAR WEB PORT WING

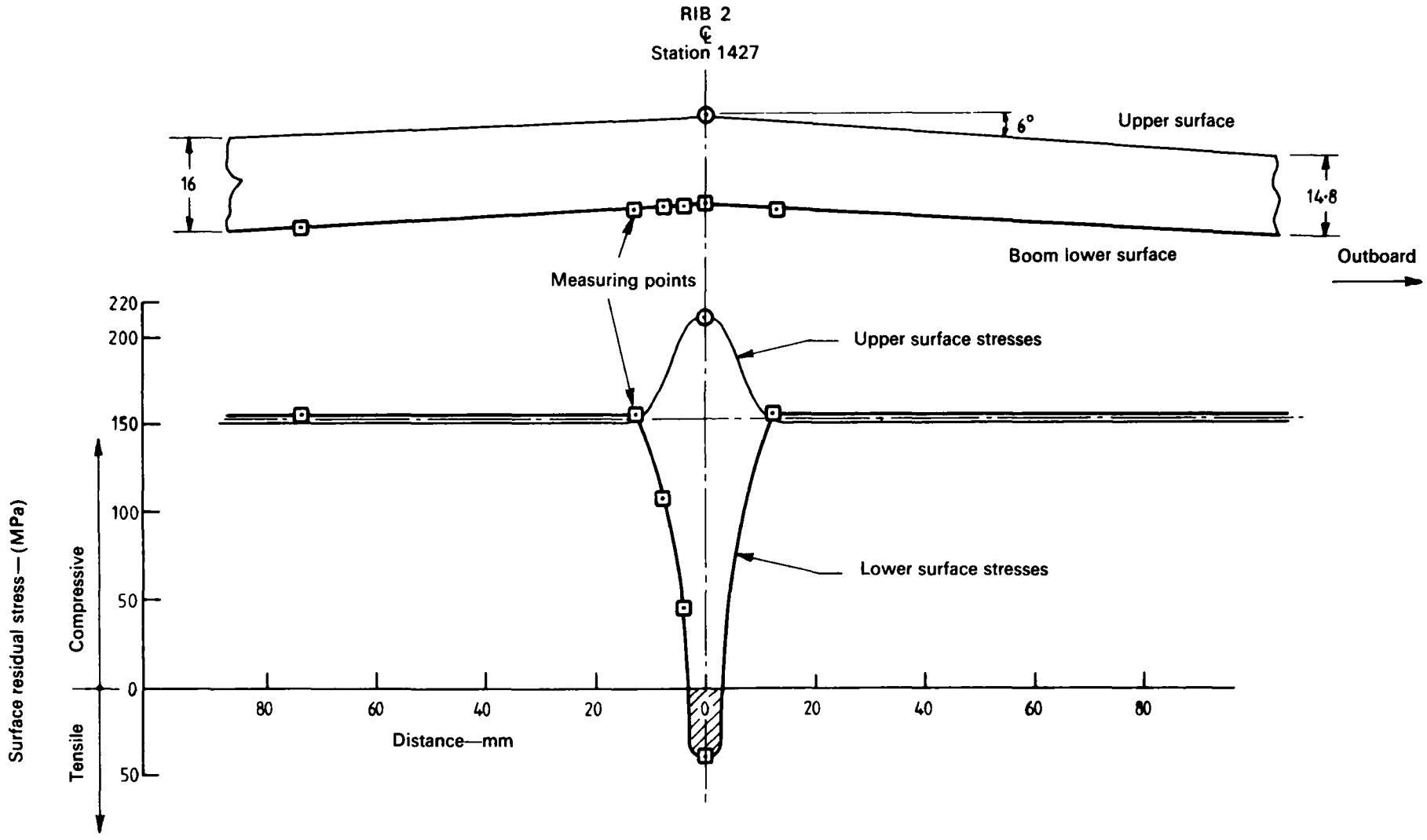

FIG. 2: RESIDUAL SURFACE STRESSES IN VAMPIRE WING LOWER SPAR BOOM AT RIB 2

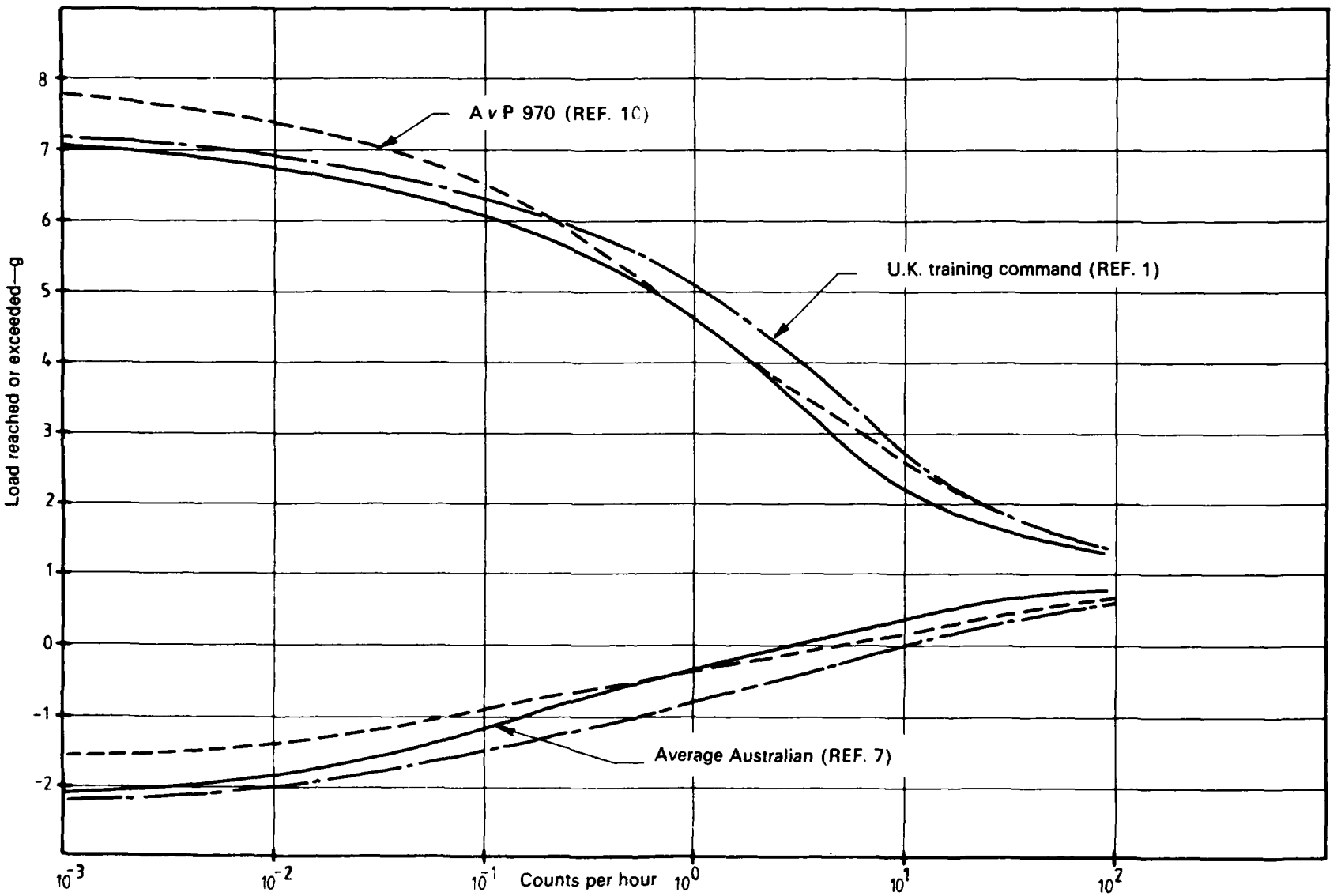

FIG. 3: VAMPIRE LOADING SPECTRA

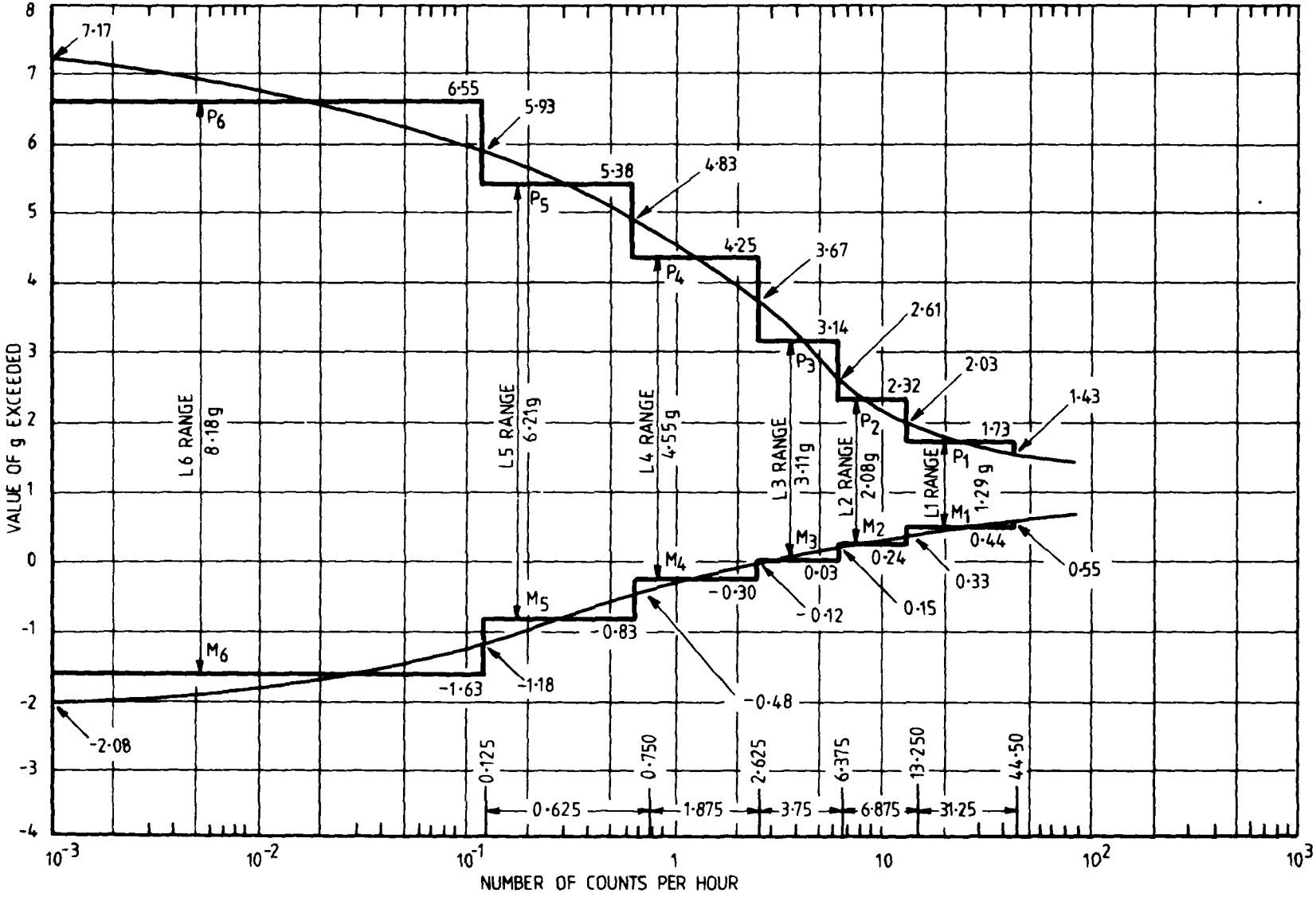

FIG. 4: AVERAGE FLYING SPECTRUM AND TEST LOADS

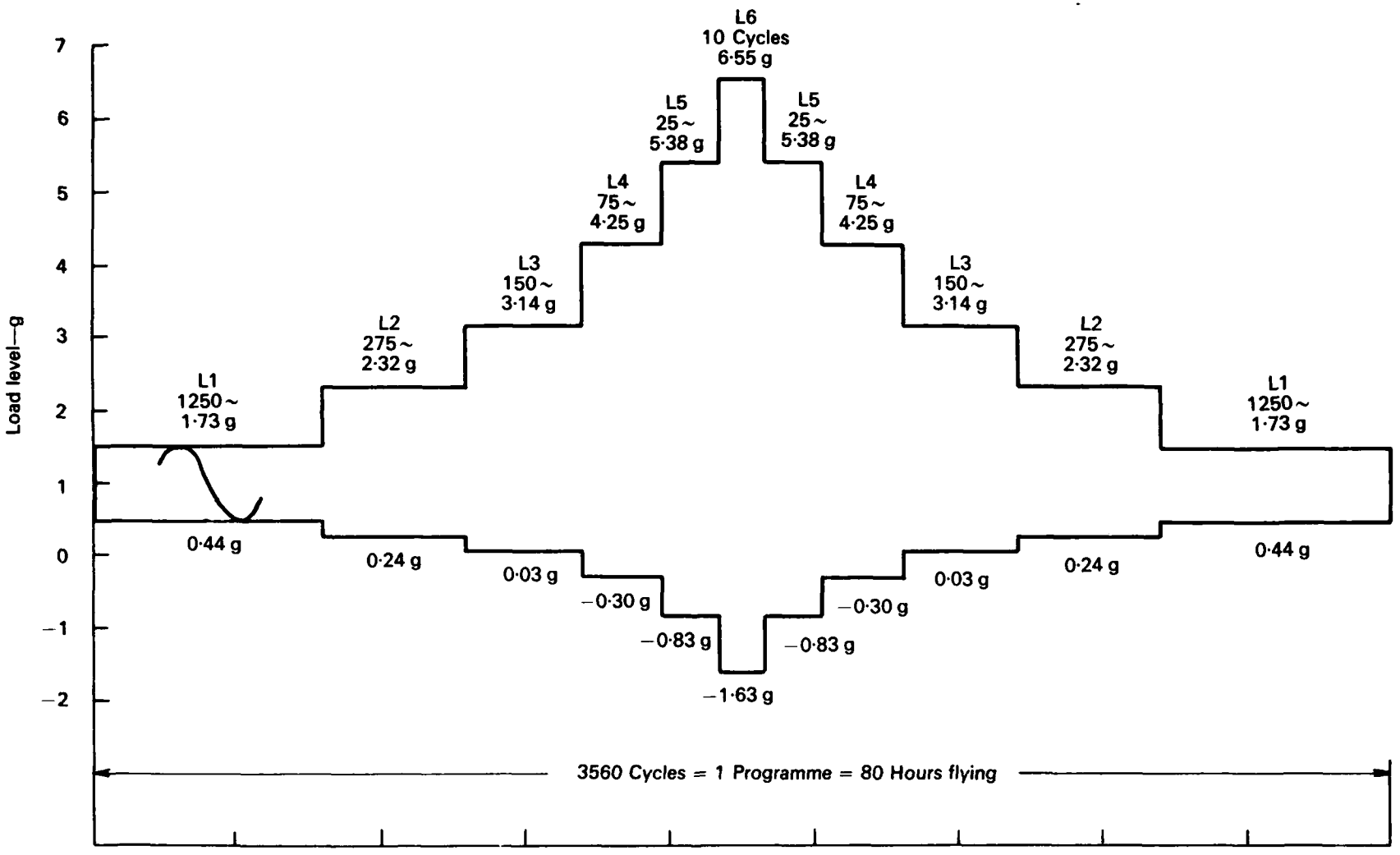

FIG. 5: PROGRAMME LOADING SEQUENCE

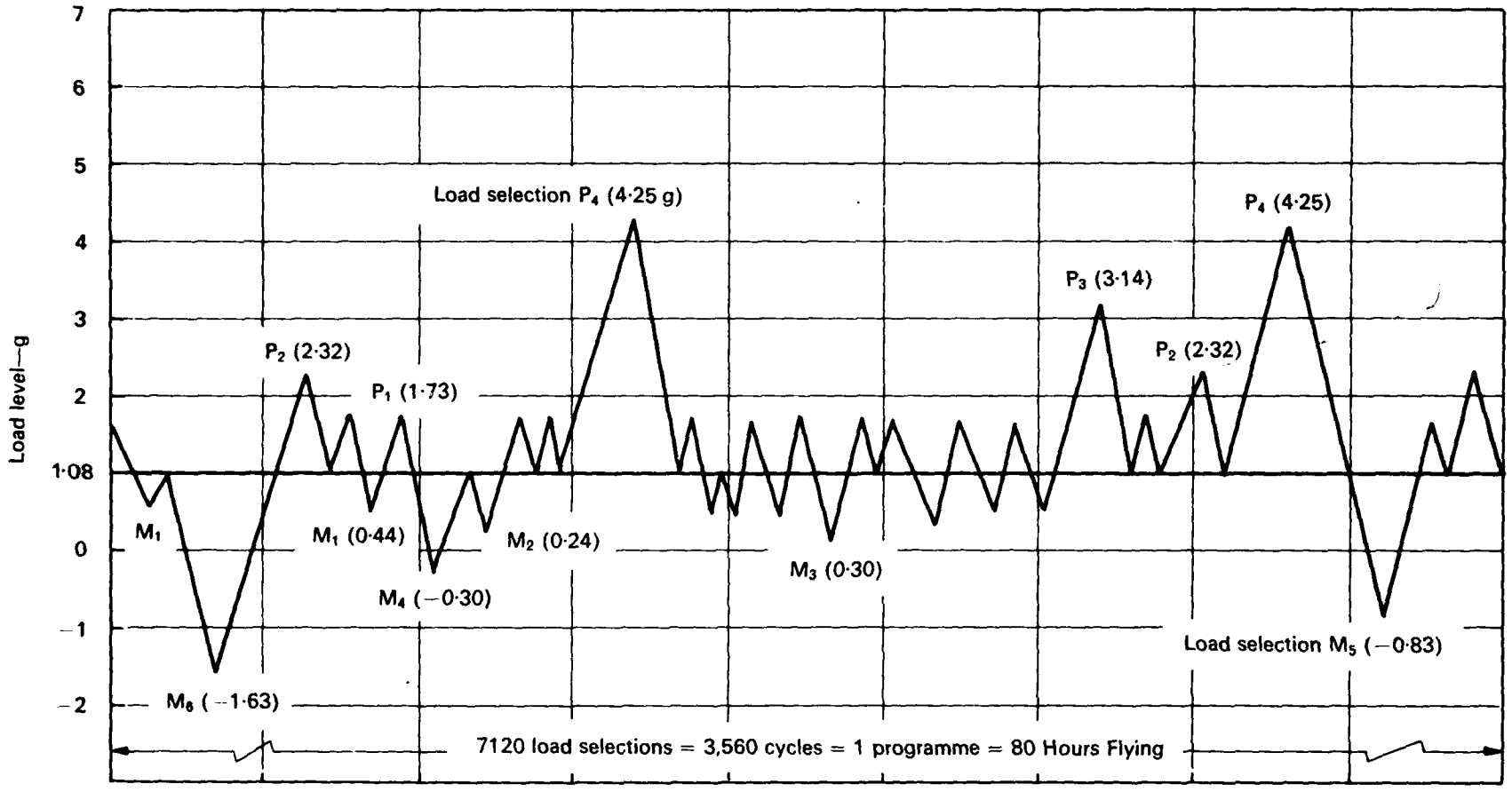

FIG. 6: RANDOM LOADING SEQUENCE (TYPICAL SAMPLE)

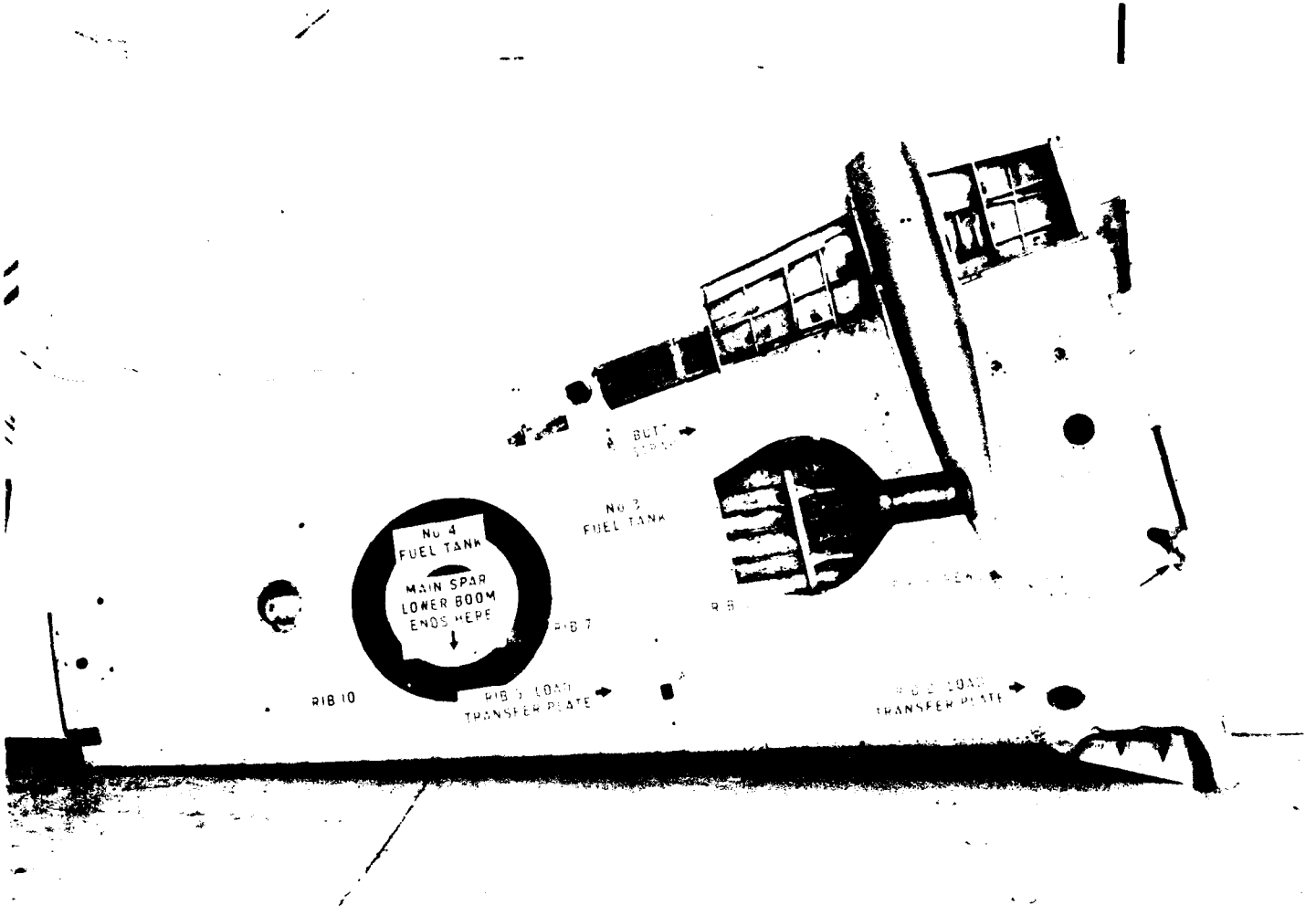

(Neg. No. 6305-A)

FIG. 7: VAMPIRE PORT WING—LOWER SURFACE

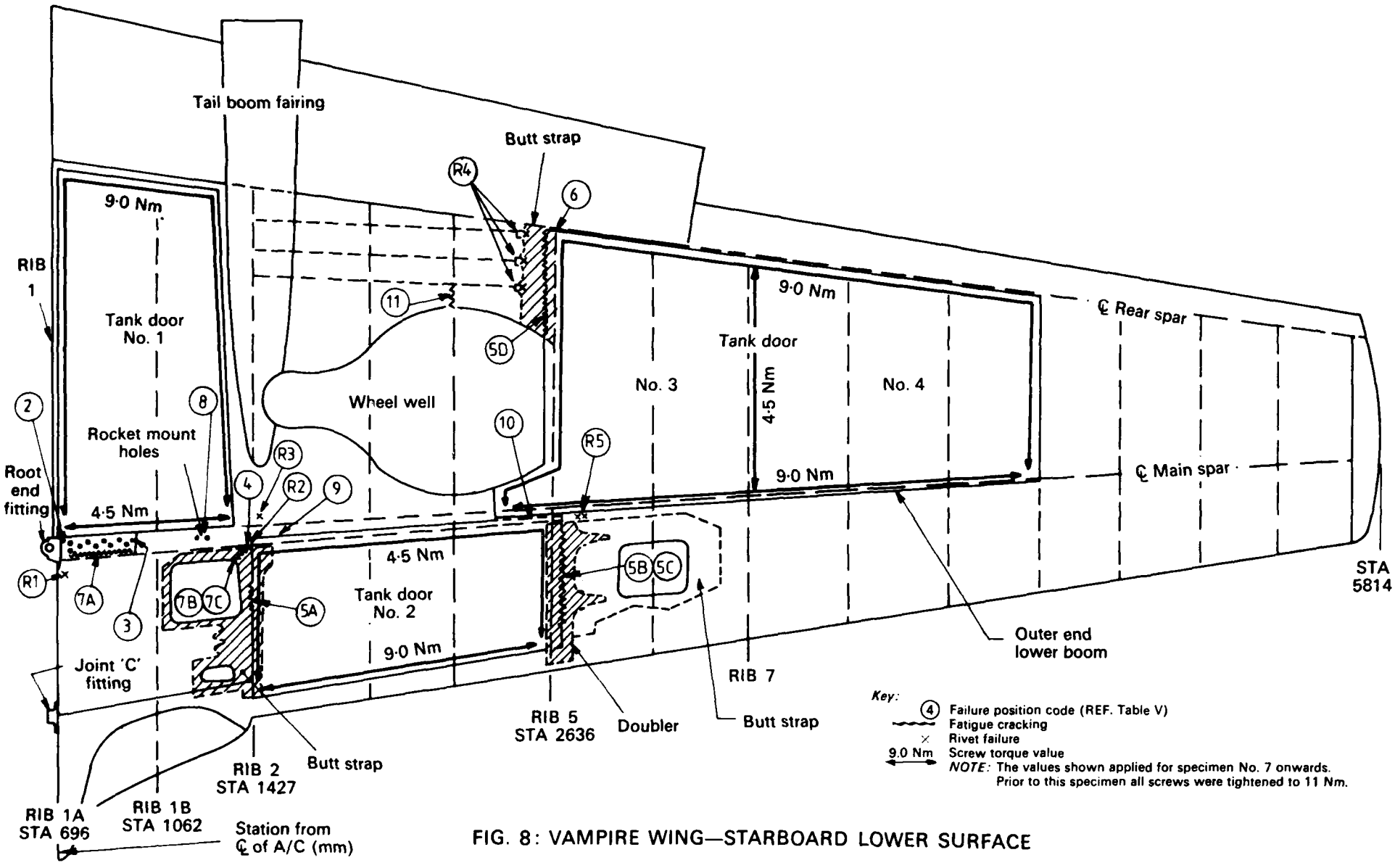

FIG. 8: VAMPIRE WING—STARBOARD LOWER SURFACE

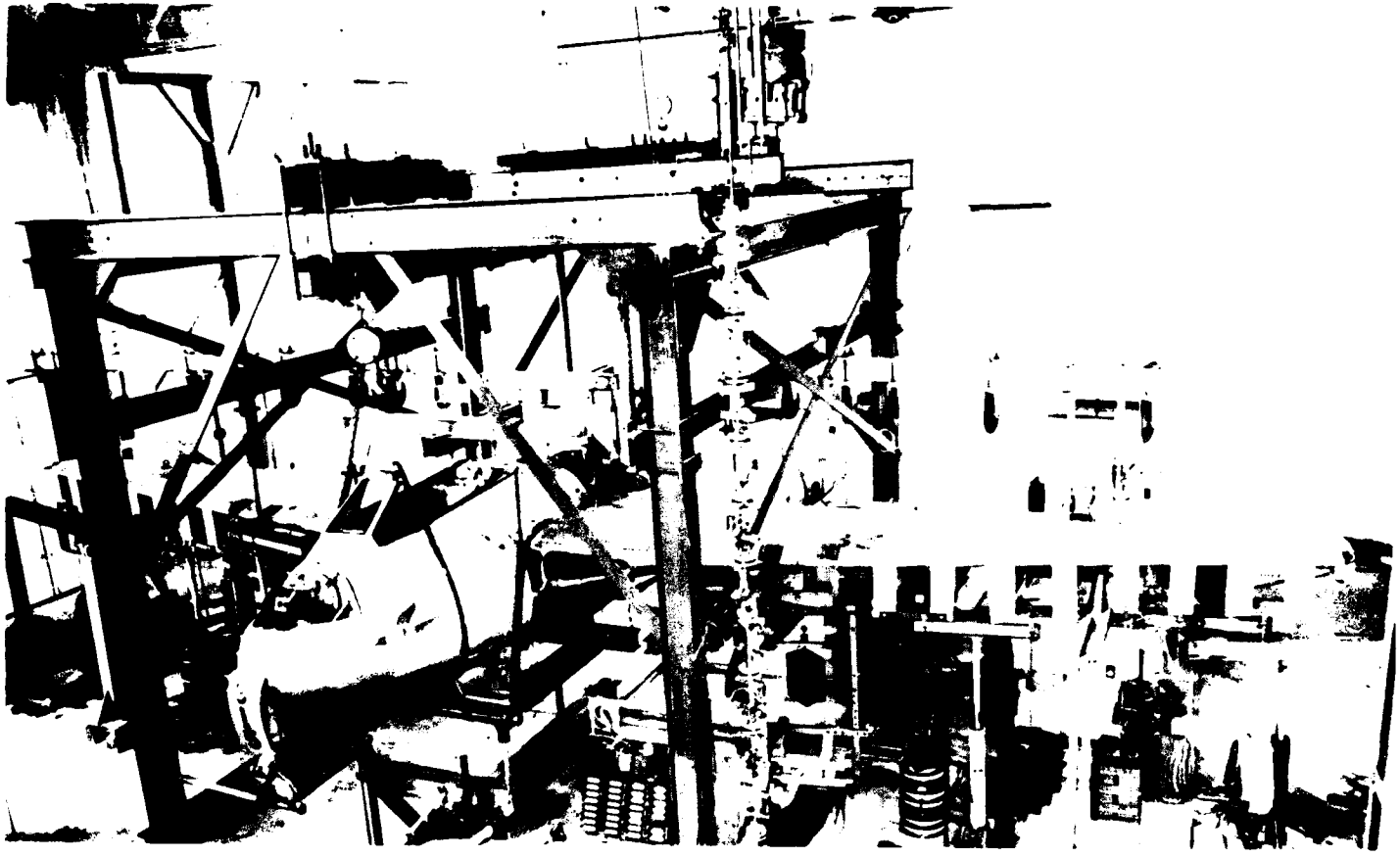

(Neg. No. 6295-A)

FIG. 9: GENERAL VIEW OF TEST RIG

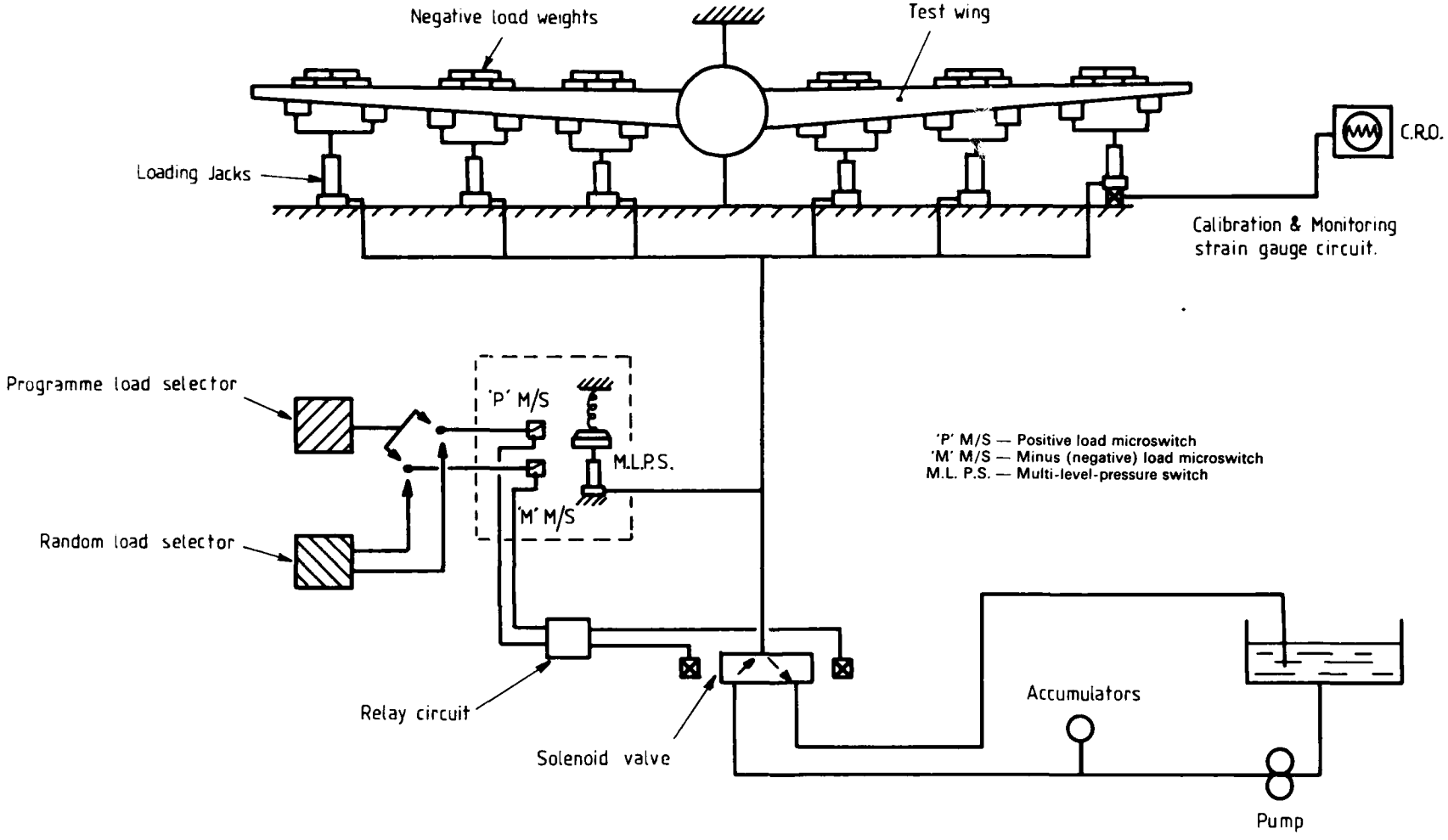

FIG. 10: SCHEMATIC HYDRAULIC AND CONTROL CIRCUITS

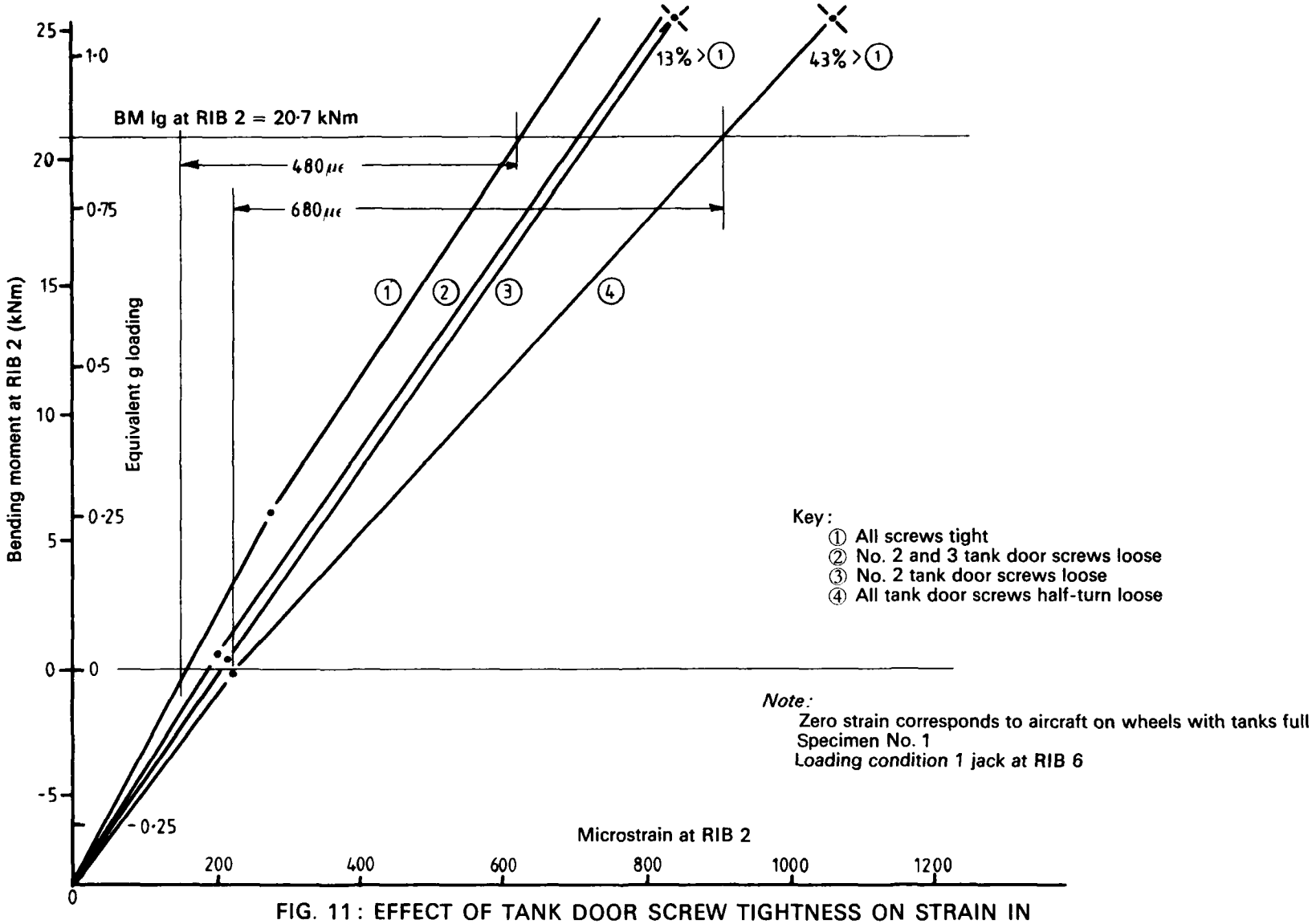

FIG. 11: EFFECT OF TANK DOOR SCREW TIGHTNESS ON STRAIN IN SPAR BOOM AT RIB 2

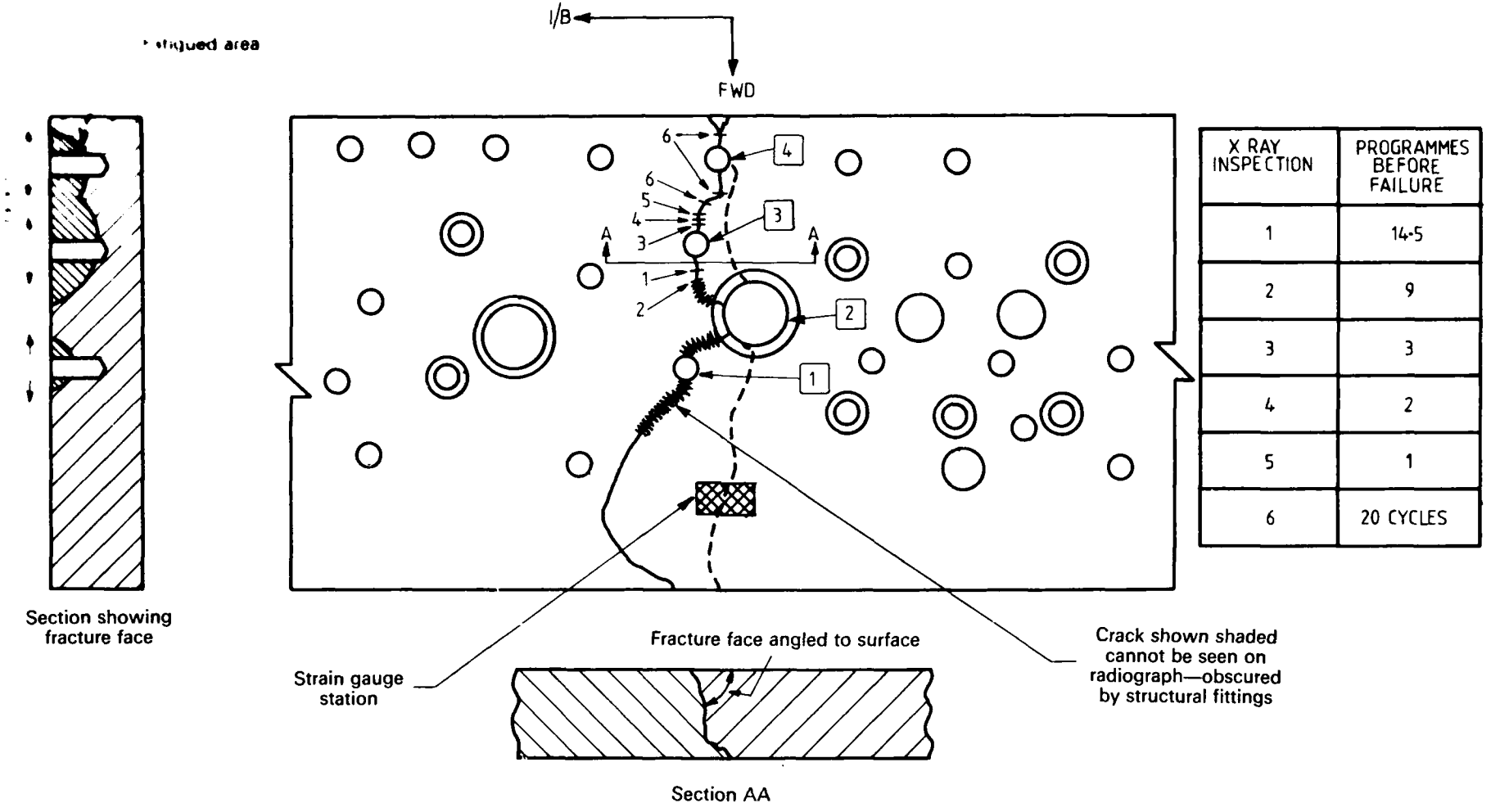

X RAY INSPECTION	PROGRAMMES BEFORE FAILURE
1	14·5
2	9
3	3
4	2
5	1
6	20 CYCLES

FIG. 12: LOWER SPAR BOOM—RIB 2 FAILURE—SPECIMEN No. 6

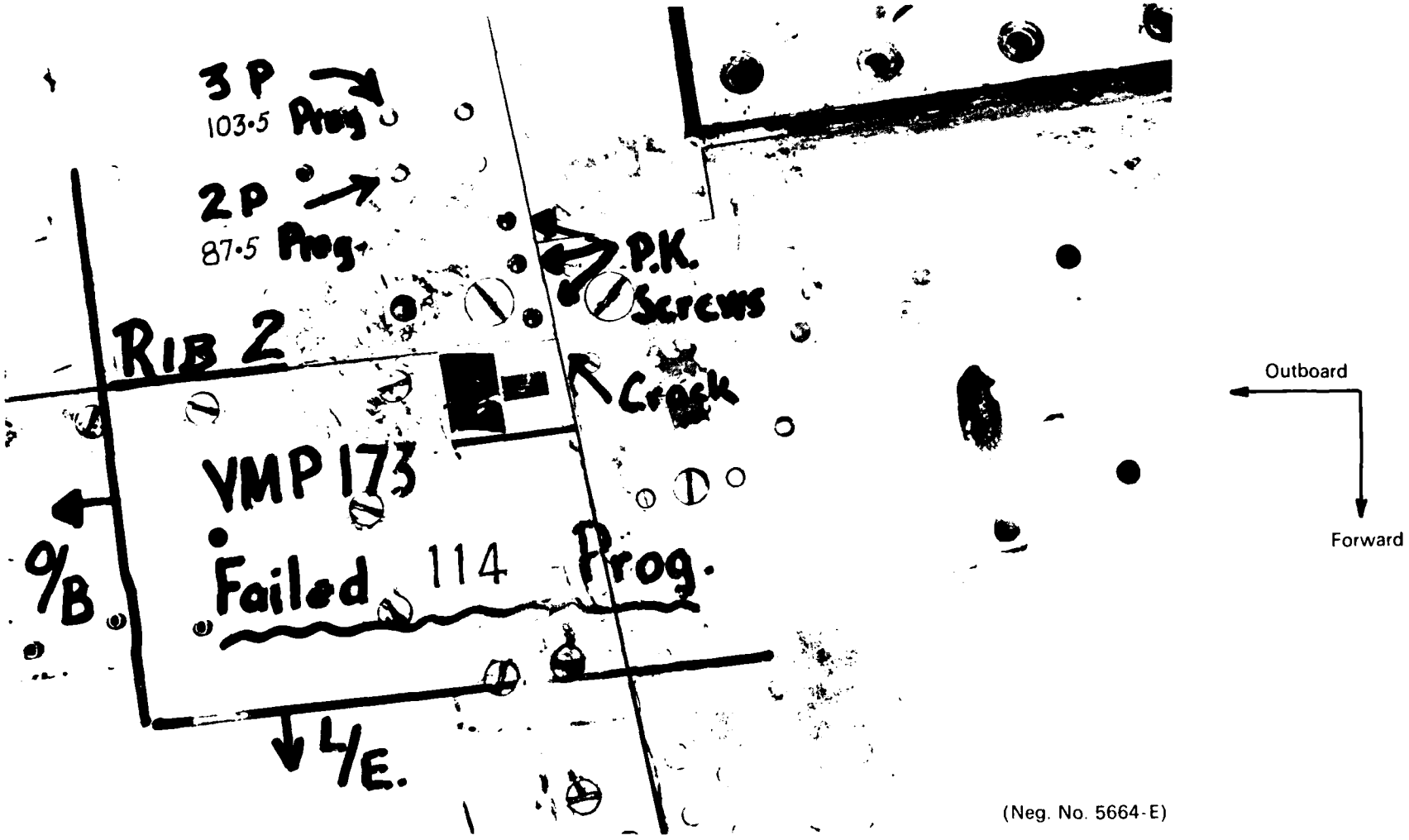

FIG. 13: LOWER SURFACE AT RIB 2 SHOWING POSITION OF P.K. SCREWS AND STRAIN GAUGE ON SPAR BOOM

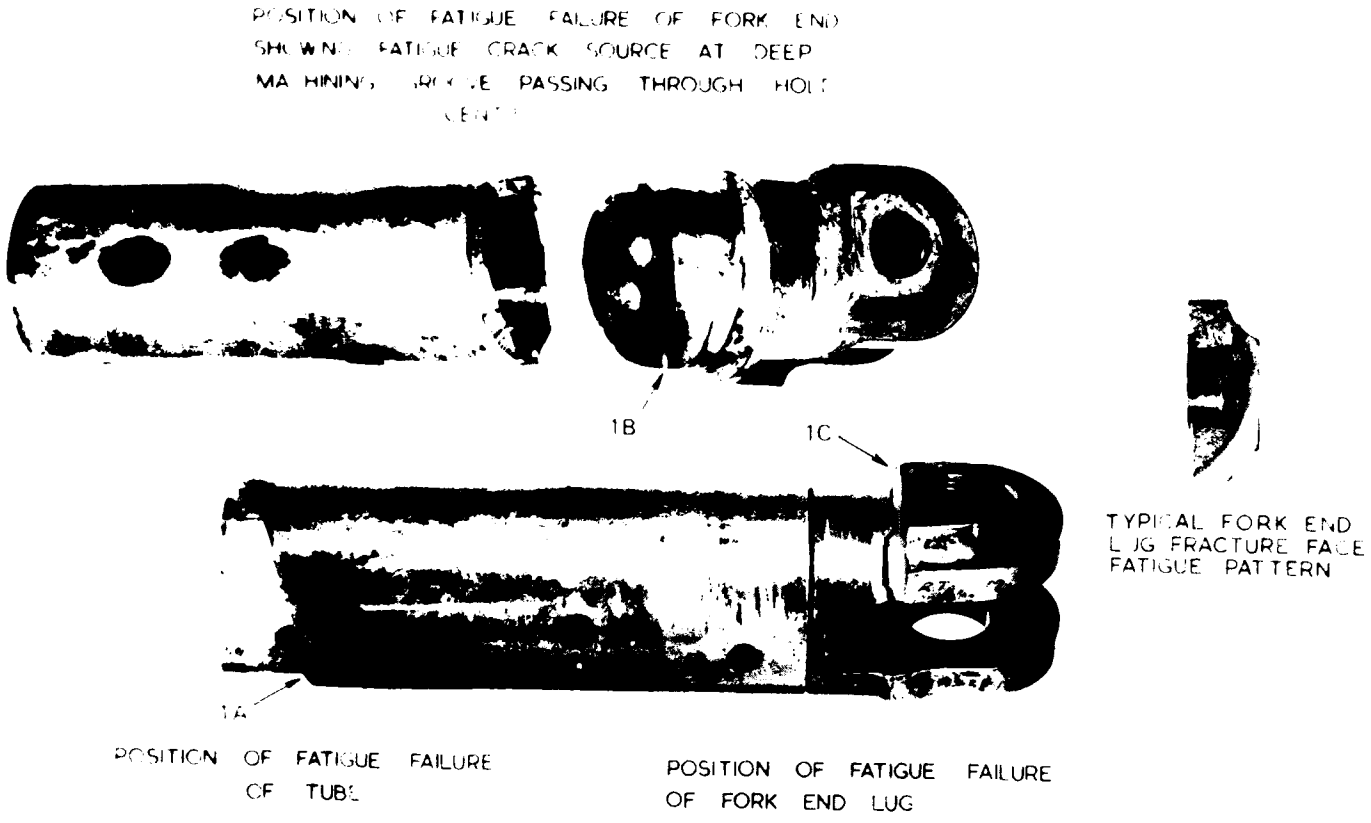

(Neg. No. 7019-13)

FIG. 14: FAILURES—LOWER CROSS-TUBE ASSEMBLY
TYPES 1A, 1B and 1C

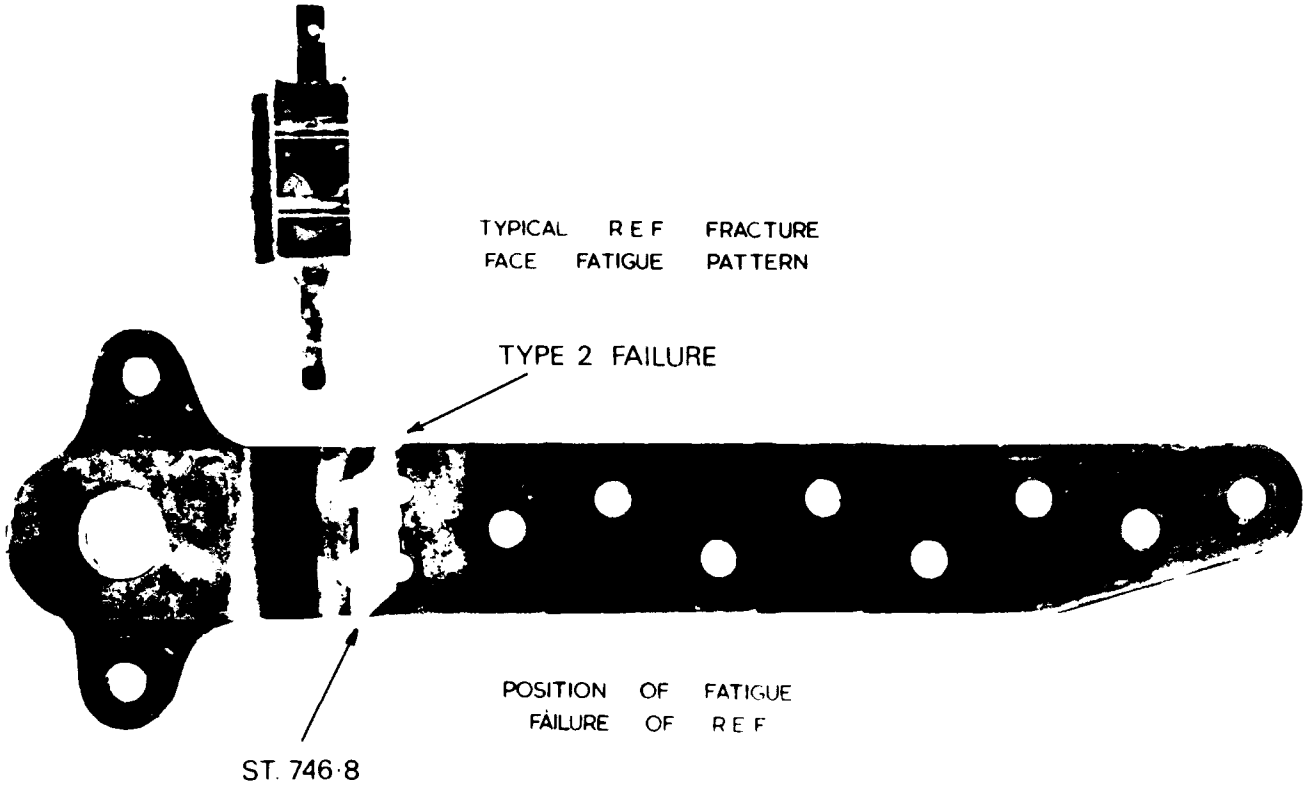

(Neg. No. 7019-A)

FIG. 15: WING ROOT END FITTING FAILURE—TYPE 2

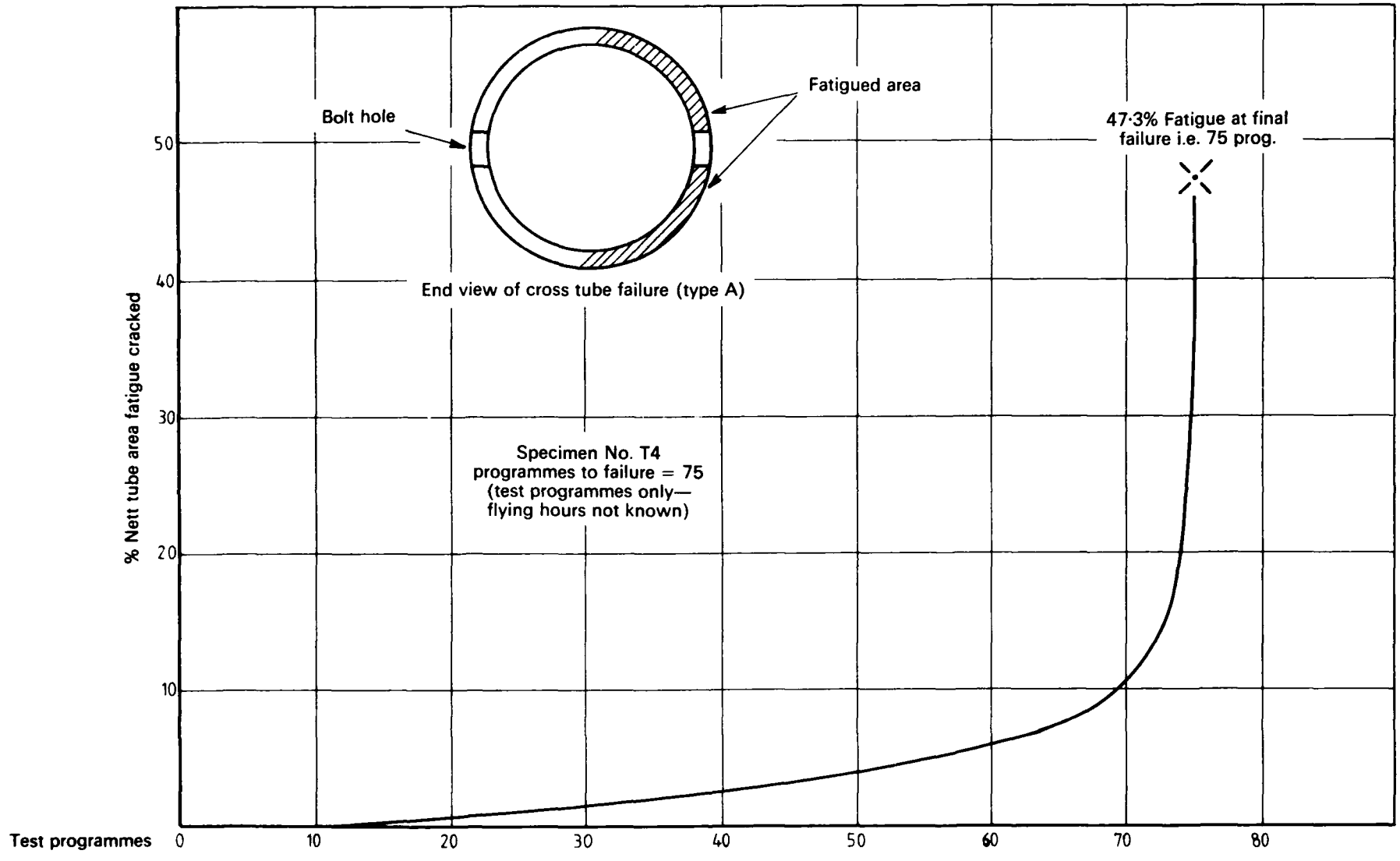

FIG. 16: CRACK PROPAGATION RATE—CENTRE SECTION LOWER CROSS TUBE

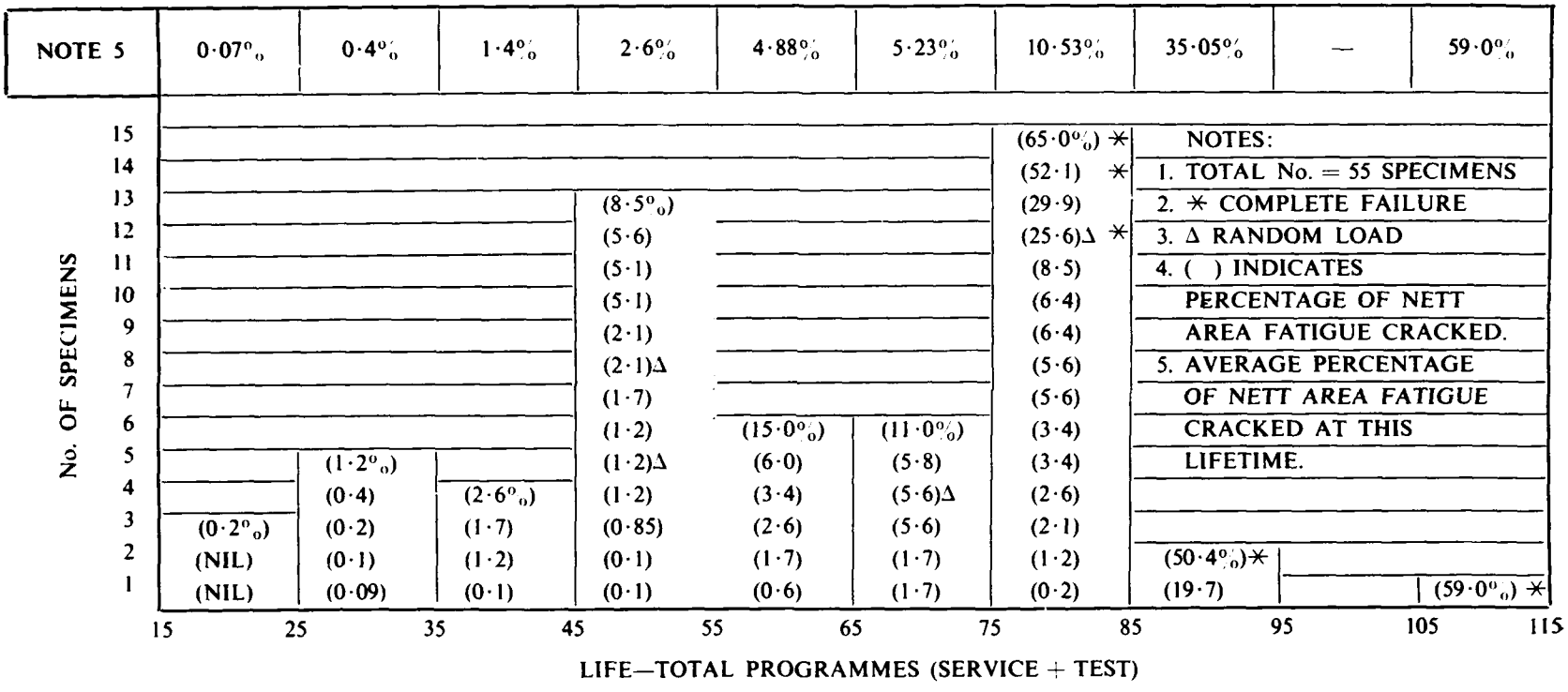

Fig. 17: Root end Fittings—Histogram of Life at Removal from Test Rig, (Indicating also the Percentage of Nett Area Fatigued)

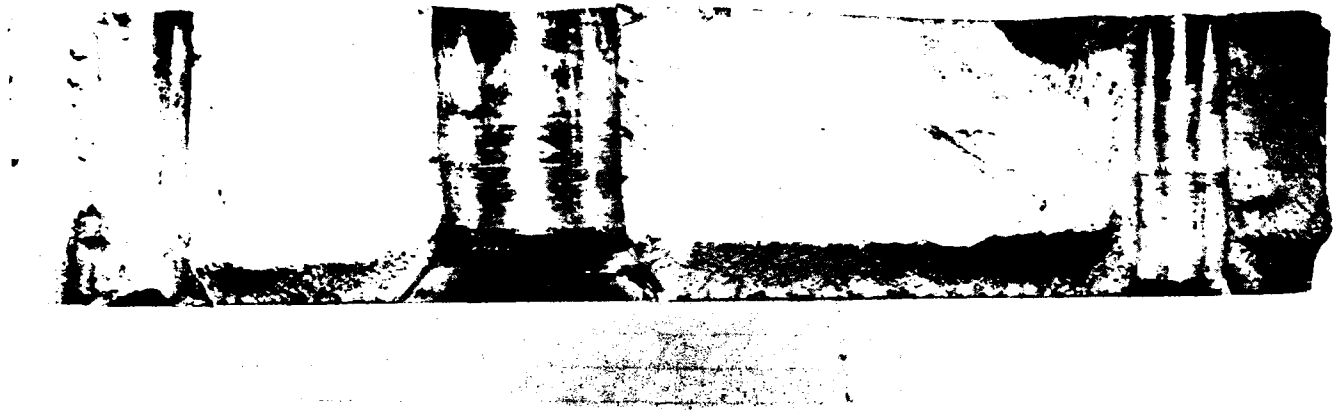

(NEG. No. 6304)

FIG. 18: TYPICAL SPAR BOOM FRACTURE AT RIB 1B (TYPE 3A)

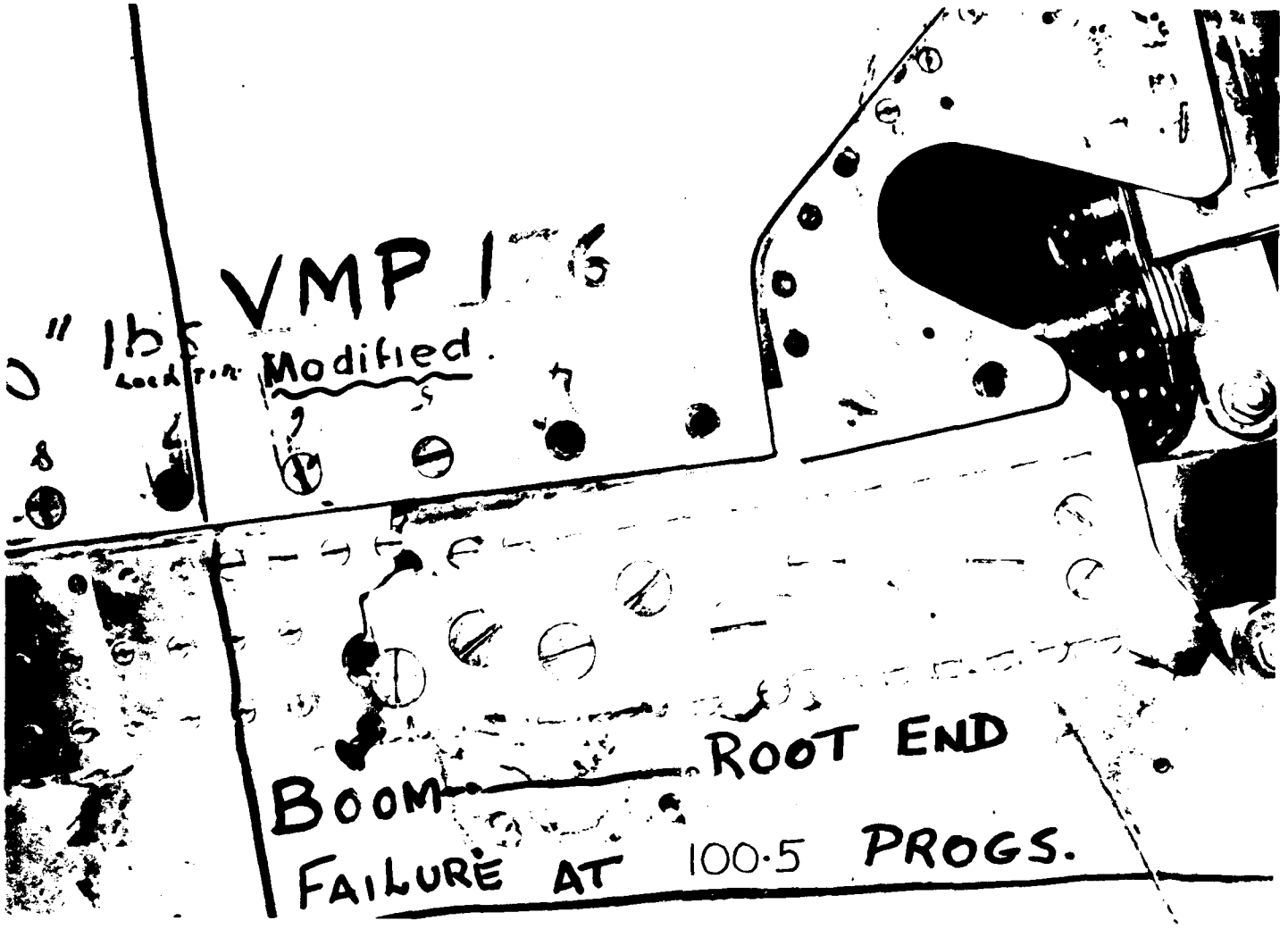

(NEG. No. 5371-B)

FIG. 19: EXTERNAL VIEW OF LOWER SURFACE FAILURE AT RIB 1B—
TYPE 3A

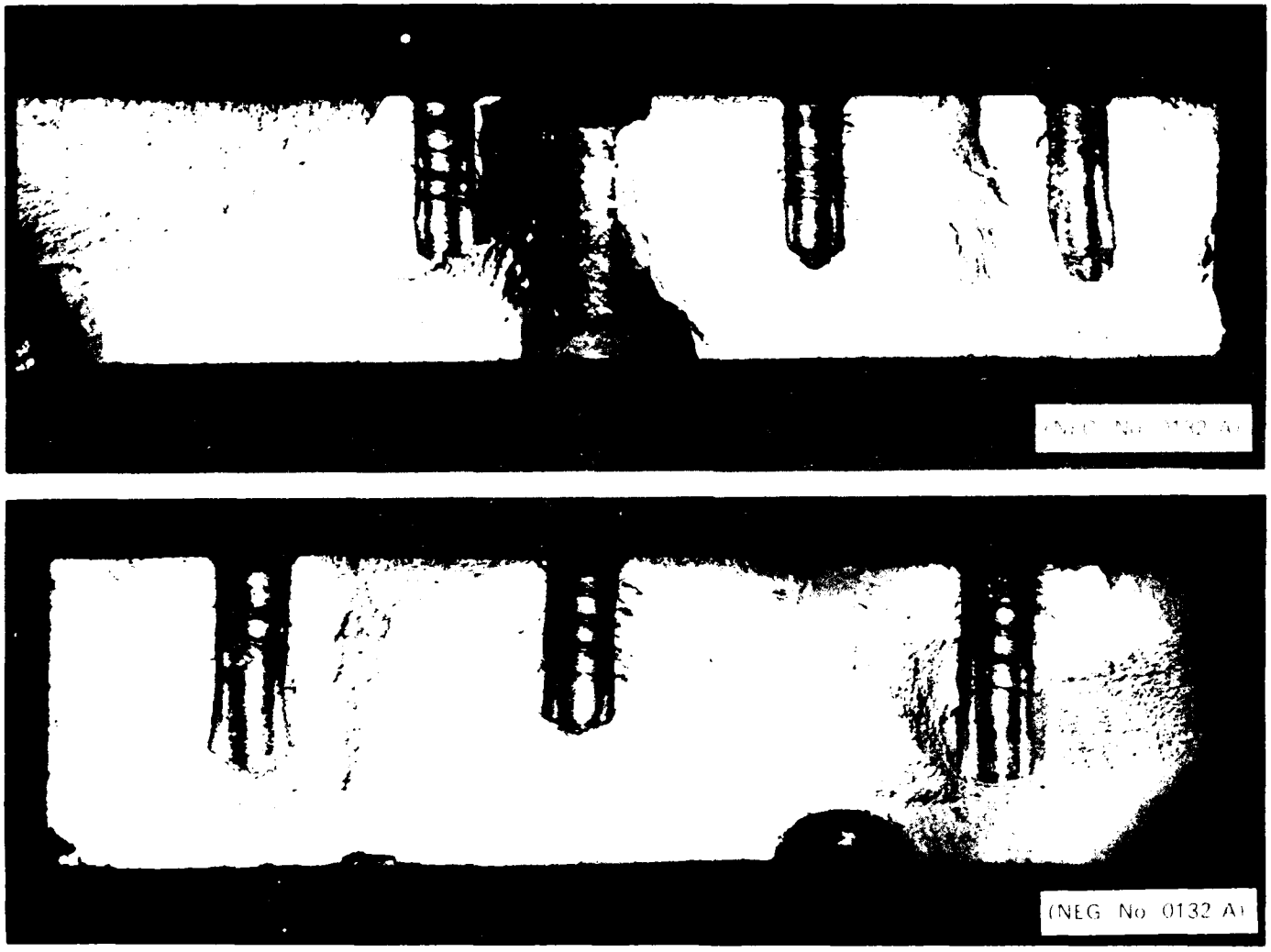

Through 9·5 mm ($\frac{3}{8}$") bolt hole

Through PK screw holes only

FIG. 20: ALTERNATE FRACTURE PATHS THROUGH SPAR BOOM AT RIB 2 (TYPE 4A)

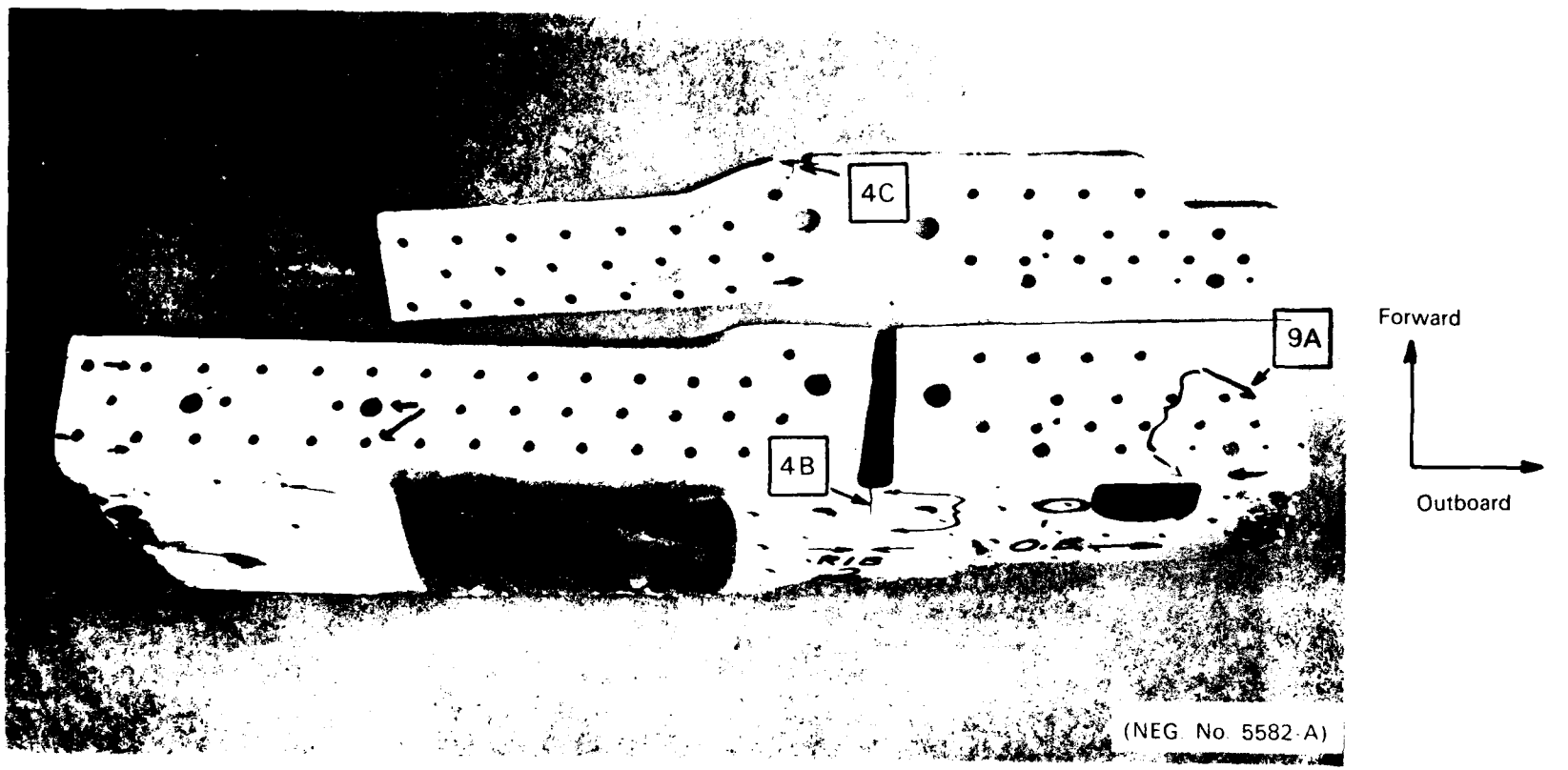

FIG. 21 : SPAR WEB AND DOUBLER FAILURES AT RIB 2
(TYPES 4B, 4C and 9A)

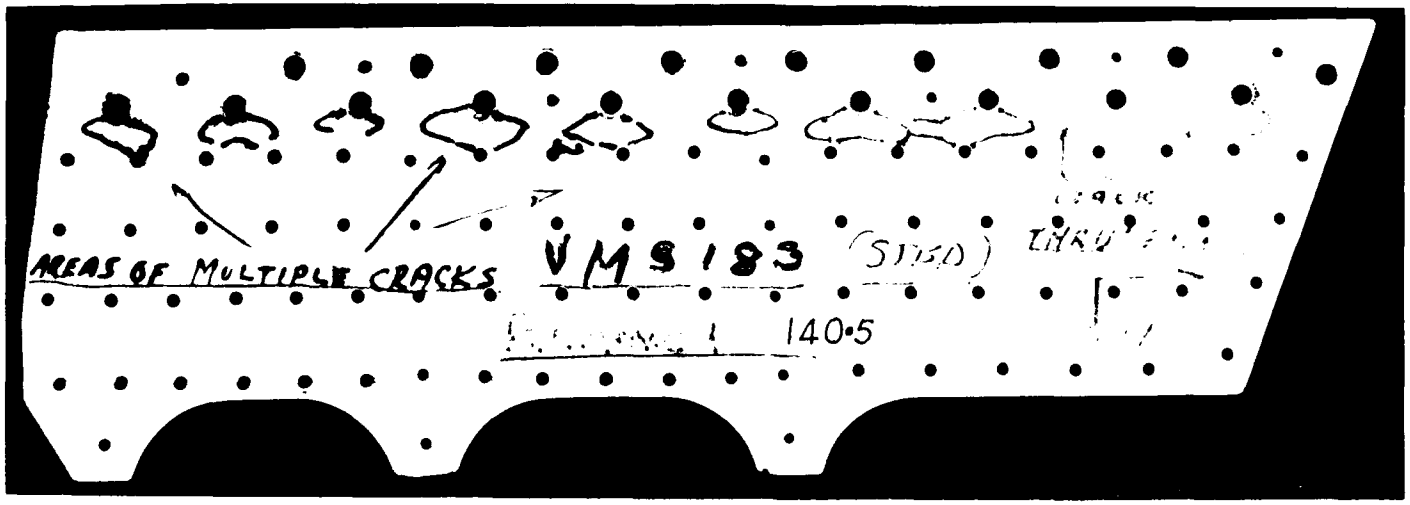

(NEG. No. 5646-E)

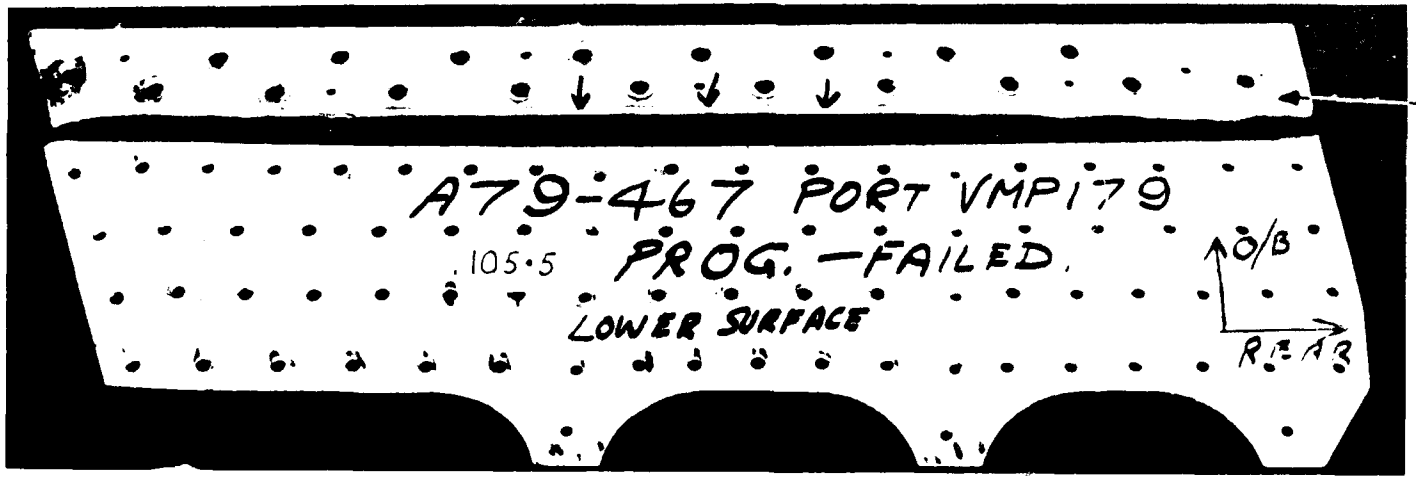

Shallow bend line

(NEG. No. 5639-A)

FIG. 22: BUTT STRAP FAILURES—TYPE 5D

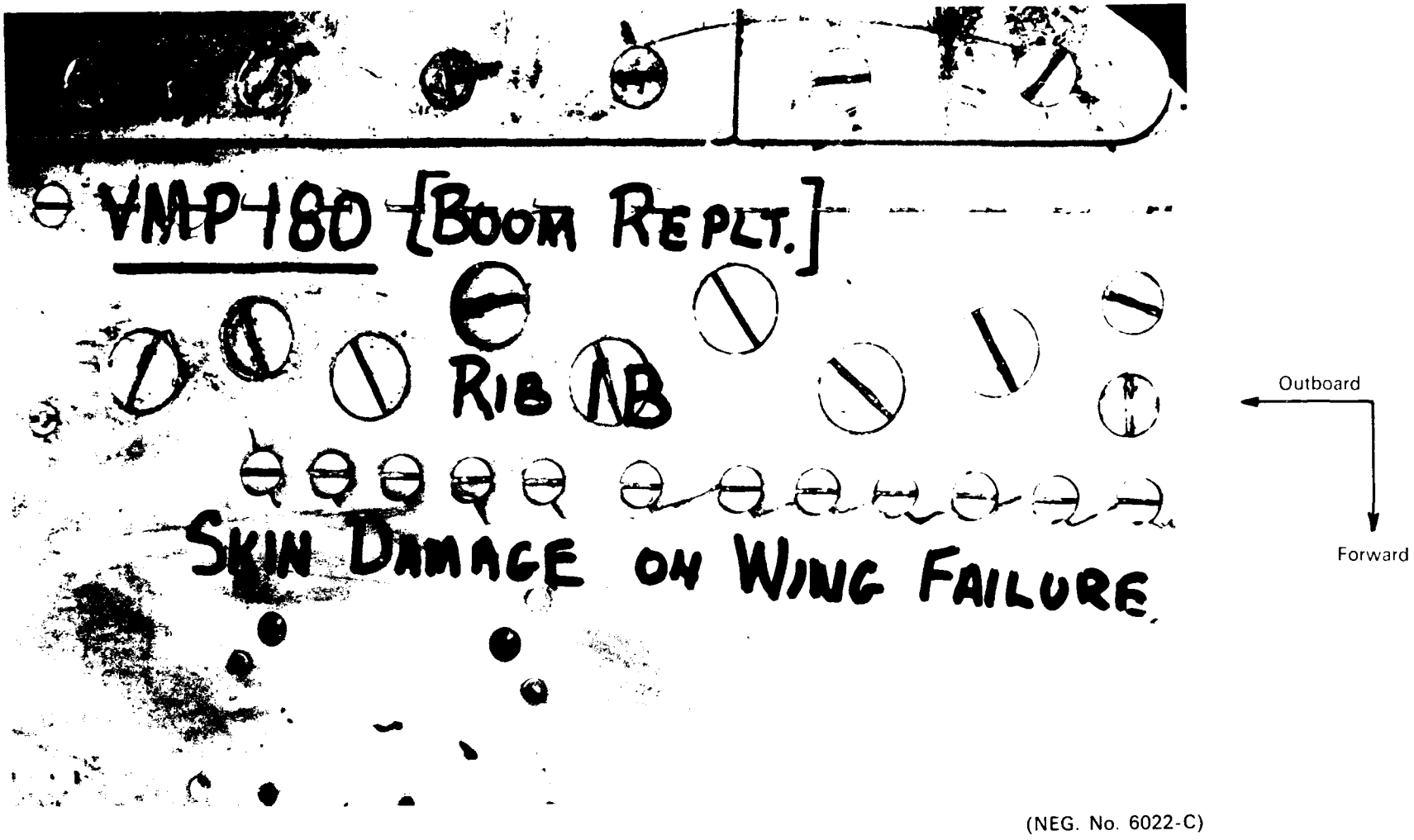

(NEG. No. 6022-C)

FIG. 23: LOWER SKIN FAILURE AT WING ROOT (TYPE 7A)

(NEG. No. 5983-F)

FIG. 24: LOCATION AND REPAIR OF LOWER SKIN FAILURE AFT OF WHEEL WELL AT STA 2248 (TYPE 11)

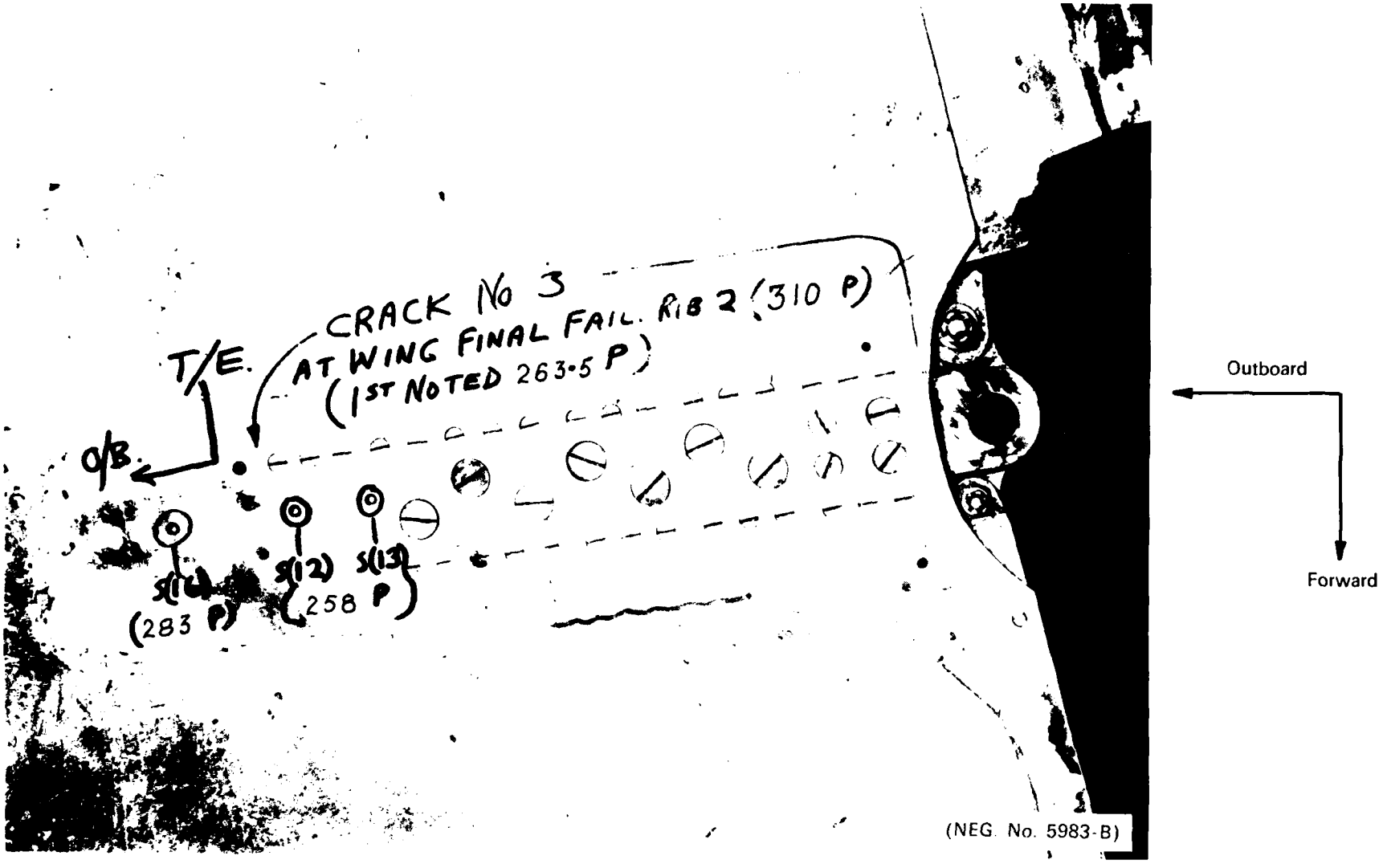

FIG. 25: UPPER SURFACE SKIN FAILURE AT ROOT END FITTING
(TYPE 12)

AD-A089 402 AERONAUTICAL RESEARCH LABS MELBOURNE (AUSTRALIA) F/G 1/3
FATIGUE TESTING OF VAMPIRE WINGS,(U)
JUN 79 R A BRUTON, C A PATCHING
UNCLASSIFIED ARL/STRUC-378 NL

2 OF 2
AD A089402

END
DATE FILMED
10-80
DTIC

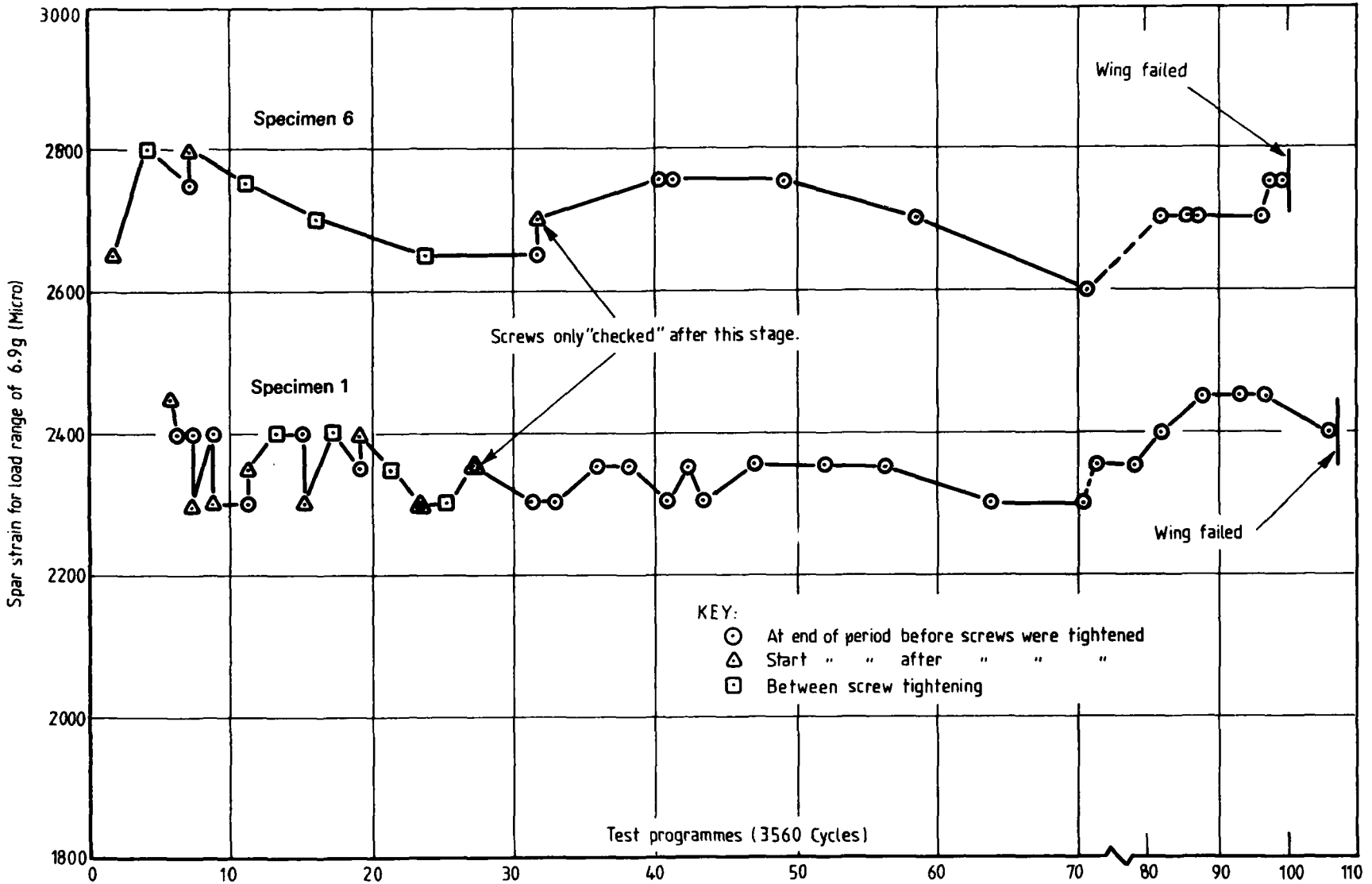

FIG. 26: PROGRESSIVE EFFECT OF SCREW TIGHTNESS ON STRAIN IN SPAR AT RIB 2

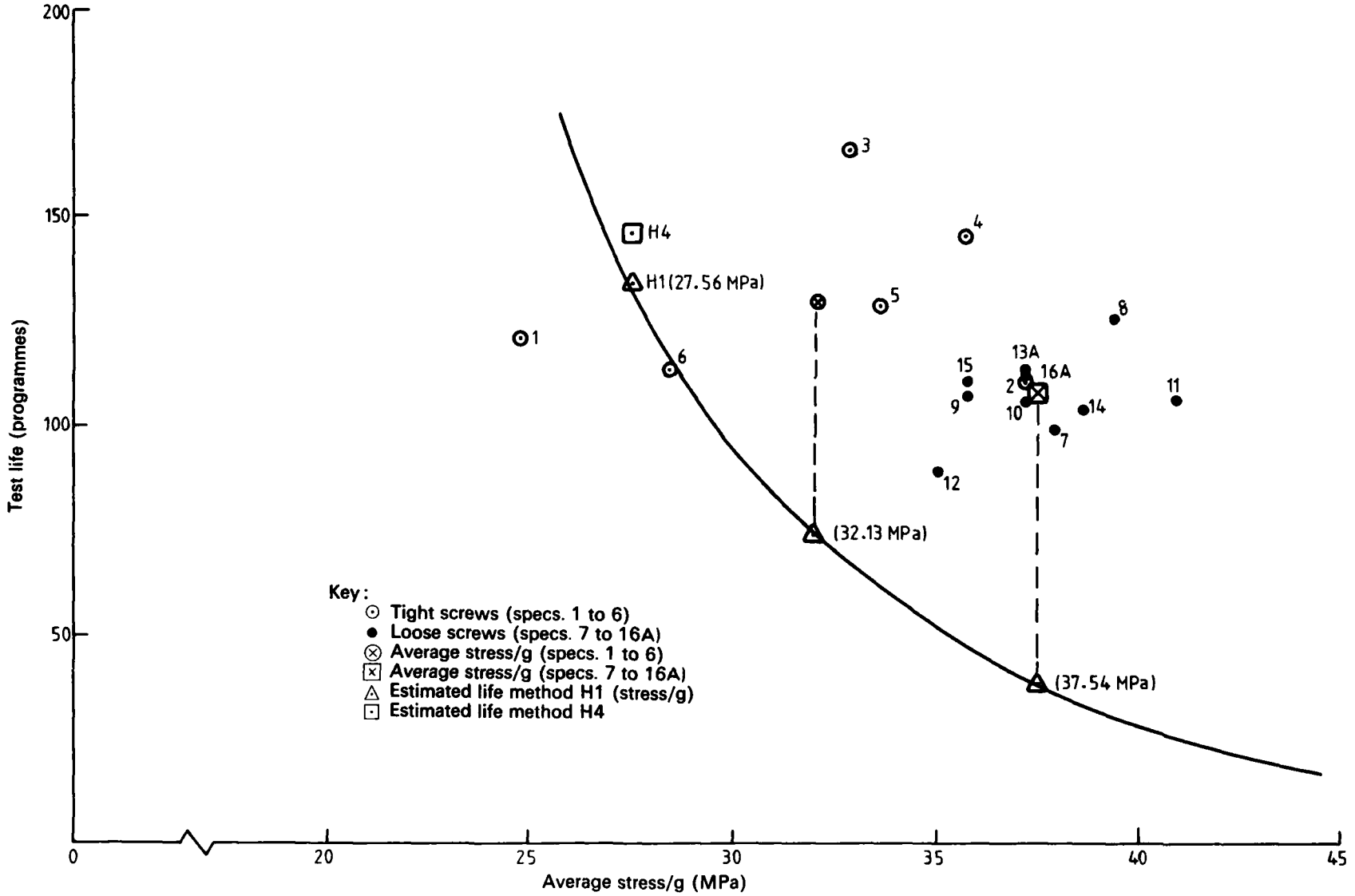

FIG. 27: LIFE-STRESS AT RIB 2

(NEG. No. 0132-B)

FIG. 28: FATIGUE INITIATION AT PK SCREWS IN SPAR BOOM

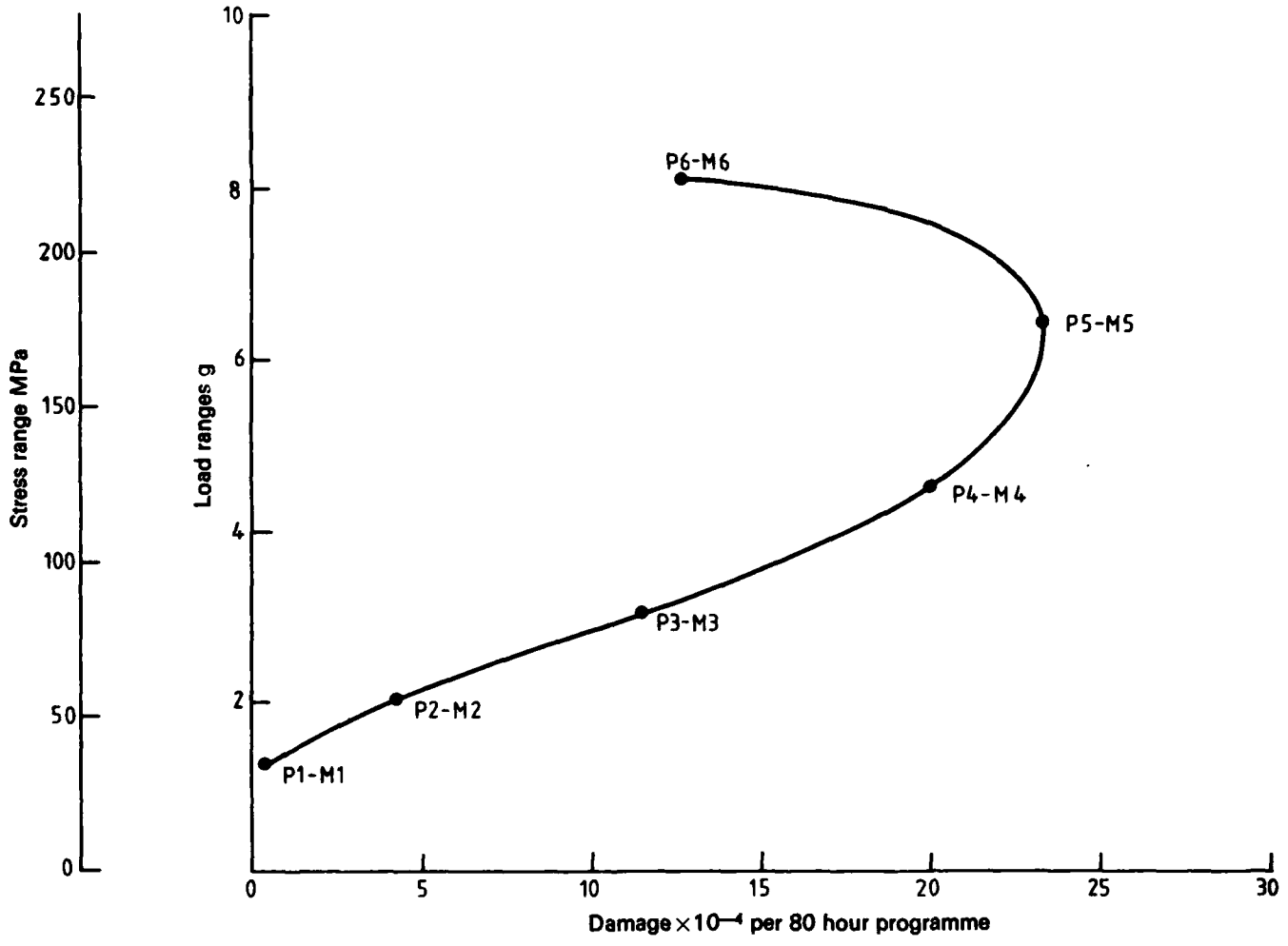

FIG. 29: PREDICTED FATIGUE DAMAGE HYPOTHESIS HI

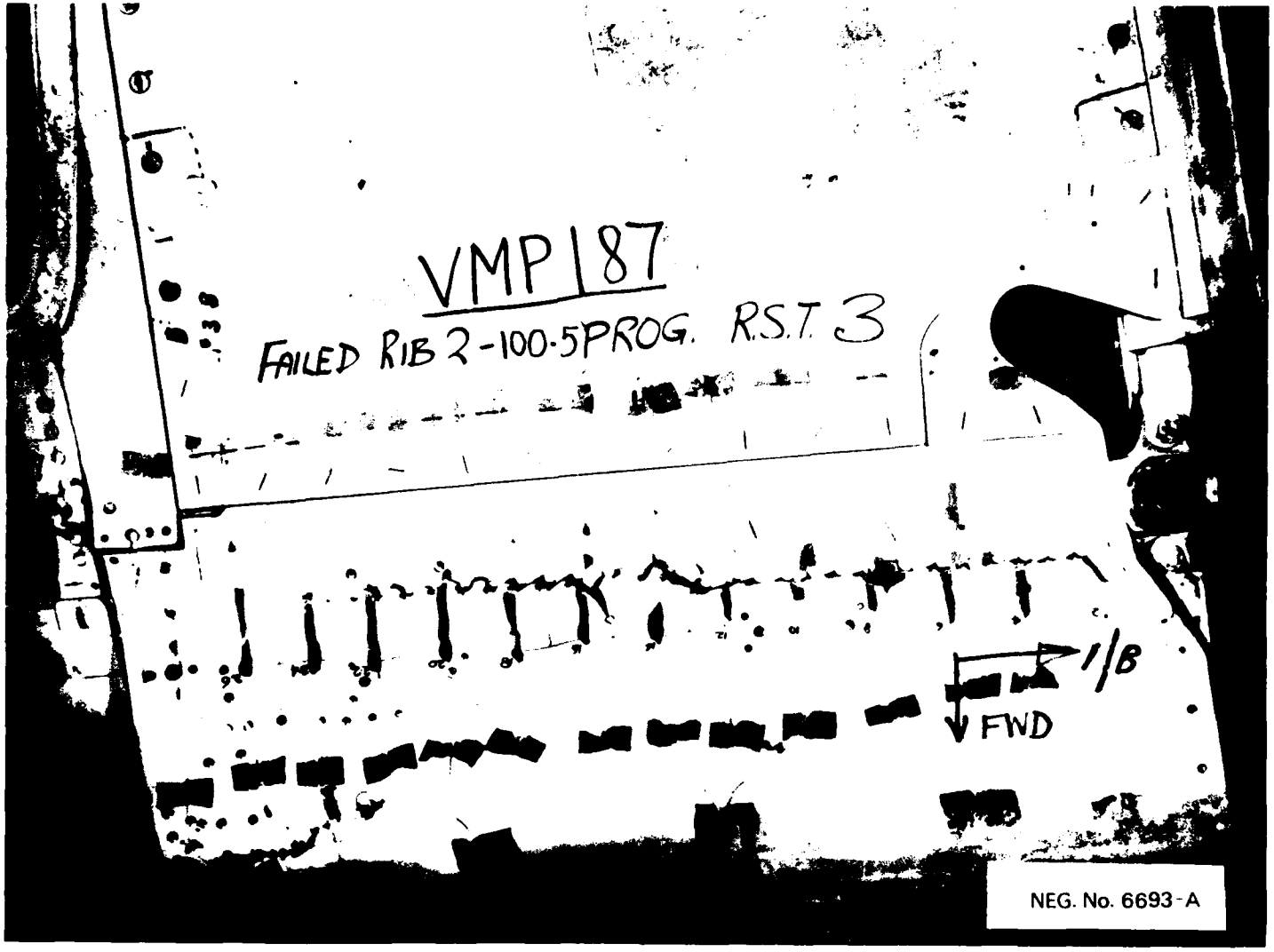

FIG. 30: CRACK PROPAGATION WIRE DETECTOR ON RESIDUAL STRENGTH TEST OF SPECIMEN No. 11

NEG. No. 6029-C

FIG. 31 : VIEW OF ENGINE MOUNT AND FUSELAGE MAIN BULKHEAD

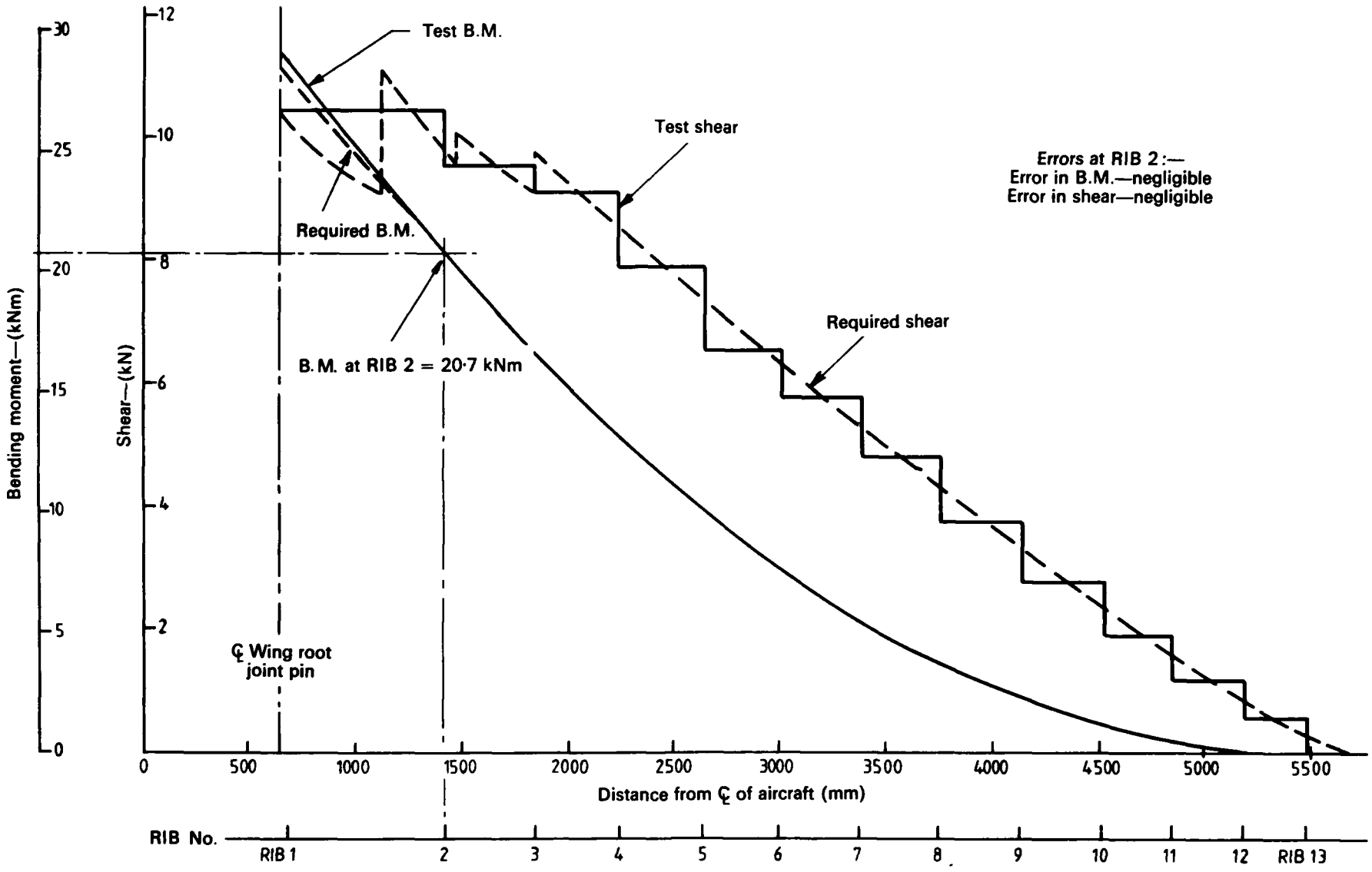

FIG. 32: 1 g INCREMENT OF LOADING — BENDING MOMENT — SHEAR

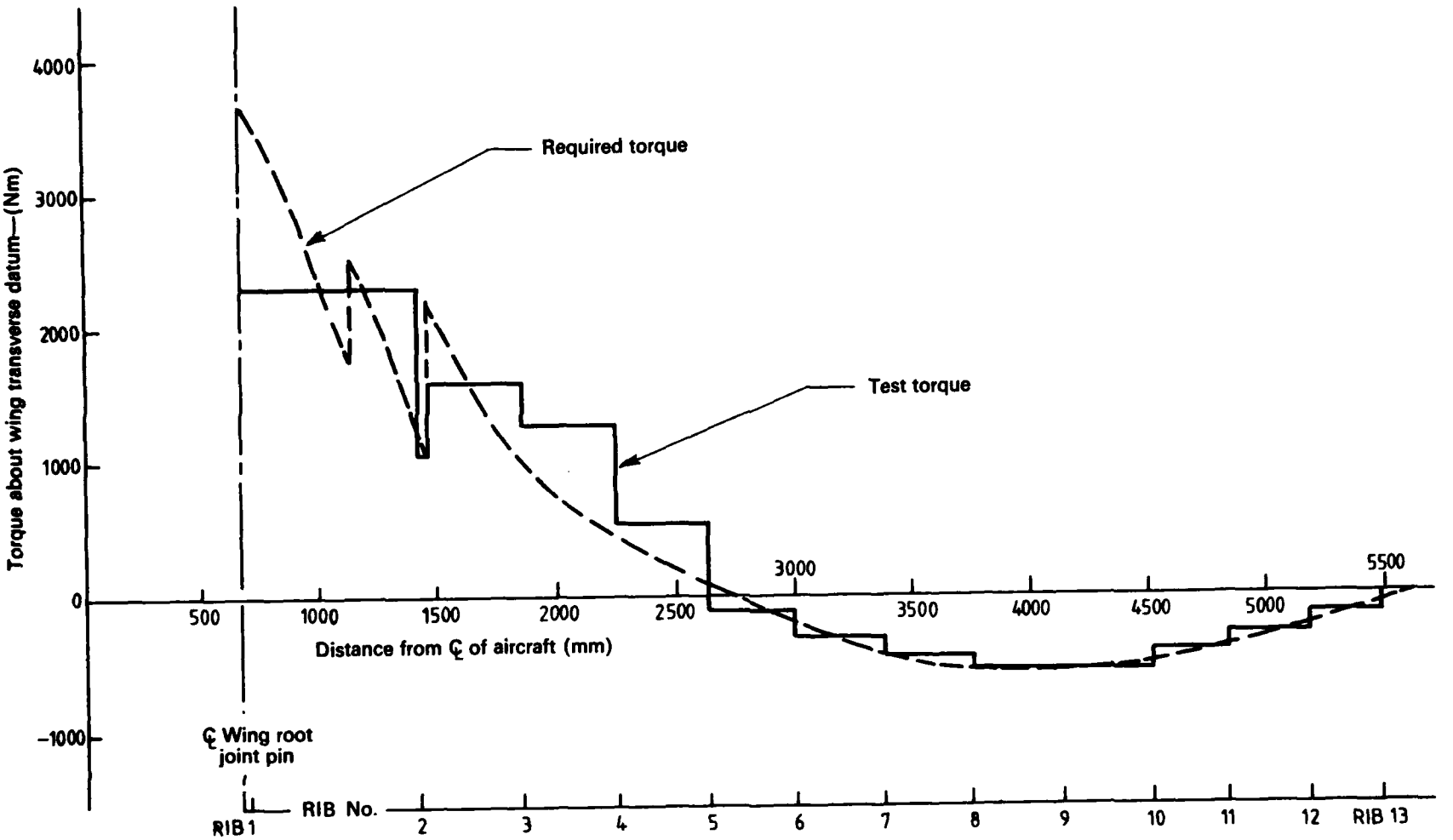

FIG. 33: 1 g INCREMENT OF LOADING — TORQUE

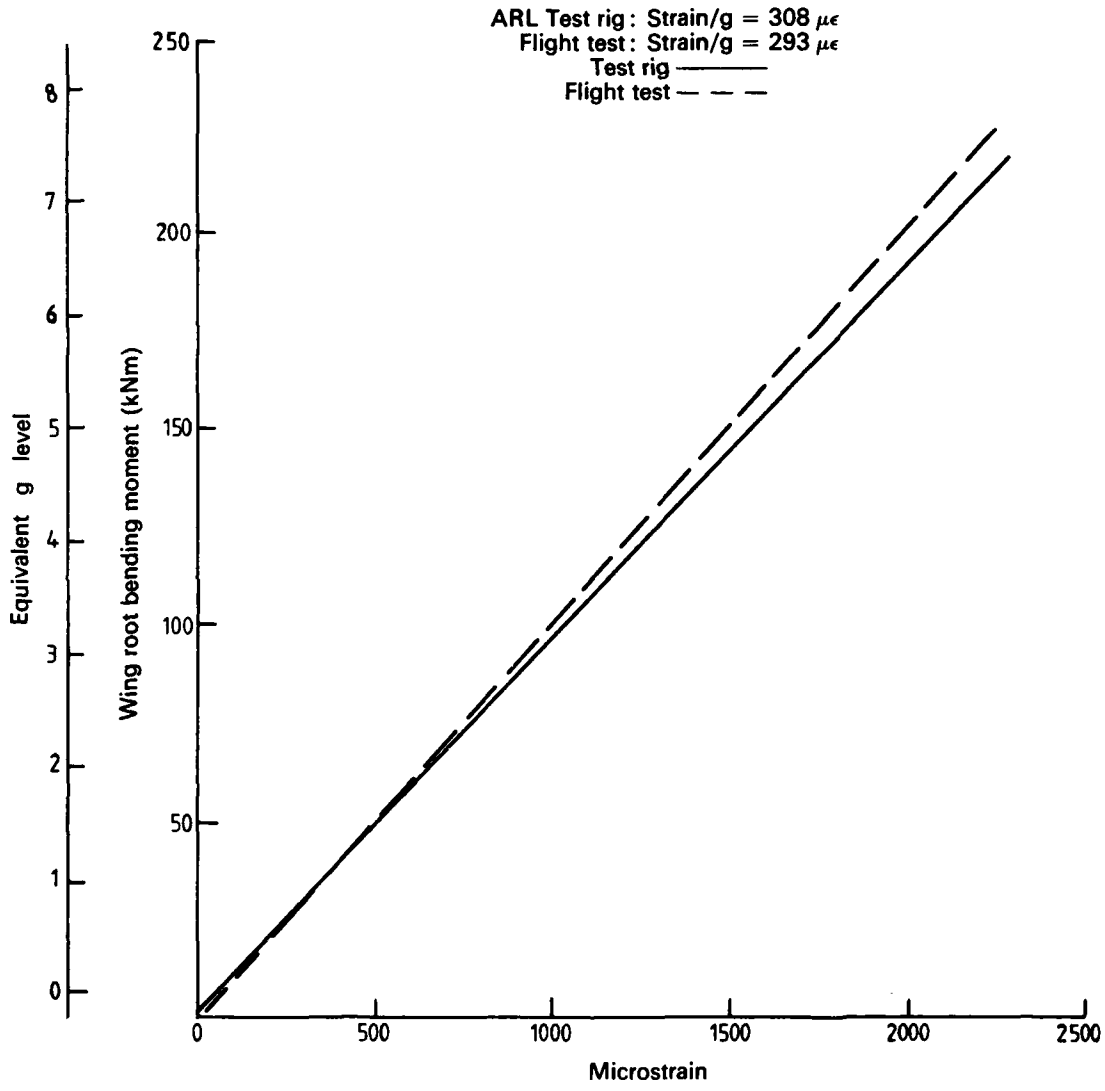

FIG. 34: BENDING MOMENT *vs* STRAIN — VAMPIRE LOWER CROSS TUBE

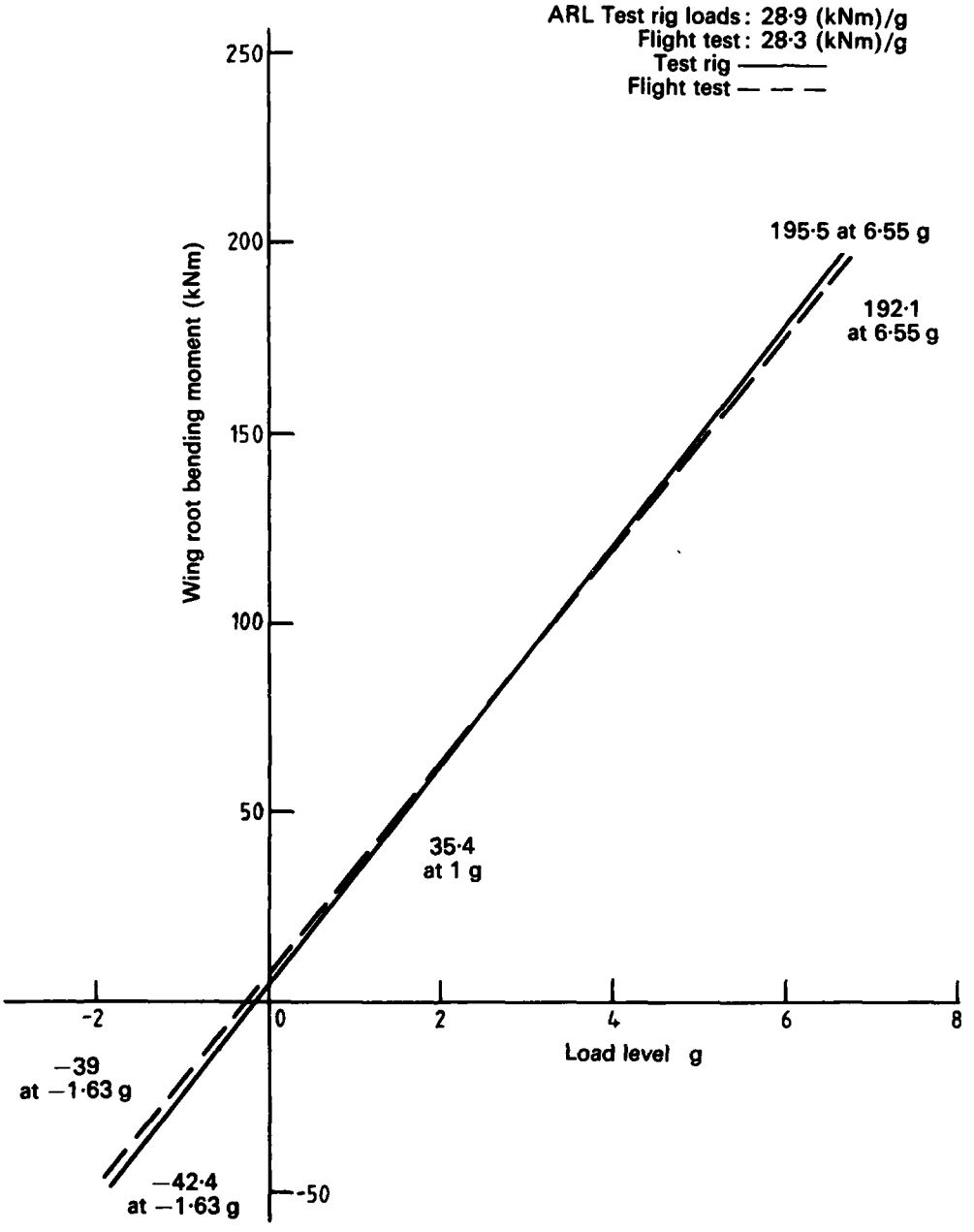

FIG. 35: COMPARISON BETWEEN FLIGHT AND TEST RIG LOADING

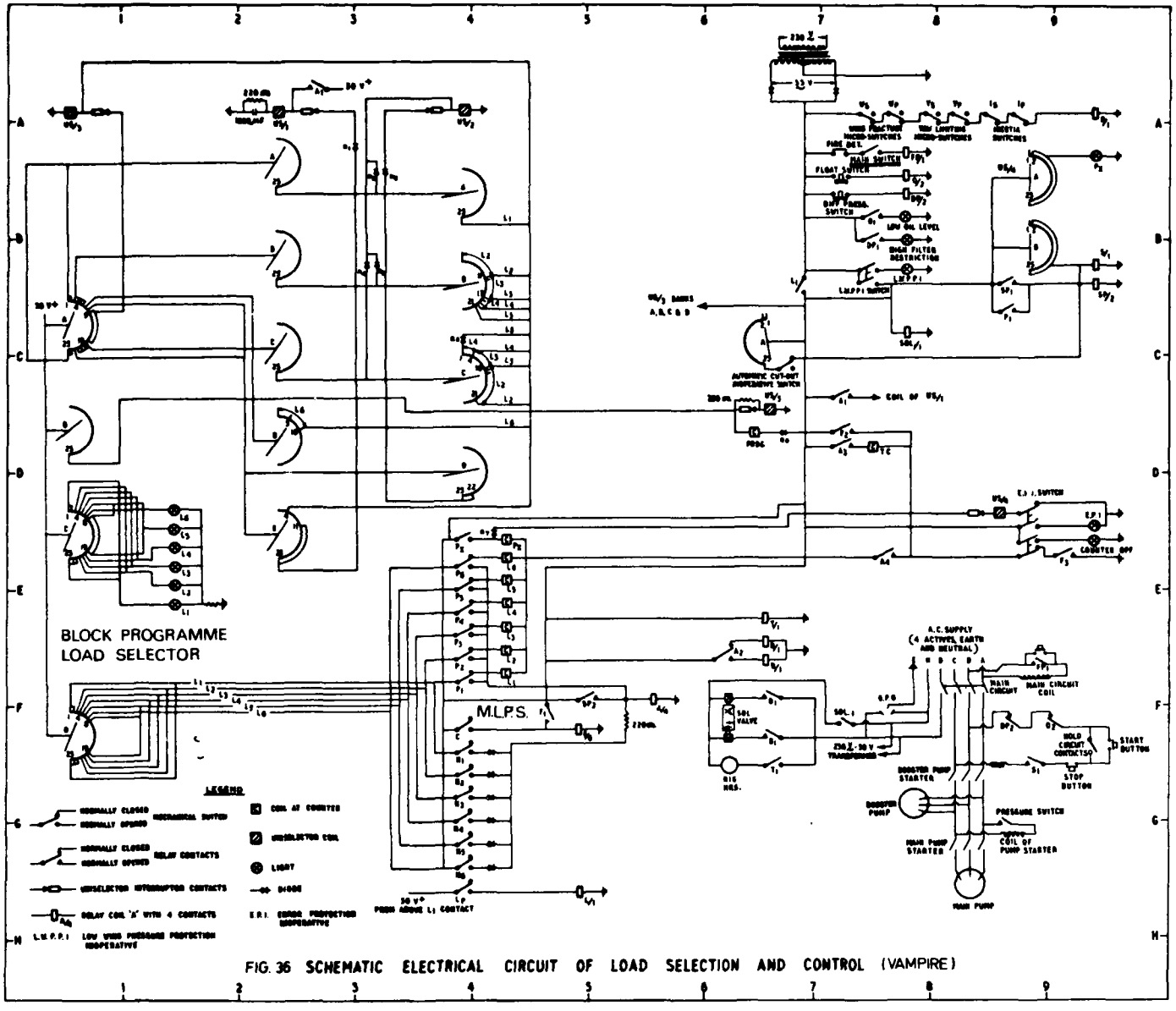

FIG. 36 SCHEMATIC ELECTRICAL CIRCUIT OF LOAD SELECTION AND CONTROL (VAMPIRE)

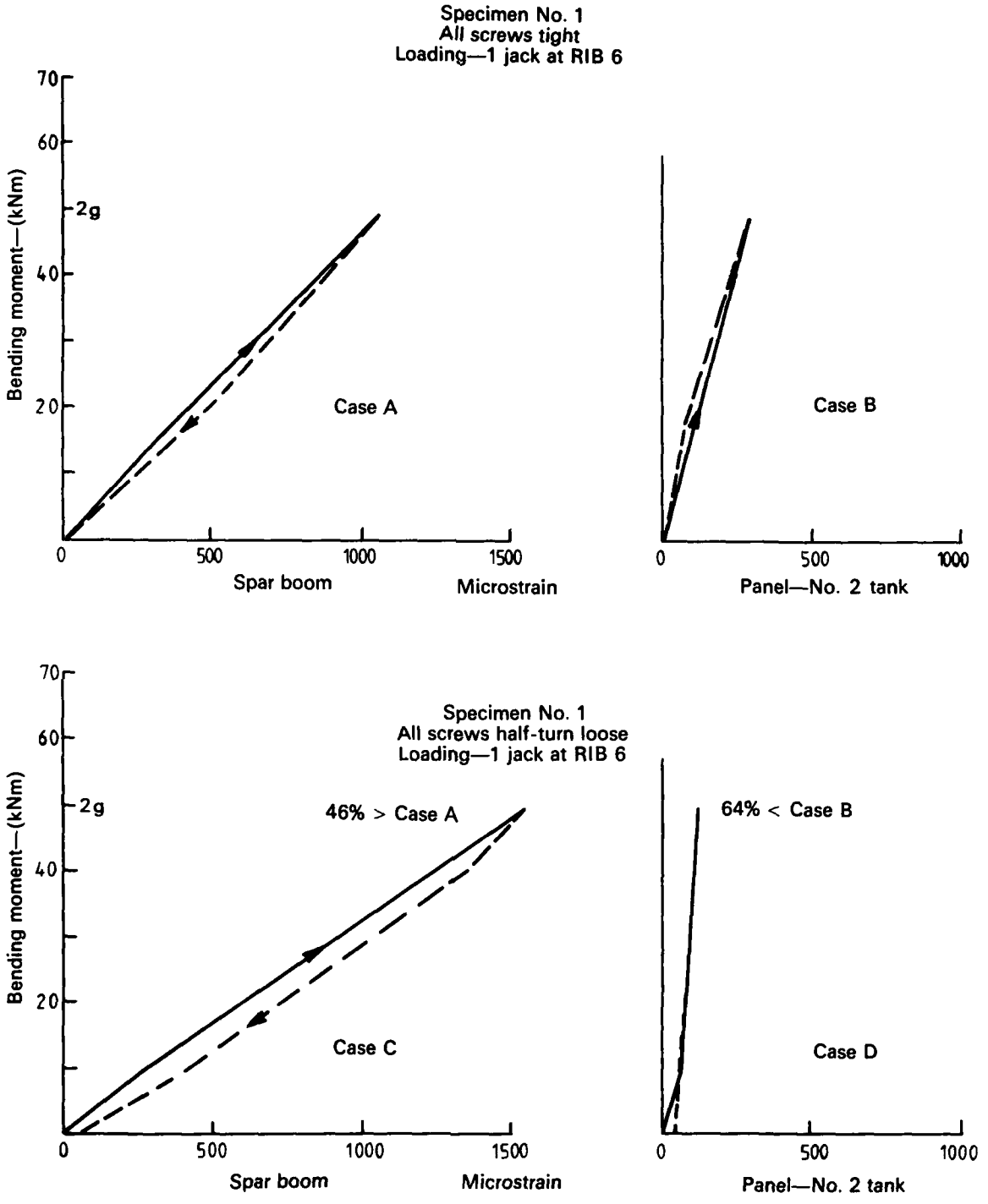

FIG. 37: EFFECT OF SCREW TIGHTNESS ON SPAR BOOM AND PANEL STRAIN AT RIB 2—LOW LOADS

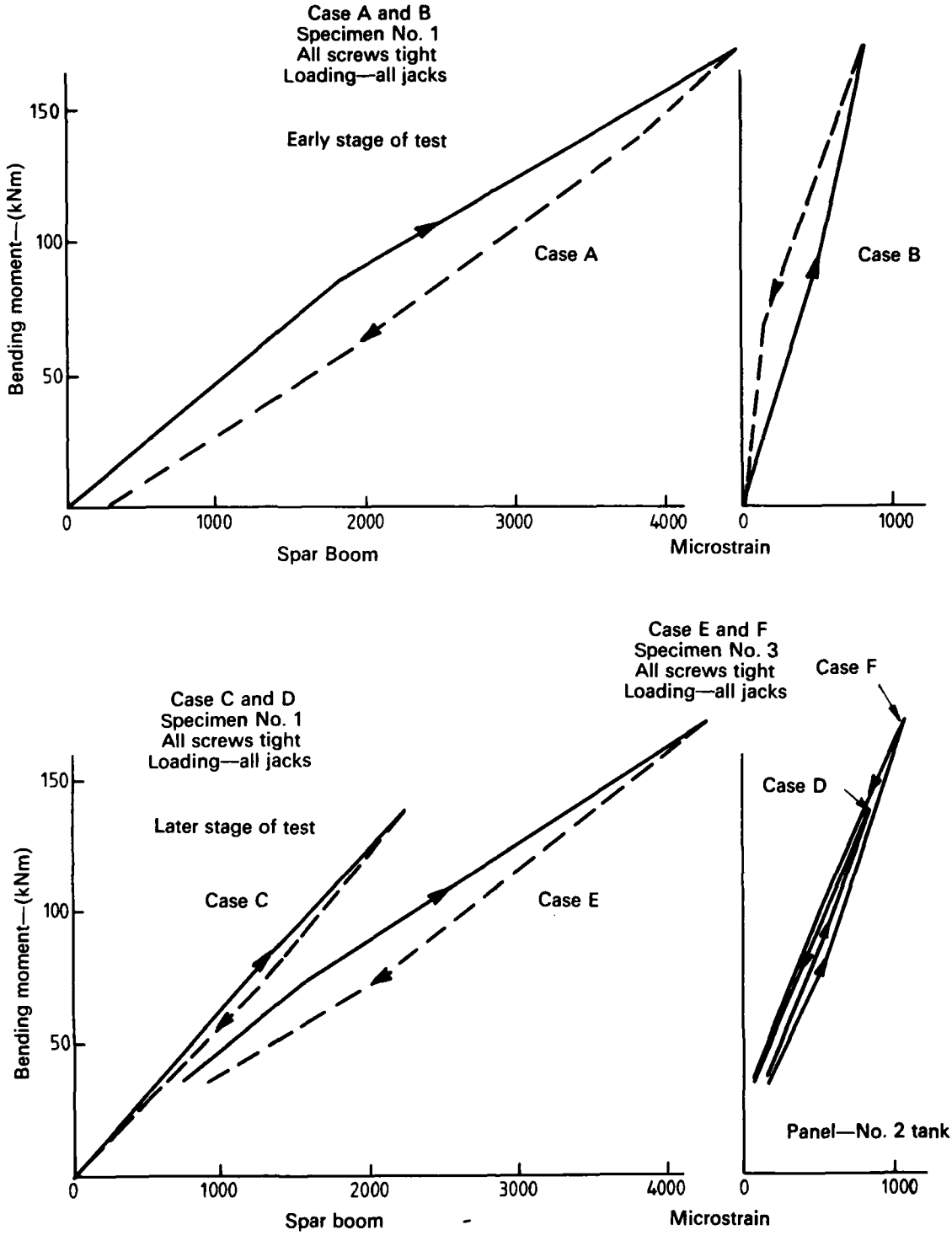

FIG. 38: EFFECT OF SCREW TIGHTNESS ON SPAR BOOM AND PANEL STRAIN AT RIB 2—HIGH LOADS

DISTRIBUTION

AUSTRALIA

	Copy No.
Department of Defence	
Central Office	
Chief Defence Scientist	1
Deputy Chief Defence Scientist	2
Superintendent, Science and Technology Programs	3
Australian Defence Scientific and Technical Representative, (U.K.)	4
Counsellor, Defence Science (U.S.A.)	5
Defence Library	6
Assistant Secretary, D.I.S.B.	7–22
Joint Intelligence Organisation	23
Aeronautical Research Laboratories	
Chief Superintendent	24
Library	25
Superintendent — Structures Division	26
Divisional File — Structures	27
Authors: R. A. Bruton	28
C. A. Patching	29
A. O. Payne	30
D. G. Ford	31
G. S. Jost	32
J. Y. Mann	33
Materials Research Laboratories	
Library	34
Defence Research Centre, Salisbury	
Library	35
Central Studies Establishment	
Library	36
Engineering Development Establishment	
Library	37
RAN Research Laboratory	
Library	38
Defence Regional Office	
Library	39
Army Office	
Royal Military College Library	40
Air Force Office	
Aircraft Research & Development Unit, Scientific Flight Group	41
Air Force Scientific Adviser	42
Technical Division Library	43
D. Air Eng.	44
HQ Support Command (SENGSO)	45
RAAF, Point Cook	46

Department of Productivity

Government Aircraft Factories

Manager/Library		47

Department of Transport

Airworthiness Group, Mr K. O'Brien		48

Statutory, State Authorities and Industry

CSIRO National Measurement Laboratory, Chief		49
CSIRO Materials Science Division, Director		50
Qantas, Library		51
Trans Australia Airlines, Library		52
Ansett Airlines of Australia, Library		53
Applied Engineering Pty. Ltd.		54
Australian Paper Manufacturers, Dr Norman		55
BHP Central Research Laboratories, NSW		56
BHP Melbourne Research Laboratories		57
BP Australia Ltd., Librarian		58
Commonwealth Aircraft Corporation, Manager		59
Commonwealth Aircraft Corporation, Manager of Engineering		60
Victorian Brown Coal Council, Dr H. K. Worner		61
Hawker de Havilland Pty. Ltd., Librarian, Bankstown		62
Hawker de Havilland Pty. Ltd., Mr Odbert, Bankstown		63
ICI Australia Ltd., Library		64
H. C. Sleigh Ltd., Technical Department Library		65

Universities and Colleges

Adelaide	Barr Smith Library	66
Australian National	Library	67
Flinders	Library	68
James Cook	Library	69
Latrobe	Library	70
Melbourne	Engineering Library	71
Monash	Library	72
	Professor I. J. Polmear	73
Newcastle	Library	74
New England	Library	75
Sydney	Engineering Library	76
	Professor G. A. Bird	77
N.S.W.	Physical Sciences Library	78
Queensland	Library	79
Tasmania	Engineering Library	80
Western Australian	Library	81
R.M.I.T.	Library	82
	Mr H. Millicer	83

CANADA

CAARC Coordinator Structures		84
International Civil Aviation Organization, Library		85
NRC, National Aeronautical Establishment, Library		86

Universities and Colleges

McGill	Library	87

FRANCE

AGARD, Library		88
ONERA, Library		89
Service de Documentation, Technique de l'Aeronautique		90

GERMANY

ZLDI		91

Brooklyn Inst. of Polytechnology	Politech. Aero. Lab., Library	203
California Inst. of Technology	Guggenheim Aero. Lab., Library	204
		205–214

Spares